# Presynaptic Gate of Pain Control: Malfunctioning Presynaptic GABAergic Inhibition in Neuropathic and Inflammatory Pain

Dissertation

zur Erlangung des Grades eines
Doktors der Naturwissenschaften

der Mathematisch-Naturwissenschaftlichen Fakultät
und
der Medizinischen Fakultät
der Eberhard-Karls-Universität Tübingen

vorgelegt
von

Da Guo (郭达)
aus Changchun, China

Mai - 2017

Tag der mündlichen Prüfung: 26.07.2017

Dekan der Math.-Nat. Fakultät: Prof. Dr. W. Rosenstiel
Dekan der Medizinischen Fakultät: Prof. Dr. I. B. Autenrieth

1. Berichterstatter: Dr. Jing Hu
2. Berichterstatter: Dr. Maria Kukley

Prüfungskommission:

Dr. Maria Kukley
PD Dr. Eva Küppers
Prof. Dr. Bernd Antkowiak
Dr. Jing Hu

*I hereby declare that I have produced the work entitled "Presynaptic Gate of Pain Control: Malfunctioning Presynaptic GABAergic Inhibition Contributes to Neuropathic and Inflammatory Pain Differently", submitted for the award of a doctorate, on my own (without external help), have used only the sources and aids indicated and have marked passages included from other works, whether verbatim or in content, as such. I swear upon oath that these statements are true and that I have not concealed anything. I am aware that making a false declaration under oath is punishable by a term of imprisonment of up to three years or by a fine.*

Tübingen, den ..... .....

Datum / Date Unterschrift /Signature

## Statement of Contributions

Own contribution: 2-photon chloride imaging, epifluorescence calcium imaging, 2-photon calcium imaging, immunohistochemistry (except NKCC1 staining) and real-time PCR experiments (with the help of Luming Zhou) and correlated data analysis and figure preparation.

Contribution of colleague: Jeremy Tsung-chieh Chen carried patch clamp and behavior experiments and related data analysis. Flavia performed NKCC1 staining and behavior and related analysis. Luming Zhou helped with RNA extraction and cDNA synthesis for real-time PCR.

Published results: Chloride imaging, cell culture calcium imaging, patch clamp, behavior results from result section 4.1 (GABAergic presynaptic modulation after peripheral nerve injury) and part of 2-photon calcium imaging on advillin-Ai38 spinal cord from result section 4.3 (A subpopulation of nociceptors crucial for presynaptic mediated mechanical allodynia in inflammatory pain) had been used in the previous published paper:

Chen JT, Guo D, Campanelli D, Frattini F, Mayer F, Zhou L, Kuner R, Heppenstall P a., Knipper M, Hu J (2014) Presynaptic GABAergic inhibition regulated by BDNF contributes to neuropathic pain induction. Nat Commun 5:5331 Available at: http://www.nature.com/doifinder/10.1038/ncomms6331 [Accessed October 30, 2014].

# Table of Contents

# i. Abbreviations

| | |
|---|---|
| BDNF | brain derived neurotrophic factor |
| BZD | benzodiazepine |
| CCC | cation-chloride cotransporters |
| CCI | chronic constriction injury |
| CFA | Complete Freud's Adjuvant |
| CGRP | calcitonin gene-related peptide |
| CNS | central nerve system |
| COX-2 | cyclooxygenase-2 |
| CUP | $Ca^{2+}$ uni-porter |
| DRG | dorsal root ganglion |
| DRR | dorsal root reflex |
| DZP | diazepam |
| ER | endoplasmic reticulum |
| FRET | Fluorescence resonance energy transfer |
| GABA | gamma-Aminobutyric acid |
| GAD | glutamic acid decarboxylase |
| GAT1 | GABA transporter 1 |
| GCT | gate control theory |
| GDNF | neurotrophic factor |
| GECI | genetically encoded calcium indicator |
| GlyR3 | glycine receptor 3 |
| IASP | International Association for the Study of Pain |
| IB4 | isolectin B4 |
| KCC2 | K-Cl co-transporter 2 |

| | |
|---|---|
| NCX | $N^{a+}/Ca^{2+}$ exchanger |
| NGF | nerve growth factor |
| NKCC1 | Na-K-2Cl co-transporter |
| PAD | primary afferent depolarization |
| PBS | phosphate-buffered saline |
| PFA | paraformaldehyde |
| PGE2 | prostaglandin E2 |
| PKA | protein kinase A |
| PMCA | plasma membrane $Ca^{2+}$-ATPase |
| PNS | peripheral nerve system |
| ROI | region of interest |
| SC | spinal cord |
| SERCA | $Ca^{2+}$-ATPase |
| TrkA | tyrosine receptor kinase A |
| TrkB | tyrosine receptor kinase B |
| TRPV1 | transient receptor potential vanilloid subfamily type 1 |

# ii. Figures and table

# 1 Abstract

GABAergic inhibition modulates nociceptive signal transmission in spinal cord via affecting both presynaptic and postsynaptic elements. Damage to nerve and/or tissue (inflammation) often disrupts this regulation and causes pathological pain. The inhibition of postsynaptic spinal neurons had been intensively studied, while the inhibition of presynaptic terminals of peripheral sensory neurons was less focused due to the technical difficulty.

I generated transgenic mice, which specifically express GCaMP3, a genetically encoded calcium indicator, in nociceptors (SNS-Ai38) or all-sensory neurons (advillin-Ai38), to investigate the GABAergic presynaptic inhibition in spinal cord. GABA showed significant inhibitory effect on presynaptic nociceptor central terminals from intact mice. However, peripheral nerve injury and inflammation almost completely abolished this inhibition, mainly due to the NKCC1-dependent upregulation of intracellular [$Cl^-$]. Moreover, inflammation could facilitate GABAergic excitatory effect, which was only observed in spinal cord from SNS-Ai38 but not from advillin-Ai38. The Nociceptor-specific and all-sensory specific GABAA receptor knockout mice (SNS-$\beta3^{-/-}$ and advillin-$\beta3^{-/-}$) were generated to examine the function of presynaptic inhibition in vivo. Both SNS-$\beta3^{-/-}$ and advillin-$\beta3^{-/-}$ were more sensitive to thermal and mechanical stimuli compare to their wild type litter mates ($\beta3^{fl/fl}$). Yet difference between these two conditional knockout line was observed. Inflammation could not further the mechanical allodynia in SNS-$\beta3^{-/-}$ to the same level as it did in their $\beta3^{fl/fl}$ litter mates. Such difference was not observed in advillin-$\beta3^{-/-}$ mice and their litter mates. The difference between results from SNS-Cre and advillin-Cre generated transgenic mice after inflammation most likely was caused by their different Cre recombinase expression patter in peptidergic nociceptors according to immunohistochemistry study. This implies that part of peptidergic nociceptors are crucial for inflammation induced mechanical allodynia.

Overall, our data reveal that GABAergic presynaptic inhibition modulates thermal and mechanical spinal nociceptive processing. Nerve injury and peripheral inflammation can both result in nociceptor [$Cl^-$] elevation and disturb the presynaptic regulation. Furthermore, the malfunctioning presynaptic control caused by them contributes to pain modalities differently.

# 2 Introduction

## 2.1 Acute and pathological pain

International Association for the Study of Pain (IASP) defines pain as "an unpleasant sensory and emotional experience associated with actual or potential tissue damage, or described in terms of such damage"[1]. In healthy subjects, acute pain is generated by noxious stimuli applied to receptive field of nociceptors. In pathological state, pain feeling maybe more intensive when noxious stimuli is applied (hyperalgesia), and pain could be induced by non-noxious stimuli (allodynia) or even without any stimuli (spontaneous pain).

One major group of pathological pain is chronic pain, which had been estimated to affect one-sixth of the population[2]. Chronic pain, not like the protective and adaptive pain in common condition, does not carry any useful purpose. Approximately 20% of the adult European population[33] and at least 116 million US adults suffer from chronic pain[4]in both the physical and emotional way. The current annual cost in society is estimated more than €200 billion in Europe and $150 billion in USA[3]. However, 79 % sufferer still have chronic pain after treatment[5]. According to etiology, peripheral nerve system (PNS) originated chronic pain can be divided into 2 subgroups, neuropathic pain and inflammatory pain. Neuropathic pain is caused by a lesion or disease of the somatosensory nervous system[1]. Chronic inflammatory pain, on the other hand, is generated by lesion of non-neural tissue and the following inflammatory factors release.

## 2.2 Peripheral sensory neurons related to nociception

### 2.2.1 Properties of sensory neurons

Primary sensory neurons in somatosensory system are cells that sense the external or internal state of body, then encode the information into electrical signal and transmit it to spinal cord (SC). They are pseudo-bipolar neurons, which have their cell soma sit in ganglia in spine, projecting one branch of axon to periphery to sense stimuli, and another to spinal cord or brain stem to relay the encoded signal to central nervous system.

Primary sensory neurons are highly specialized. Various cutaneous stimuli, such as gentle touch, temperature, pinch etc, are conveyed by different sensory fibers. The thickest myelinated Aβ fiber neurons have a low mechanical threshold and respond to innocuous tactile stimulus. And the majority of thin myelinated Aδ fiber and unmyelinated C fiber neurons are nociceptors or thermoreceptors. Due to the fact that most Aδ and C fiber neurons are smaller than Aβ fiber neurons, size is commonly used to separate nociceptors from non-nociceptors. In mice, dorsal root ganglion (DRG) neurons can be generally classified into small (diameter < 25 μm, putative nociceptors) and large (diameter >= 25 μm, putative non-nociceptors).

### 2.2.2 Nociceptors classification based on molecular markers

Nociceptors can be further subdivided into peptidergic and non-peptidergic neurons. Peptidergic neurons are recognized by their expression of peptides, such as substance P and calcitonin gene-related peptide (CGRP). They require nerve growth factor (NGF) binding to their tyrosine receptor kinase A (TrkA) for development[6]. Capsaicin receptor, transient receptor potential vanilloid subfamily type 1 (TRPV1), is also expressed by many of these neurons[7,8]. Non-peptidergic nociceptors, on the other hand, switch their NGF-TrkA dependency to glial cell line-derived neurotrophic factor (GDNF)/Ret as animal matures[6], and are characterized by their binding of plant lectin isolectin B4 (IB4). Although peptidergic and non-peptidergic neurons are commonly used term to divide nociceptors, a notable overlapping of these 2 subpopulations had been reported by several studies[9–12].

## 2.3 Spinal cord anatomy related to nociception

The anatomy of spinal cord dorsal was thoroughly studied, and its neuronal components had been well reviewed[13,14]. The gray matter in spinal cord is divided into 10 laminae (I – X) from dorsal horn to ventral horn according to functionally distinct populations of neurons (**Figure 1**). Cutaneous sensory input is relayed into dorsal horn laminae including number I – V. Lamina I, which is composed of projection neurons and interneurons, is a thin layer located in the most superficial part of dorsal horn gray matter. It receives input from small myelinated Aδ fiber and unmyelinated C fiber. Multiple modalities signal such as warm, cold, itch, and pain is transmitted into this layer. Peptidergic nociceptors mainly target lamina I and therefore CGRP and substance P are usually used to mark this layer. Inhibitory and excitatory interneurons highly populate in laminae II and III. They receive information from primary afferents and finally pass it to projection neurons lie in Laminae I, IV and V. Although these interneurons also make connections to each other, and this network is believed to be important for input processing, the exact circuits for different modality inputs are still under investigated due to technical difficulty. Non-peptidergic nociceptors mainly send input into lamina II, thus, IB4 is commonly used to label this layer. The deeper layers of dorsal horn including laminae III, IV and V are the main targets of myelinated Aβ fiber, which transmit non-noxious tactile stimulus.

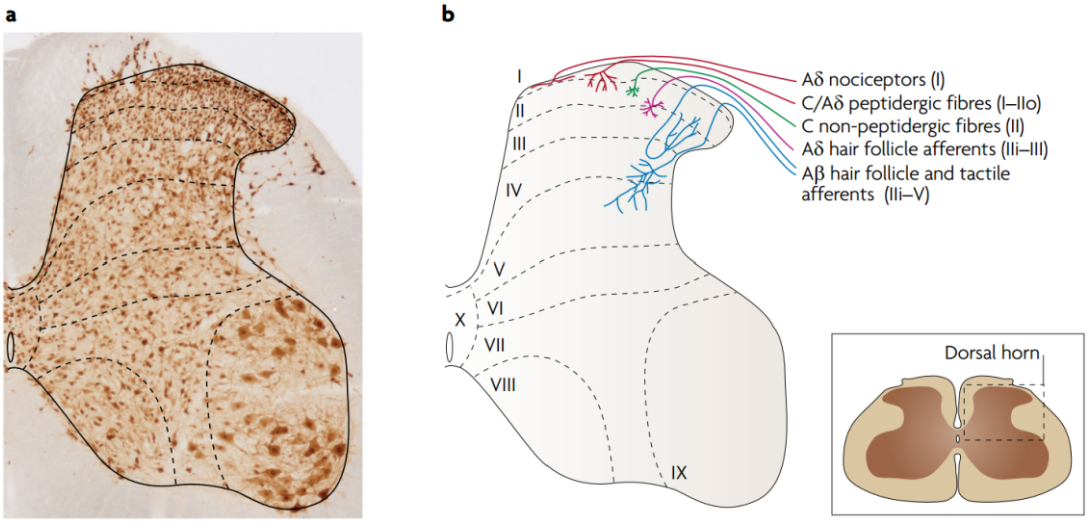


Figure 1: Spinal cord laminar organization and primary afferents innervation. Spinal cord gray matter is divided into 10 parallel laminae according to variations in the size and density of neurons. (**a**) Rat spinal cord section stained with NeuN antibody labeling neurons. Lamina I and Lamina II (also known as substantia gelatinosa) form superficial layer. Lamina II can be further divide into outer (IIo) and inner (IIi) layers. (**b**) The innervation pattern of primary afferents is well organized. Spinal dorsal horn (Laminae I – V) receive input from primary afferents. Deep layers, laminae III – V, of dorsal horn are innervated by Aβ fibers transmitting non-nociceptive signal. Aδ fibers end mainly in superficial layers with some extension into lamina III. Peptidergic fibers arborize within lamina I and IIo layers. Non-peptidergic fibers end in lamina II layer. (From Todd, 2010[14])

# 2.4 Spinal cord circuit gating nociception

## 2.4.1 Gate control theory.

Melzack and Wall published their Gate Control Theory (GCT) half century ago[15] (**Figure 2**). GCT suggests pain signal generation and transmission does not solely depend on pain specific pathway or is simply different from non-painful signal on magnitude described in previous published theories. It hypothesizes that a circuit lying in spinal cord dorsal horn, where signals from nociceptive and non-nociceptive afferents converge via interneurons, is able to dynamically modify the pain signal flow from PNS to central nerve system (CNS) like opening and closing a gate. When signal transmitted in large-diameter (non-nociceptive) afferents activates inhibitory interneurons, input from small-diameter (nociceptive) afferents to projection neurons is suppressed by these interneurons. In other words, the gate is closed. However, noxious stimuli gener-

ated activity in small-diameter afferents can turn the key to the opposite direction by inhibiting interneurons firing, and thus open the gate. In addition to external stimuli, descending input from brain is also applied to this circuit, which explains the role of emotion state on pain perceptive.

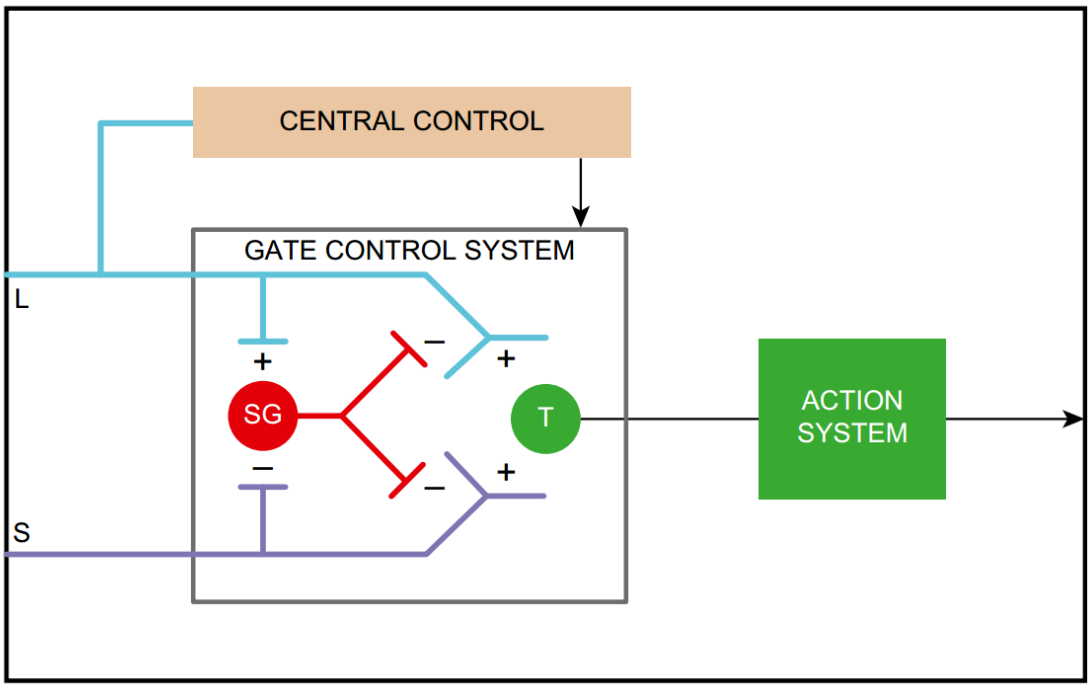


Figure 2: Gate control theory (GCT). The original idea introduced a neuronal circuit in spinal dorsal horn consisting of primary afferents (L, large diameter putative non-nociceptors; S, small diameter putative nociceptors), projection/transmission (T) cells, lamina II (substantia gelatinosa [SG]) interneurons, and supraspinal central control. The core element of GCT is SG interneurons which regulate signal transmission from large and small diameter primary afferents to T cells with presynaptic and postsynaptic connections. Non-nociceptive signal activates large diameter fibers, and in turn activates interneurons which inhibit signal transmission to T cells, i.e. closing the gate. Small diameter fibers can open the gate by inhibiting the output from interneurons. The successful delivery of signal to T cells depends on the balance between the input from large and small diameter fibers. (From Braz et al., 2014[13])

The critical component of GCT, inhibitory interneurons, were merely speculative cells when Melzack and Wall published their theory. Following studies proved the existence of these neurons in spinal dorsal horn with immunochemistry and electrophysiology[16–18]. Furthermore, Bohlhalter et at.[19] have displayed the distribution pattern of $GABA_A$ receptor in rodent spinal cord dorsal horn in detail. These studies showed evidence supporting GCT interneuron concept on cellular and molecular level.

### 2.4.2 Spinal GABA inhibition

gama Aminobutyric acid (GABA) is the major inhibitory neurotransmitter in the PNS as well as in the CNS. It is released from GABAergic neurons and binds to both of chloride permeable $GABA_A$ receptors and $GABA_B$ receptors, which are G protein coupled receptors. $GABA_A$ receptors mediate principal effect of GABA by increasing membrane permeability to chloride.

Mammalian $GABA_A$ receptors are ligand-gated chloride channels comprised of 5 subunits out of 19, including α1-6, β1-3, γ1-3, δ, ε, θ, π, and ρ1-3 (**Figure 3**). In spite of the large diversity of isoforms, the majority of $GABA_A$ receptors contain two α subunits, two

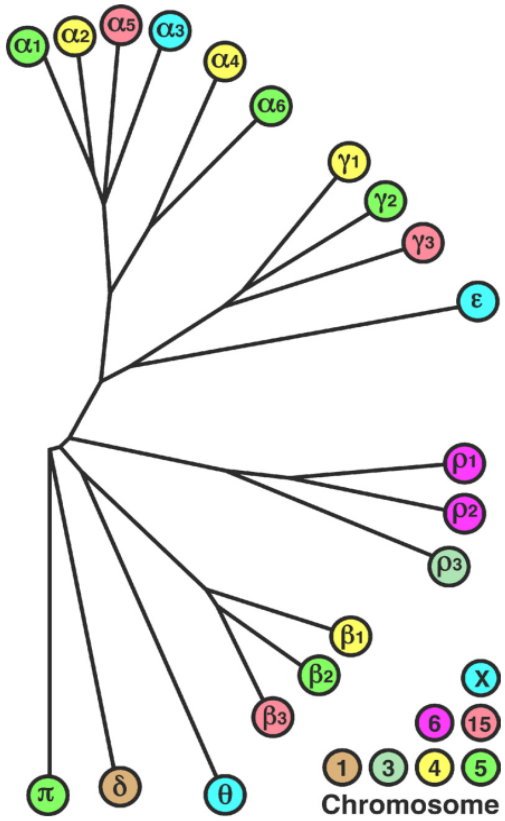


Figure 3: Dendrogram of 19 genes coding human $GABA_A$ receptor subunits. (From Sigel et al., 2012[20])

β subunits, and one γ subunit (**Figure 4**). They commonly have two GABA binding sites located at α/β subunit interface, and one bensodiazepine (an exogenous modulator) site located at α/γ subunit interface[20].The expression pattern of $GABA_A$ receptor

subunits have been mainly studied on mRNA level and protein level in rats and mice[19,21]. In these studies, α3, β2/3, and γ2 subunits exhibited widespread expression in the whole dorsal horn, and α1, α2 and α5 subunits were found to be expressed in multiple laminae, but distribute differently. Staining for α1 and α5 subunits appeared in laminae II-V, but was absent in lamina I. α2 subunits staining could be found in the whole dorsal horn, but most prominent in superficial layer laminae I and II. These subunits were suggested to be expressed on both spinal neurons and primary afferent terminals[19,21].

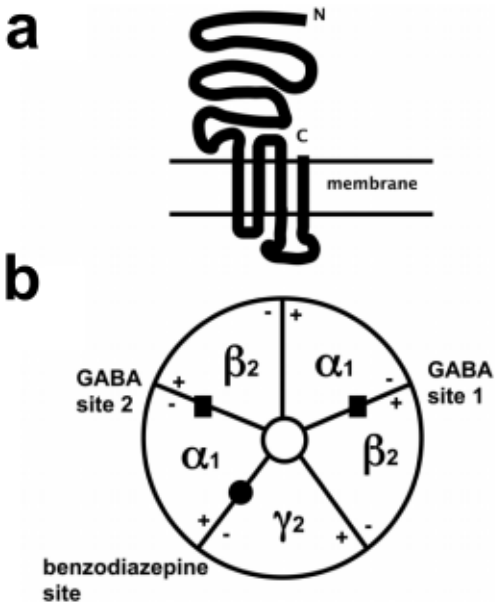


Figure 4: Schematic structure of $GABA_A$ receptor. (**a**) membrane topology of a single subunit. (**b**) Top view of a $GABA_A$ receptor subtype, α1β2γ2, with 2 GABA binding site between α and β subunits, and a bensodiazepine between a and γ subunits. The sidedness of the subunits is symbolized + and -. (From Sigel et al., 2012[20])

In rat spinal cord dorsal horn, ~25%, 30% and 40% neurons are GABAergic in lamina I, lamina II and lamina III respectively[22]. These GABAergic interneurons have various morphology and express diverse chemical markers[13,14]. Dual patch clamp recordings suggest GABAergic interneurons receive input from primary afferents[23]. Further, previous anatomical studies have revealed that GABAergic interneurons make contact to projection neurons[14]. However, the patterns of signal flow in the circuit composed of

primary afferents, interneurons (inhibitory and excitatory) and projection neurons are far from clear.

Intrathecal injection of GABA or positive allosteric $GABA_A$ receptor modulator benzodiazepine (BZD), such as diazepam (DZP), shows anti-nociceptive effect and rescues nerve injury induced chronic pain via enhancing spinal GABAergic inhibition[24–28]. Prohibiting GABAergic inhibition exhibits opposite effect, i.e. increasing pain behavior when nociceptive stimuli applied (hyperalgesia) or even generating pain behavior with only non-nociceptive stimuli applied (allodynia)[24,29–33]. These pharmacological and behavior studies suggested a spinal inhibition in pain perception regulation, which is most possibly carried by GABAergic interneurons.

### 2.4.3 Postsynaptic inhibition

Original GCT only proposes pre-synaptic inhibition for gating information flow, yet the postsynaptic regulation on projection neuron is not excluded. In fact, the information flows from primary afferents to interneurons, and finally to projections had been proved[13,14,28].

The effect of $GABA_A$ receptor activation depends on intracellular chloride concentration. If the intracellular $[Cl^-]$ is high enough to cause the reversal potential of chloride ($E_{Cl}$) positive to neuron's membrane potential ($V_m$), the opening of chloride permeable pore in $GABA_A$ receptor results in chloride efflux, which consequently depolarizes the neuron. If the $[Cl^-]$ is so low that the $E_{Cl}$ is negative to neuron's $V_m$, activation of $GABA_A$ receptor causes hyperpolarization of the neuron due to the chloride ion influx. The $[Cl^-]$ is mainly regulated by various cation-chloride cotransporters (CCC). In mammalian neurons, the accumulation of chloride is mainly driven by Na-K-2Cl co-transporter (NKCC1), and the extrusion is largely mediated by K-Cl co-transporter 2 (KCC2). In CNS, neurons have high NKCC1 expression but very low KCC2 expression during development[34]. However, in mature animal, accompanied with downregulation of NKCC1, the increase of KCC2 reduces the $[Cl^-]$, and thus hyperpolarizes the $E_{cl}$, which is low enough to generate chloride influx when $GABA_A$ receptor is open[34]. In intact mature animal, the postsynaptic neurons, i.e. CNS neurons in spinal dorsal horn, are inhibited by GABA with this mechanism.

### 2.4.4 Pre-synaptic inhibition

Compare to the postsynaptic inhibition, the story of pre-synaptic side, primary afferents, is different. Unlike CNS neurons, DRG neurons keep high expression level of NKCC1 in adults, while KCC2 is expressed at very low level or even absent[35–38]. Therefore, DRG neurons in adults maintain a high intracellular chloride concentration which cause the reversal potential of chloride ($E_{Cl}$) more depolarized than resting membrane potential[39]. Consequently, when GABA binding opens central pore of $GABA_A$ receptor, the outflow of chloride induces depolarization rather than hyperpolarization. It has been decades that GABA is considered to be the important transmitter to induce presynaptic inhibition via generating primary afferent depolarization (PAD), which reduces excitatory transmitter release from primary afferent central terminal[40]. Several mechanisms had been proposed to explain the inhibitory effect of PAD[41]. Depolarization on nociceptor central terminals may cause inactivation of voltage-gated calcium channels, and thus reduces calcium influx and transmitter release. Voltage-gated sodium channels may also be inactivated by PAD, together with shunting effect by opening $GABA_A$ receptor, propagation of action potential towards primary afferents terminal could be hampered.

## 2.5 Alterations of inhibitory synaptic transmission in pathological states

Pain perception is not generated by a plain signal relay induced by noxious stimuli, but a redundant and dynamic system, in which the transmission of noxious stimuli generated signal is regulated by both internal (from brain) and external (from non-noxious and/or noxious stimuli) input via multiple pathways involving various types of cell. Malfunctioning component(s) may break the balance in this system and interrupt coding of somatosensory stimuli, thus causing pathological pain, such as hyperalgesia and allodynia[28,42–44]. Previous studies showed intrathecal injection of $GABA_A$ receptor antagonist, bicuculline, resulted a dose-dependent allodynia and hyperalgesia[45,46]. Further, Baba et al. reported that bicuculline effectively facilitated primary afferents evoked polysynaptic EPSCs in lamina II neurons[47]. And this effect of bicuculline was dramatically diminished after nerve injury and inflammation[47,48]. Another study observed primary afferents evoked IPSCs in lamina II neurons was reduced after various types of

nerve injury, and $GABA_A$ receptor-mediated IPSCs was decreased as well[49]. These evidence suggests $GABA_A$ receptors dependent inhibition in spinal dorsal horn is altered by nerve injury and this may contribute to allodynia and hyperalgesia caused by nerve injury and inflammation.

### 2.5.1 Change of postsynaptic inhibition

Because $GABA_A$ receptors mediated inhibition has different mechanisms for presynaptic central terminals and postsynaptic spinal neurons. The alterations caused by nerve injury and/or inflammation may also differ. For spinal neurons, Coull et al. reported that $[Cl^-]$ in lamina I neurons was elevated due to the reduction of KCC2 after nerve injury, and the subsequently shifted reversal potential of chloride greatly diminished GABAergic inhibitory controls or even switch it to exciatation[50]. The same group afterwards revealed the role of microglia in this change of postsynaptic inhibition[51]. In brief, after nerve injury, microglias release brain derived neurotrophic factor (BDNF) upon the stimulation of ATP, the binding of BDNF on lamina I neurons tyrosine receptor kinase B (TrkB) receptors causes downregulation of KCC2 and the following $[Cl^-]$ elevation[51] (**Figure 5**).

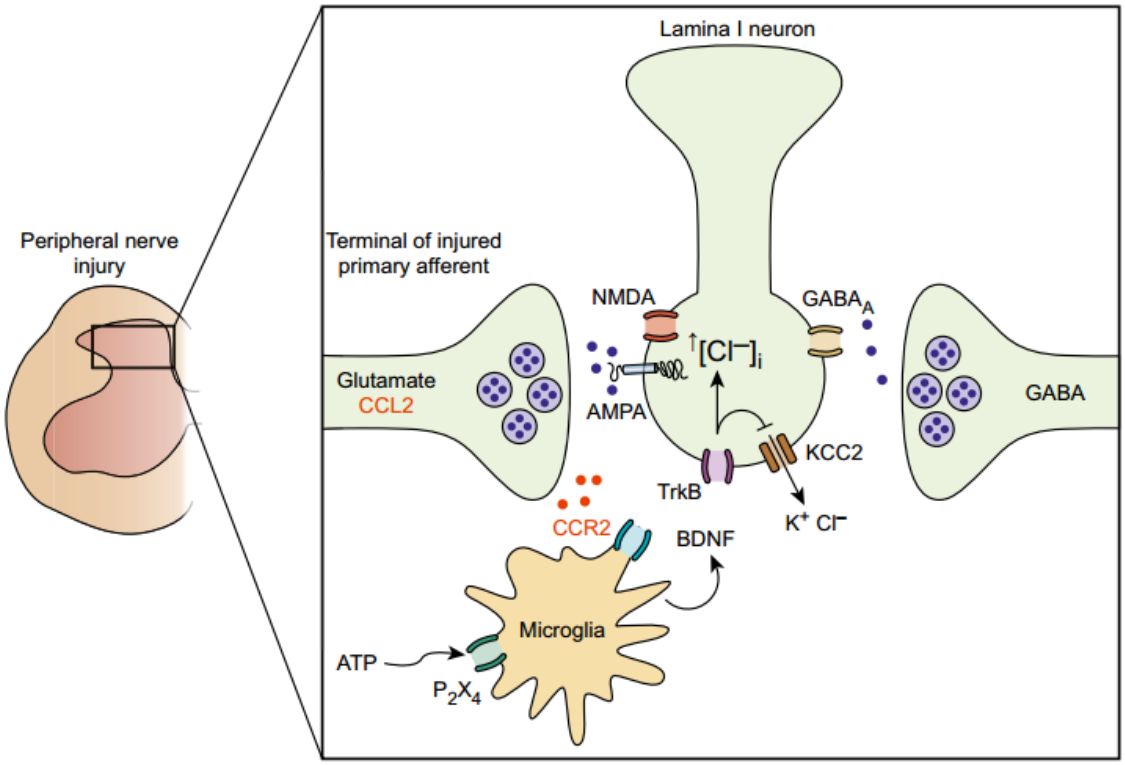


Figure 5: Postsynaptic change in neuropathic pain. Peripheral nerve injury activates spinal microglia via ATP and/or chemokine ligand 2 (CCL2). The activated microglia release BDNF, which binds to TrkB receptors on lamina I neurons. BDNF-TrkB signaling downregulate chloride co-transporter KCC2, which causes the rise of intracellular [$Cl^-$] in lamina I neurons. This [$Cl^-$] change disrupts the $GABA_A$ receptor mediated postsynaptic inhibition, which generates inward flow of $Cl^-$ and hyperpolarizes the postsynaptic neurons in physiological condition. (From Braz et al., 2014[13])

### 2.5.2 Change of presynaptic inhibition

Due to the technical difficulty, the physiological recording of presynaptic inhibition and its change in pathological condition were mainly studied by recording the central stump of a cut filament of a dorsal root. Willis had reviewed that when PAD reached firing threshold, it could generate a back-traveled action potential from primary afferent terminal to peripheral side, which was named as dorsal root reflex (DRR)[52]. DRRs were reported to increase after inflammation, and increased DRRs caused release of neurotransmitters which generated neurogenic inflammation on peripheral side and increased excitability of postsynaptic neurons on central side[52]. Possible reasons for the increase in DRRs might be the upregulation of GABAergic system in spinal dorsal horn or the activity increase of NKCC1, both of which may intensify the chloride outflow gen-

erated membrane depolarization. Funk et al. reported an upregulation of intracellular [$Cl^-$] of DRG neurons, which might be contributed by enhanced NKCC1 activity, after inflammatory mediators treatment[53]. However, whether pathological conditions, such as nerve injury and peripheral inflammation, has the similar impact on DRG neuron [$Cl^-$] remains unclear. In addition, the influence of the elevated intracellular [$Cl^-$] on the physiological function of presynaptic terminals has not been discovered yet.

## 2.6 Objectives

DRG neurons respond to cutaneous stimulation and convey the information to central nervous system in spinal dorsal horn. This input information is then processed by postsynaptic interneurons and projection neurons there. Studies had confirmed GABAergic spinal inhibition, and the function of postsynaptic inhibition in physiological and pathological conditions had been well characterized. However, the presynaptic side, central terminals of primary afferents, was less focused due to the technical difficulty. Electrophysiological technique such as patch clamp is commonly used to study neuron activity. The function of GABA on spinal dorsal horn neurons were well investigated with this method. Unfortunately, it can not be applied on presynapses. Besides, calcium imaging, which is another frequently used technique for live cell study, were prevented from recording presynapse-only signals due to the difficulty of mass labeling central terminals in acute spinal cord slices. Cre-Lox recombination makes it possible to specifically express genetically encoded calcium indicator (GECI) in sensory neurons with proper transgenic mouse lines, thus allowing calcium recording on central terminals of primary afferents.

The objective of this project includes: (1) Generating conditional GECI expressing mice and use them to examine the proposed GABAergic presynaptic inhibition; (2) Investigating whether the proposed presynaptic inhibition is affected by nerve injury and peripheral inflammation.

# 3 Methods

## 3.1 Animal

Experiments were carried out in adult C57BL/6 and several lines of transgenic mice (male, aged 6-12 weeks, 20-25g in weight). Mice were housed 2 to 5 per cage, and maintained in a temperature and humidity-controlled room on a 12/12h light/dark cycle with access to rodent chow and water ad libitum. All experiments were conducted according to the guidelines of German Animal Protection Law.

### 3.1.1 Transgenic mice

Transgenic mice expressing Clomeleon[54], a ratiometric $Cl^-$ indicator, under the control of the Thy1 promoter were used for chloride imaging.

Two Cre mice lines were used for the study. Cre recombinase is expressed under the regulatory elements of mouse *Scn10a* gene, and of mouse *advillin* gene in SNS-Cre[55] and advillin-Cre[56] mice lines respectively. The former transgenic mice line is from the group of Dr. Kuner, and the latter is from the group of Dr. Heppenstall. *Scn10a* gene encodes the tetrodotoxin-resistant Nav1.8 sodium channel which is mainly expressed nociceptors[57], while *advillin* gene encodes the homonymous actin regulatory/binding protein restrictedly expressed in DRG neurons and superior cervical ganglia neurons[58–60].

Ai38 (#014538) and Gabrb3-loxP mice (B6;129-Gabrb3$^{tm2.1Geh1Geh}$/J, #008310) are from the Jackson Laboratory. In Ai38 mice, a loxP-flanked STOP cassette prevents transcription of the downstream GCaMP3 fusion gene until exposed to Cre recombinase. Offspring of Ai38 and Cre mice will have STOP cassette deleted in Cre expressing tissue, and express calcium indicator protein, GCaMP3, which has low EGFP fluorescence in the absence of calcium, and brighter fluorescence when binded by calcium. Gabrb3-loxP mice possess loxP sites on either side of exon 3 of gene encoding $GABA_A$ receptor β3 subunit. When Gabrb3-loxP mice are bred to Cre expressing mice, Offspring will have exon 3 deleted in Cre-expressing cells.

SNS-Ai38 and advillin-Ai38 were generated by breeding SNS-Cre mice and advillin-Cre mice to Ai38 mice respectively. SNS-$\beta3^{-/-}$ and advillin-$\beta3^{-/-}$ mice were generated by breeding SNS-Cre mice and advillin-Cre mice to Gabrb3-loxP mice respectively.

Mouse genotype was verified by PCR using primers as follows: SNS-cre Forward: 5'-GAA AGC AGC CAT GTC CAA TTT ACT GAC CGT AC-3'; Reverse: 5'-GCG CGC CTG AAG ATA TAG AAG A-3'. Advillin-cre Forward: 5'- GCA CTG ATT TCG ACC AGG TT-3'; Reverse: 5'-GAG TCA TCC TTA GCG CCG TA-3'. Ai38 Mutant Forward: 5'-CTT CAA GAT CCG CCA CAA CAT CG-3'; Mutant Reverse: 5'-TTG AAG AAG ATG GTG CGC TCC TG-3'. Ai38 Wild type Forward: 5'-CCA AAG TCG CTC TGA GTT GTT ATC-3'; Wild type Reverse: 5'-GAG CGG GAG AAA TGG ATA TG-3'. Gabrb3-loxP Forward: 5'-ATT CGC CTG AGA CCC GAC T-3'; Reverse: 5'-GTT CAT CCC CAC GCA GAC-3'.

## 3.2 Induction of chronic pain

Chronic constriction injury (CCI)[61] was used to induce neuropathic pain in mice. In brief, animal was deeply anesthetized with 2 % isoflurane (CP-Pharma, Germany). Skin incision was made on one side after hair shaved. Sciatic nerve at the level of the right mid-thigh was exposed by tearing connective tissue between the gluteus superficialis and biceps femoris muscles. Four loose silk ligatures (4/0) were placed (with ~0.5 mm spacing) around the sciatic nerve. Ligatures were tied until they elicited a brief twitch in the respective hind limb[62]. The wound was closed with sutures in the muscle and staples in the skin.

Inflammatory pain in mice was induced by intradermal injection of Complete Freud's Adjuvant (CFA), which consists of inactive Mycobacterium tuberculosis in mineral oil. Animal was deeply anesthetized with 2 % isoflurane. Syringe with 25 gauge needle was inserted approximately 2 mm, bevel up, into the metatarsal region of hindpaw and 20 µl CFA was slowly delivered. Needle was held still for 10 s to keep pressure before withdrawing (adapted from Fehrenbacher et al.[63]).

Animal used for CCI or CFA injection were placed back to cage after surgery and allowed to recover for at least 24 h before any behavior test.

## 3.3 Behavior

Animal underwent CCI or CFA injection were examined by behavior test to verify the effect of injury or inflammation. Animal were habituated on behavior test setups for at lease 30 min 1 day prior to baseline tests, which were performed before surgery. 2-day later, same tests were applied again and the effect of surgery was evaluated by comparing these results with baseline data. All tests were taken in the morning. Mechanical sensitivity was measured with von Frey hairs from 0.008 to 1.4 g (0.008, 0.02, 0.04, 0.07, 0.16, 0.4, 0.6, 1, and 1.4 g)[64]. Animal were placed in transparent plastic box sitting on a metal mesh. The setup allows experimenter to observe animal behavior while applying mechanical stimulation with von Frey hair. The hair was lifted perpendicular to the mid-plantar surface of hind paw until slightly bended, and held for about 6 s. A quick withdraw of stimulated hind paw or immediate flinching upon removal of the hair were considered a positive response. Other cases, such as slow withdraw, animal walking away etc, required a repeat test. 5 tests were applied with each hair with a interval of at least 5 s (adapted from Chaplan et al.[64]).

Plantar test with hargreaves apparatus (ugo basile, Italy) was employed to examine the sensitivity of animal to thermal stimulation. Animal were placed in the same type of plastic box used for von Frey test, but on glass pane instead of metal mesh. A movable infrared generator with the intensity of 270±10 mW/cm$^2$ under the glass pane applied infrared heat stimulus and measured hind paw withdraw latency automatically. 3 or 4 measurement were taken for each animal with an interval of 5 min to avoid repeated heat stimulation generated.

## 3.4 Cell culture

Mouse L4 and L5 DRGs were dissected and collected in-ice cold phosphate-buffered saline (PBS). DRGs were washed once with PBS prior to incubation with 2 different enzymes, collagenase and trypsin which were used to dissociate DRG cells from each other. DRGs were first treated with 1 ug/ml collagenase type IV (Sigma, Germany) in 1 ml of PBS at 37 °C for 40 min. The supernatant was removed, and DRGs were incubated with 1 ml of 0.05 % trypsin (Sigma, Germany) in PBS for another 30 min. The supernatant was removed and DRG medium consisting of DMEM/Hams-F-12, 8 mg ml$^{-1}$

glucose, 100 U $ml^{-1}$ penicillin, 100 μg $mg^{-1}$ streptomycin, and 10% heat inactivated horse serum, was added. DRGs were gently dissociated with pipette to obtain single cell suspension and centrifuged at 800 RPM for 5 min. The supernatant was removed, and the cells were resuspended in DRG medium and seeded on poly-lysine (500 μg $ml^{-1}$, at 37 °C for 18 h) and laminin (20 μg $ml^{-1}$, at 37 °C for 1 h) coated coverslips. After 3-4 h, additional DRG medium was added to cells. Cells were cultured for 12-24 h at 37 °C in incubator.

## 3.5 Acute spinal cord slice

Animal was deeply anesthetized with ketamin : xylazine : saline (1.5 : 0.75 : 7.75). The total volume of anesthetic is 1% of animal weight. The anesthetic was delivered by intra-peritoneal injection in 3 divided doses at 5 min interval. ½ of the total volume was administrated for the first dose, ¼ of total volume was administrated for the second and third doses. Animal back was shaved, and skin incision was made along lumbar vertebrae. Spinal laminectomy was applied to expose lumbosacral spinal cord innervated by L4 and L5 spinal nerve. This part of spinal cord was isolated after pia mater removed, and placed in cold Prep-Ringer solution (2–4 °C; 87mM NaCl, 1.25mM $NaH_2PO_4$, 25mM$NaHCO_3$, 2.5mM KCl, 7mM $MgCl_2$, 0.5mM $CaCl_2$, 25mM glucose, 75mM sucrose). Next, it was embedded in 2% low melting agarose (Bio-Rad Laboratoried, CA 94547). A 300 μm transverse slice was cut from the embedded spinal cord on a vibrating blade microtome (Leica VT1200, Leica, Germany). The spinal cord slice was stored on a cellulose nitrate filter (Sartorius Stedim Biotech GmbH, Germany) perfused with Ringer solution saturated with 95% $O_2$ and 5% $CO_2$ at room temperature following 45–60 min perfusion at 33–34 °C for slice recovery.

## 3.6 Chloride imaging

Clomeleon is a fusion protein consisting of $Cl^-$ insensitive CFP and $Cl^-$ sensitive YFP[65]. Fluorescence resonance energy transfer (FRET) occurs between two fluorophores due to close spatial proximity. Quenching of YFP by $Cl^-$ causes the ratio of fluorescence

emission to change in response to $[Cl^-]$[66]. Thus, Clomeleon can be used as a ratiometric indicator for $Cl^-$.

L4 and L5 DRG were removed from clomeleon mice and stored in oxygenized Ringer's solution (124 mM NaCl, 1.25 mM $NaH_2PO_4$, 26 mM $NaHCO_3$, 3 mM KCl, 2 mM $MgCl_2$, 2 mM CaCl2, 10 mM glucose) at room temperature. A commercial 2-photon setup (LaVision, Germany) consisting of an upright microscope (Olympus BX51WI) and imaging software ImSpector Pro (LaVision, Germany) was used for ratiometric $Cl^-$ imaging. A 1.0 numerical aperture 20× water immersion lens (Plan- APOCHROMAT, Zeiss) was used for the experiment. Fluorescence was elicited using a Ti: Sapphire laser (Mai Tai HP DeepSee, Spectra-physics, Mountain View, CA) tuned to 870 nm. CFP signals (filter: 480BP 36) and YFP signals (filter: 537 BP 42) were separated by a beamsplitter (500 LP) and recorded simultaneously. Images were acquired from Clomeleon-positive cells in whole DRG. The data were analyzed offline with ImageJ (http://rsbweb.nih.gov/ij/) and Matlab (MathWorks, Natick, Massachusetts). The fluorescence intensity of YFP ($F_{YFP}$) and CFP ($F_{CFP}$) and their associated background signal ($B_{YFP}$ and $B_{CFP}$) of DRG neurons were read out in ImageJ. The ratio of YFP and CFP intensity ( $R=\frac{F_{YFP}-B_{YFP}}{F_{CFP}-B_{CFP}}$ ), which is negatively correlated to the $Cl^-$ concentration, and related statistics were calculated in Matlab.

## 3.7 Perforated patch clamp

Recordings were made from DRG neurons using fire-polished glass pipette with a resistance of 3–7 MΩ. Extracellular solution contained 150 mM NaCl, 5 mM KCl, 2 mM $CaCl_2$, 1 mM $MgCl_2$, 10 mM glucose and 10 mM HEPES (pH 7.4). Internal solution used to fill glass pipette contained 140 mM KCl, 5 mM EGTA and 10 mM HEPES (pH 7.3). Lucifer Yellow and gramicidin were freshly added into internal solution prio to recording to reach to final concentration 0.1% and 50 - 100 μg $ml^{-1}$ respectivily. Membrane current and voltage were amplified and acquired using EPC-10 amplifier (HEKA Electronik GmbH, Germany) sampled at 10 kHz. The formation of gramicidin perforation were monitored by the Patchmaster programme (HEKA Electronik GmbH, Germany) and the measurement was started until serious resistance dropped to < 40 MΩ. 1 mM GABA was applied to recorded neuron at a series of holding potentials (-60, -40, -20, 0

and 20 mV). Data was analysed with Fitmaster software (HEKA Electronik GmbH, Germany). The reversal potential of GABA-induced current ($E_{Cl}$) was calculated using a series of current amplitudes recorded at various holding potentials. The conductance of $GABA_A$ receptors was calculated according to ohm's law.

# 3.8 Calcium imaging

## 3.8.1 Imaging of cultured DRG neurons

Briefly, fluorescence microscopy was done on an Observer A1 inverted microscope (Zeiss, Germany) using a 0.8 numerical aperture 25× water immersion objective (Zeiss, Germany), and a 175W Xenon lamp as a light source. Before imaging, DRG neurons were incubated with 2 mM Fura-2 in extracellular solution containing 150 mM NaCl, 5 mM KCl, 2 mM $CaCl_2$, 1 mM $MgCl_2$, 10 mM glucose and 10 mM HEPES at 37 °C for 40 min and washed with extracellular solution at 37 °C for another 30 min. When IB4 marker (Sigma, Germany) was used, cells were incubated with 2 μg $ml^-$ IB4 in extracellular solution at 37 °C for 20 min directly after Fura-2 incubation.

Excitation light was passed either through a 340-BP 30 filter or a 387-BP 16 filter. Two filters were switched by an ultra-high speed wavelength switcher Lambda DG-4 (Sutter, Novato, CA). Emissions elicited from both excitation wavelengths were passed through a 510-BP 90 filter and collected by a charge-coupled device camera (Zeiss). Different solutions were applied by multi barrel perfusion system (WAS02, DITEL, Prague). AxioVision software (Zeiss) was used to record image data. After background ($B_{340}$, $B_{380}$) subtraction in each channel ($F_{340}$, $F_{380}$), the ratio ($R_{340/380}$) of fluorescence elicited by excitation light at wavelength 340 nm and 380 nm, was calculated: $R=\frac{(F_{340}-B_{340})}{(F_{380}-B_{380})}$ . A high KCl extracellular solution was used to stimulate neurons and generate calcium transient. It contains 115 mM NaCl, 40 mM KCl, 1 mM MgCl2, 2 mM CaCl2, 10 mM glucose and 10 mM HEPES. Drugs were perfused in either extracellular solution or high KCl extracellular solution. If the 4th highest R was larger than threshold $\left(R_0+5\,std_{R_0}\right)$ , the cell was considered to show a calcium transient in response to a stimulus. $R_o$ is the mean value of baseline ratio.

Data were analyzed by using AxioVision and Matlab (MathWorks, Natick, Massachusetts).

### 3.8.2 Imaging of acute spinal cord slices

Spinal cord slice was transferred to recording chamber of the 2-photon setup and perfused with oxygenized Ringer's solution. 2-photon imaging setup is same as for chloride imaging experiments, except the laser was tuned to 920 nm. GCaMP3 signal (filter: 562 BP 40) was recorded. Time series of images were acquired from the spinal cord dorsal horn. Superficial layer of dorsal horn (not deeper than 100 mm from the spinal cord dorsal outline) was imaged. Scanning frequency was 1 Hz. A high KCl Ringer's solution was used to stimulate neurons. It contains 87 mM NaCl, 1.25 mM NaH2PO4, 26 mM NaHCO3, 40 mM KCl, 2 mM MgCl2, 2 mM CaCl2, 10 mM glucose. To avoid the effect of activation of glutamate receptor, 10 mM NMDA (N-methyl-D-aspartate) antagonist (RS)-CPP (Tocris Bioscience, UK) and 10 mM AMPA (a-amino-3- hydroxy-5-methyl-4-isoxazolepropionic acid) antagonist CNQX (abcamBiochem- icals, UK) were added into high KCl Ringer's solution. Ringer's solution with 1mM GABA was used to investigate neuron response to GABA. Short time perfusion with Ringer's solution with GABA followed by high KCl Ringer's solution with CPP, CNQX and GABA was used to investigate influence of GABA on neuron excitation. All chemicals were either perfused to the whole recording chamber or to the adjacent area of recording field (< 500 μm).

2-photon live imaging data was exported from LaVison customized version of ImSpector software (http://www.imspector.de), and was analyzed offline with ImageJ and Matlab (MathWorks, Natick, Massachusetts). Image stacks underwent sample moving correction with ImageJ plugin, Image Stabilizer (K. Li, "The image stabilizer plugin for ImageJ," http://www.cs.cmu.edu/~kangli/code/Image_Stabilizer.html, February, 2008.), utilizing Lucas–Kanade method. Each recording was segmented into 5 x 5 μm square shape regions of interest (ROIs). Average of all pixels' intensity in each ROI from a single frame was calculated and used as fluorescence intensity (F). All data points were also smoothed by using LOESS method, which is a local regression using weighted linear least squares and a 2$^{nd}$ degree polynomial, with a span of 10% of data points, and collected as FS.

Mean value of F and FS from 30 frames prior to simulation were used as baseline fluorescence intensity ($F_o$ and $FS_o$). 180 frames following stimulation were used for re-

sponse analysis. When the maximum F ($F_{max}$) from these 180 response frames exceeded threshold $\left(F_0+5\,std_{F_0}\right)$ by $\frac{\left(F_{max}-F_{min}\right)}{2}$ while the maximum FS ($Fs_{max}$) exceeded threshold $\left(FS_0+2\,std_{FS_0}\right)$ by $\frac{\left(FS_{max}-FS_{min}\right)}{2}$, a ROI was considered to have a positive response. $std_{F_0}$ And $std_{SF_0}$ are the standard deviations of $F_o$ and $SF_o$ respectively. $F_{min}$ and $FS_{min}$ are the minimum F and FS from response frames. $F_{max}$ was converted to ΔF using the formula $\Delta F=F_{max}-F_0$. In a given ROI, GABA is considered to decrease high KCl evoked calcium transient and have inhibitory effect when $\frac{\left(\Delta F_{KCl}-\Delta F_{K\,Cl+GABA}\right)}{\Delta F_{KCl}}>0.5$, or there is no response to high KCl Ringer's solution combine with GABA. When $\frac{\left(\Delta F_{KCl+GABA}-\Delta F_{KCl}\right)}{\Delta F_{KCl}}>0.5$, or the ROI responds to high KCl Ringer's solution with GABA, but not high KCl Ringer's solution alone, GABA is considered to facilitate calcium transient evoked by high KCl and be excitatory. If $\frac{\left|\Delta F_{KCl}-\Delta F_{KCl+GABA}\right|}{\Delta F_{KCl}}\leqslant 0.5$, GABA influence is categorized as no influence.

In GABA alone stimulation piece, only ROIs showed positive responses in KCl stimulation piece from the same trial were used for analysis.

## 3.9 Immunohistochemistry

Mice were deeply anesthetized with isofluorane, and were perfused with 4% paraformaldehyde (PFA) in PBS pH 7.4. DRGs and spinal cords were then dissected from perfused mice and post-fixed with 1% and 4% PFA overnight respectively. 10% sucrose in PBS 1h, 20% sucrose in PBS 1h, and 30% sucrose in PBS overnight incubation were applied to all tissue. For NKCC1 staining, DRGs and spinal cords were isolated

from non-perfused animal and fixed with 2% PFA in PBS pH 7.4 overnight and then incubated in 25% sucrose-hanks in PBS overnight.

O.C.T. compound (Tissue-tek, Sakura Finetek) were used to embed tissue and bind to specimen block of cryotome (Leica) for slicing. 10 - 14 µm thick samples were mounted on SuperFrostr® Plus microscope slides (R. Langenbrinck Labor- u. Medizintechnik) and stored at -20 °C.

For CGRP and IB4 staining, the sections were permeablized and blocked with 0.1% Triton X-100 (Roth) and 5% donkey serum in PBS for 1 h, and incubated with primary antibody anti-calcitonin gene-related peptide (CGRP) (goat, ab36001) diluted 1:1000, or isolectin GS-IB4 (griffonia simplicifolia, Alexa Fluor® 568 conjugated, I21412) diluted 1:400 in PBS with 0.05% Triton X-100 and 5% donkey serum at 4 °C for 18 h. Secondary antibody donkey-anti-goat (cy3 conjugated) 1 h incubation at room temperature was used to label CGRP antibody. To label NKCC1, the sections were permeablized 3 min with 0.1% Triton X-100 (Sigma-Aldrich) in PBS, blocked 30 min in 1% BSA (Sigma-Aldrich) in PBS, and incubated with primary antibody anti-NKCC1 (goat, Santa Cruz Biotechnology) diluted 1:500 at 4 °C for 18 h followed by 1h secondary antibody, donkey-anti-goat (cy3 conjugated) incubation at room temperature.

Coverslips were mounted with vectashield mounting medium (Vector Laboratories, Inc. Burlingame). Samples were imaged with epifluorescence microscope (Zeiss) equipped with fluorescence lamp and monochrome camera. The acquired images were analyzed using ImageJ (NIH, Bethesda, MD; USA).

## 3.10 Real-time PCR

Total RNA was extracted from DRGs using peqGOLD TriFast (peqlab) following the manufacturer's protocol. RNA was determined with a peqlab NanoDrop ND-1000. Complementary DNA was synthesized from 5 mg of total RNA using the SuperScript TM II Reverse Transcriptase kit (Invitrogen, Carlsbad, CA, USA) with oligo(dT) primers, according to the manufacturer's protocol.

The volume of each reaction was 20 µl composed of 10 µl ABsolute QPCR SYBR Green ROX Mix (Thermo Scientific), 1 µl 1:5 diluted cDNA and 1 µl forward and reverse primers. 3 replications were prepared for every test. The real-time PCRs were per-

formed on an ABI 7500 Real Time PCR System (ABS/ Life Technologies). Primers used were listed in **Table 1**.

Relative amounts of mRNA were determined using comparative CT method[67]. In brief, $C_T$ of each reaction was readout, $\Delta C_T$ was calculated using $\Delta C_T = C_T - C_{T(GAPDH)}$. $C_{T(GAPDH)}$ is the $C_T$ value of housekeeping gene GAPDH. Then $\Delta\Delta C_T$ was calculated with $\Delta\Delta C_T = \Delta C_T - \Delta C_{T(control)}$. $\Delta C_{T(control)}$ is the $\Delta C_T$ of the tested gene from control sample. Finally, the fold change was calculated as $2^{-\Delta\Delta C_T}$.

| **Gene** | **Forward (5' - 3')** | **Reverse (5' - 3')** |
|---|---|---|
| Gabra1 | CCAAGTCTCCTTCTGGCTCAACA | GGGAGGGAATTTCTGGCACTGAT |
| Gabra2 | TTACAGTCCAAGCCGAATGTCCC | ACTTCTGAGGTTGTGTAAGCGTAGC |
| Gabra3 | CAAGAACCTGGGGACTTTGTGAA | AGCCGATCCAAGATTCTAGTGAA |
| Gabra5 | CGCGTAGGCGTCAAGATCAAGT | TCATAGCCATCCAAGAGTCCGTC |
| Gabrb3 | GCC AGC ATC GAC ATG GTT TC | GCG GAT CAT GCG GTT TTT CA |
| NKCC1 | TCC TCA GTC AGC CAT ACC CAA A | ATC CCG AAC AAC ACA CGA ACC |
| BDNF | AGT CTC CAG GAC AGC AAA GC | TCG TCA GAC CTC TCG AAC CT |
| Trkb truncated | ATC TGC AAC GAC GAT GAC TCT G | GTA GCA CTC GGC AAG GAA AAC T |
| Trkb full-length | CCC AAA TTA CCC TGT AGT CCT CT | ACC CAT CCA GTG CGA TCT TAT |
| GAD65 | CGC ATT GCC AAA CAA CTC TAA A | AGT CTG CTG CTA ATC CAA CCA T |
| GAD67 | GCC ACA AAC TCA GCG GCA TA | CCC GGT GTC ATA GGA GAC GT |
| GAT1 | CTC CAA CTA CAG CCT GGT CAA TAC | GCA GAA ATA CAC GAG CAC CCA |
| GAPDH | ACC CTG TTG CTG TAG CCG TAT CA | TCA ACA GCA ACT CCC ACT CTC CA |

Table 1: Sequence of primers used for real-time PCR experiments.

# 4 Results

## 4.1 GABAergic presynaptic modulation after peripheral nerve injury

### 4.1.1 Increased [$Cl^-$] in DRGs after nerve injury

Chronic constriction injury (CCI) of sciatic nerve was reported to generate various pathological symptoms, such as mechanical allodynia, mechanical and thermal hyperalgesia, and therefore is widely used as an animal model to study neuropathic pain[44]. The effect of CCI in mouse had been assessed by my colleague with von Frey and plantar tests and confirmed that both mechanical and thermal pain behaviors were induced in this injury model[61]. The sensitivity of injured mice reached to peak 2 days after CCI, and lasted at least 28 days. My interest is the early stage of chronic pain development, therefore, 2 days post injury animal were used for further study.

The principle inhibitory effect of GABA is achieved by activating $GABA_A$ receptor which generate chloride current and hyperpolarize cell. Therefore, the intracellular chloride concentration is crucial. Coull et al. reported potassium-chloride cotransporters KCC2 on lamina I projection neurons were downregulated after peripheral nerve injury[50]. This event, in turn, elevated intracellular [$Cl^-$]. As a result, GABA induced postsynaptic inhibition on projection neurons was lost or even switched to excitation due to chloride gradient shift. I wondered whether peripheral nerve injury could also change the intracellular [$Cl^-$] in presynaptic DRG neurons, and interfere presynaptic inhibition. Therefore, 2-photon chloride imaging were performed on acutely dissected DRGs from transgenic clomeleon mice, which express chloride indicators in neurons, to investigate if CCI influence the [$Cl^-$] of DRG neurons (**Figure 6**). These indicators contain both CFP and YFP fluorophores. The ratio of YFP to CFP fluorescence (YFP/CFP) negatively correlates with [$Cl^-$]. I observed significantly decrease of YFP/CFP, representing the increase of [$Cl^-$], in both small (Control: 0.18 ± 0.003; CCI 0.13 ± 0.004) and large diameter DRG neurons (Control: 0.20 ± 0.003; CCI: 0.13 ± 0.002) from nerve injured mice (**Figure 6**).

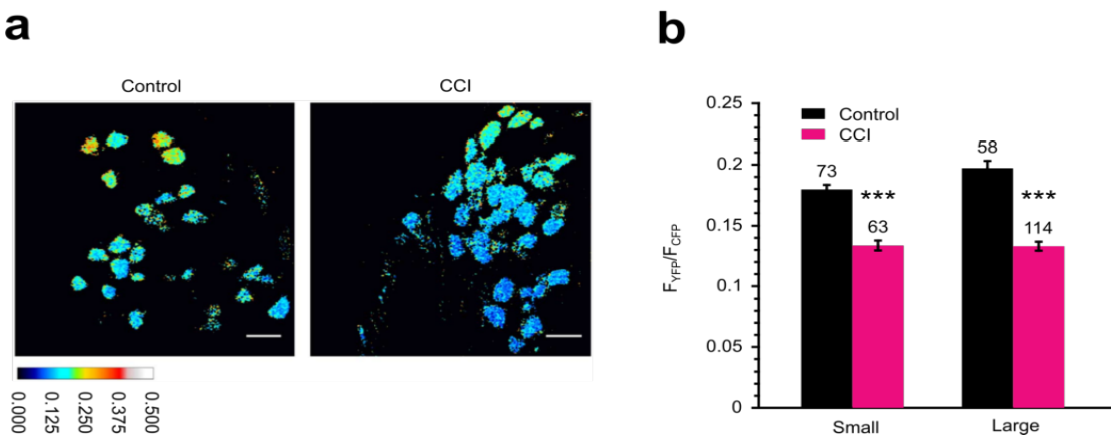


Figure 6: CCI upregulate intracellular [$Cl^-$] of DRG neurons. (a) The 2-photon images of Clomeleon signal ($F_{YFP}/F_{CFP}$) in acutely dissected DRGs from intact (left) and 2-day post CCI animal. (b) The increase of intracellular [$Cl^-$] in both small and large DRG neurons after CCI indicated by the decrease of $F_{YFP}/F_{CFP}$ (small control: n = 73; small CCI: n = 63; large control: n = 58; large CCI n= 114; small control vs small CCI, unpaired student t-test, P < 0.001; large control vs large CCI, unpaired student t-test, P < 0.001). Error bars indicate standard error of the mean (SEM). Scale bars (a) 50 μm. ***P < 0.001.

My colleague, Jeremy Tsung-Chieh Chen, performed perforated patch clamp to investigate the function of $Cl^-$ permeable $GABA_A$ receptors of DRG neurons from intact and nerve injured mice (**Figure 7**). The results indicated that the reversal potential of $Cl^-$ ($E_{Cl}$) are – 35.2 ± 2.5 mV and – 37.5 ± 2.4 mV in small and large neurons repectively from control mice. And nerve injury depolarizingly shifted $E_{Cl}$ in both small (22.7 ± 2.4 mV) and large neurons (– 28.3 ± 3.4 mV respectively). The depolarizing shift of $E_{Cl}$ suggests an increase of intracellular [$Cl^-$] which is consistent with my chloride imaging result. Noticeably, the conductance of $GABA_A$ receptors ($G_{GABA}$) was downregulated in both small and large neurons by nerve injury (**Figure 7d**).

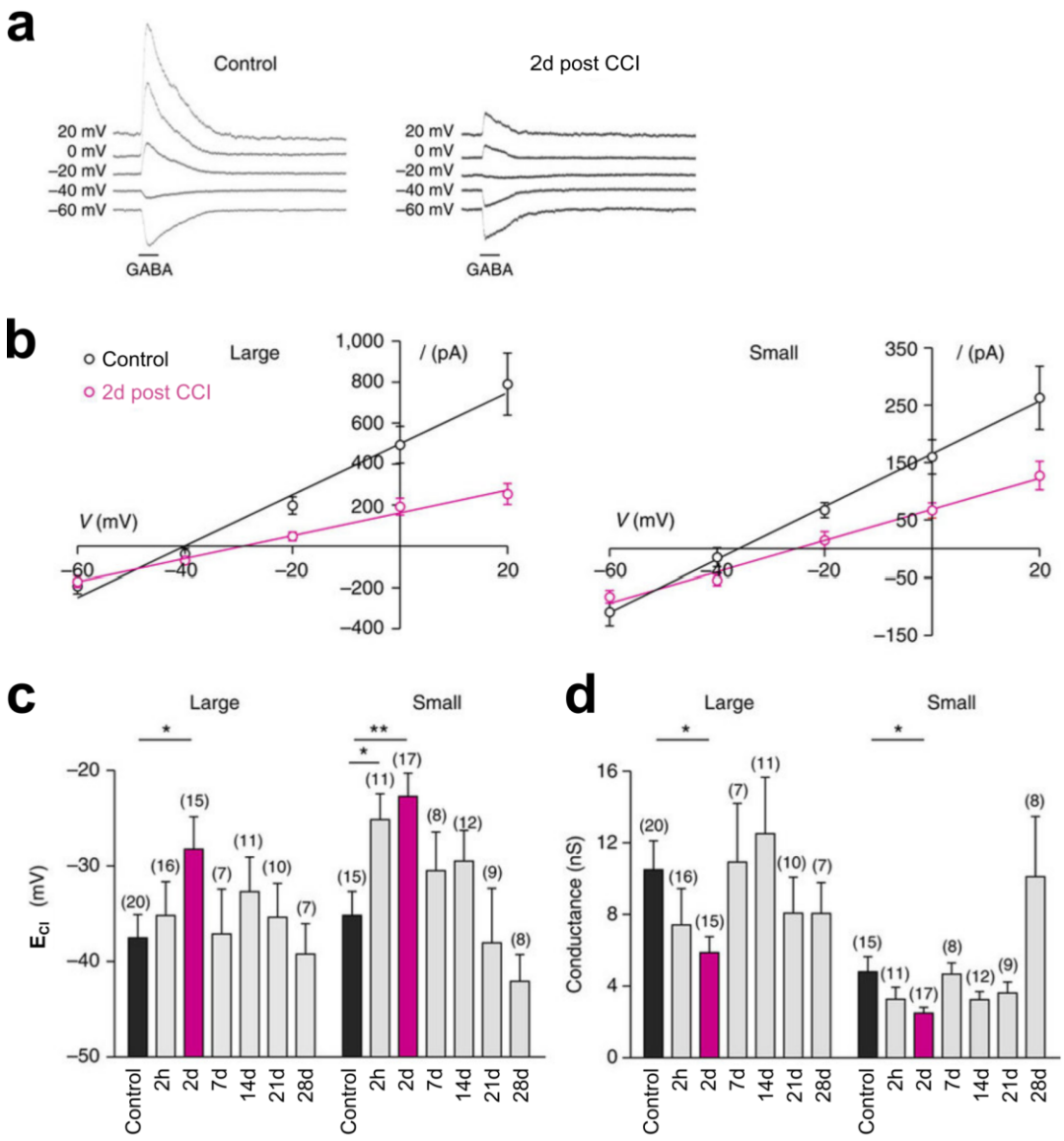


Figure 7: Nerve injury (CCI) induced a transient depolarizing shift of $E_{Cl}$ and reduction of conductance of GABA induced current in primary sensory neurons. (**a**) Representative traces of GABA-activated currents recorded in DRG neurons during gramicidin perforated patch at various holding potential mV. (**b**) Current–voltage relationship for GABA-activated response from large (left) and small (right) neurons. (**c**) Bar graph showing the time course of the changes in $E_{Cl}$. (**d**) Bar graph showing the time course of the changes in conductance of $GABA_A$ receptors. The number of neurons recorded is indicated on top of each bar in (**c**) and (**d**). *P < 0.05; **P < 0.01; unpaired t-test. Error bars indicate SEM.

In conclusion, nerve injury caused an increase of $[Cl^-]$ possibly potentiating the depolarization induced by activation of $GABA_A$ receptors. However, the associated decrease of $G_{GABA}$ may limit such depolarization.

### 4.1.2 Proportion of DRG neurons activated by GABA is not changed by nerve injury

Due to the nature that DRG neuron [$Cl^-$] is high enough to cause the $E_{Cl}$ more depolarized than membrane potential, the activation of $GABA_A$ receptors would lead to an outflow of chloride ions and depolarize the cell[39,40]. This depolarization, as previous studies advocated, was suggested to be the principal component of presynaptic inhibition induced by GABA[28]. However, when this depolarization reaches firing threshold, the inhibitory effect could be impaired. The CCI generated rise of [$Cl^-$] in DRG neurons

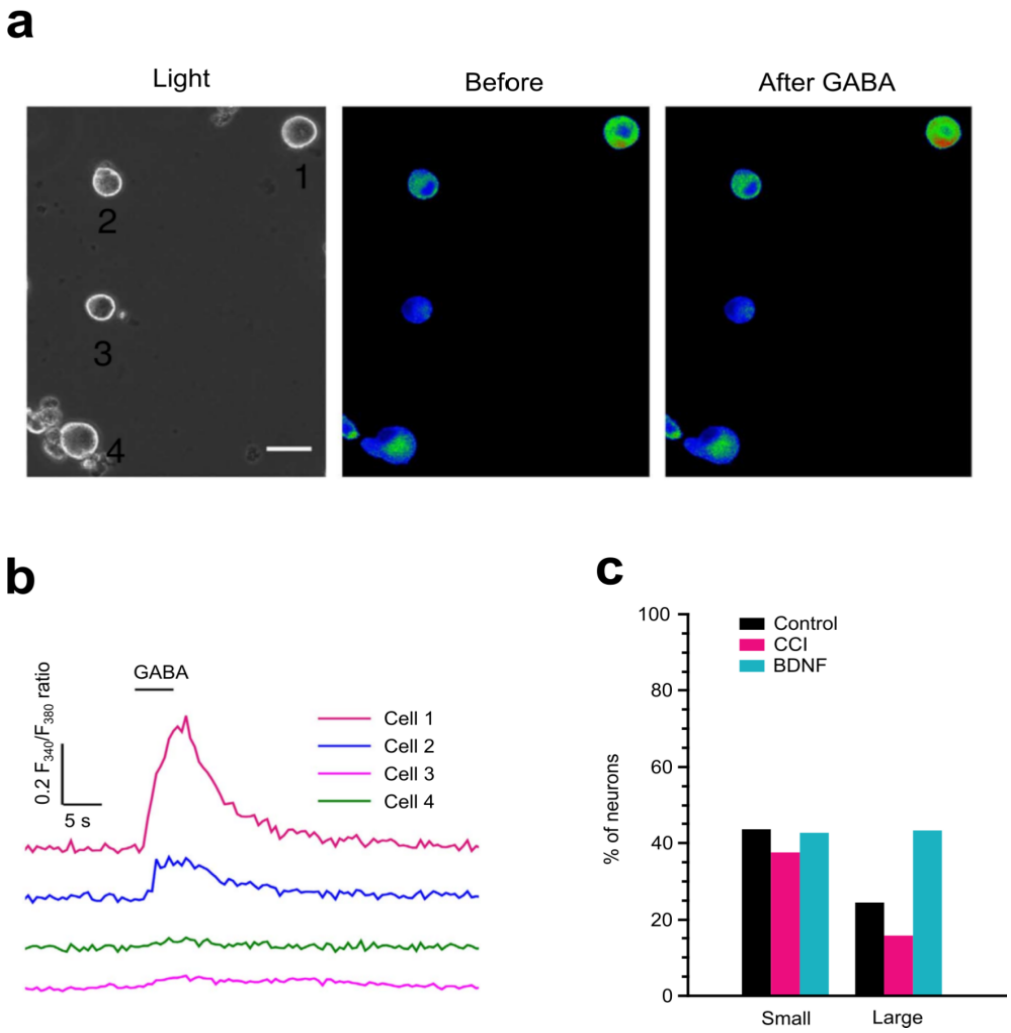


Figure 8: CCI did not change the proportion of DRG neurons displaying GABA evoked calcium transient. (**a**) The bright field (left) and Fura-2 signal ($F_{340}/F_{380}$) images taken before (middle) and immediately after (right) GABA application. (**b**) Representative traces showing intracellular [$Ca^{2+}$] along time in labeled cells in **a**. (**c**) Proportions of neurons displaying GABA evoked calcium transient (small control: n = 236; small CCI: n = 149; small BDNF: n = 110; large control: n = 45; large CCI: n = 19; large BDNF n = 30; Fisher's exact test, all P > 0.05). Scale bar (**a**) 30 μm.

caused a larger electrical potential across membrane, which might increase the $GABA_A$ receptor mediated chloride current outflow. Whether the slightly elevated $[Cl^-]$ can change the effect of GABA, for example, to excitation is unclear. To figure this out, DRGs from intact and injured animal were cultivated, and used for Fura-2-AM loaded cell calcium imaging, which indirectly showed neuron activity by monitoring intracellular calcium influx (**Figure 8a**). Locally applied 1 mM GABA, which is in the same concentration range as in synaptic cleft, was found to trigger calcium transient in 44% of small neurons and 24% of large neurons from intact animal (**Figure 8c**). And these proportions were not significantly changed in neurons from injured mice (38% in small neurons, 16% in large neurons) (**Figure 8c**). This result showed that the GABA induced depolarization could not trigger calcium transient in a bigger proportion of DRG neurons after nerve injury. This may be due to the downregulated $G_{GABA}$, which limits the inward current to depolarize neurons.

### 4.1.3 GABA loses inhibitory effect on presynapses in nerve injured mice

The intracellular $[Cl^-]$ increase was observed in DRG neuron somas from nerve injured mice, but whether $[Cl^-]$ in central terminals, which locate in spinal cord dorsal horn, rise together with neuron somas is still unclear. Besides, GABA was not found to acquire excitatory effect on DRG neurons from injured mice, but its effect on presynapses is still unclear if $[Cl^-]$ also rises there. Therefore, 2-photon calcium imaging was utilized to investigate the central terminals of nociceptors.

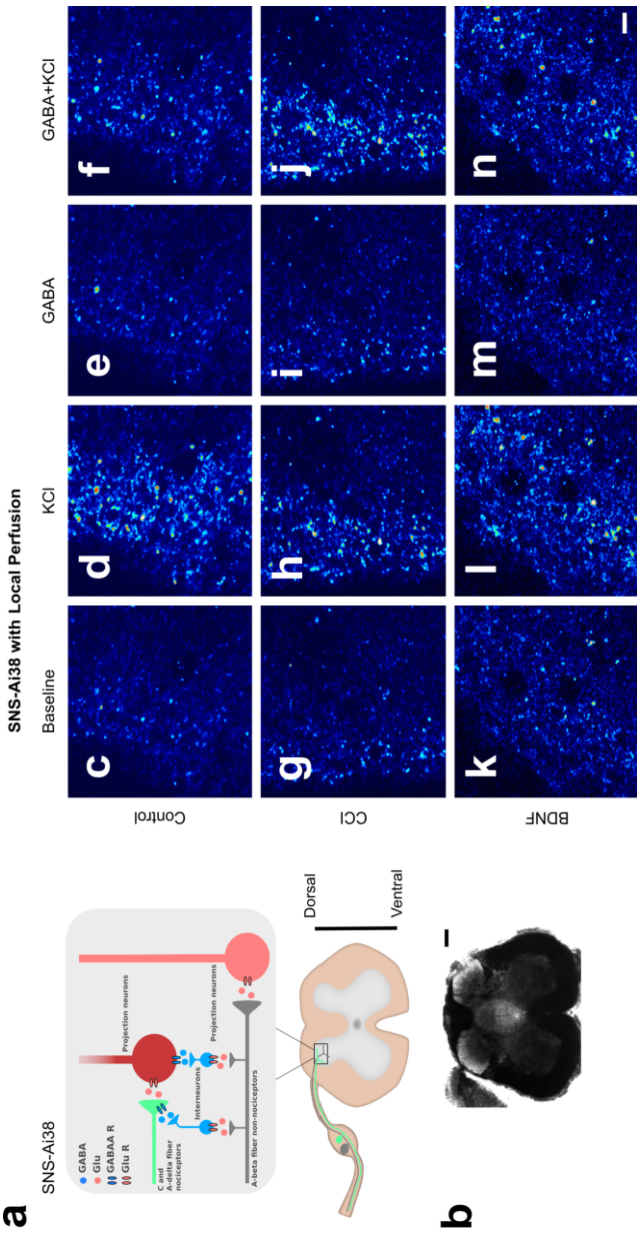


Figure 9: 2-photon images of acutely dissected spinal cord slices from SNS-Ai38 mice (control, CCI and BDNF). (**a**) A diagram showing expression patter of GCaMP3 signal in advillin-Ai38 mice. (**b**) Bright field image of spinal cord slice used for 2-photon calcium imaging. (**c - n**) 2-photon microscope imaged GCaMP3 signal indicating [$Ca^{2+}$] in Control (**c - f**), CCI (**g - j**) and BDNF (**k - n**) spinal cord superficial layer in response to various stimuli. Scale bars, (**b**) 200 μm; (**c - n**) 10 μm (only shown in **n**)

To cope with the difficulty of recognizing presynapses, I bred SNS-Cre mice, which expressed Cre recombinase in nociceptors, to Ai38 mice, in which a loxP-flanked STOP cassette prevented transcription of the downstream fluorescent calcium indicator GCaMP3 fusion gene. The offspring (SNS-Ai38) carried both Cre recombinase and GCaMP3 fusion gene had GCaMP3 specifically expressed in nociceptors and thus all calcium signal observed in spinal cord was from central terminals of neurons (**Figure 9a**).

Spinal cord innervated by L4 or L5 nerve were sliced and superficial layers of dorsal horn, where most nociceptors innervate, was imaged with 2-photon microscopy (**Figure 9b**). Considering synaptic $GABA_A$ receptors are less sensitive to GABA compare to extrasynaptic $GABA_A$ receptors[68], and the perfusion to whole recording chamber might unable to deliver the expected concentration (1 mM) of GABA and activated majority of synaptic $GABA_A$ receptors, recordings with local perfusion (less than 500 μm from

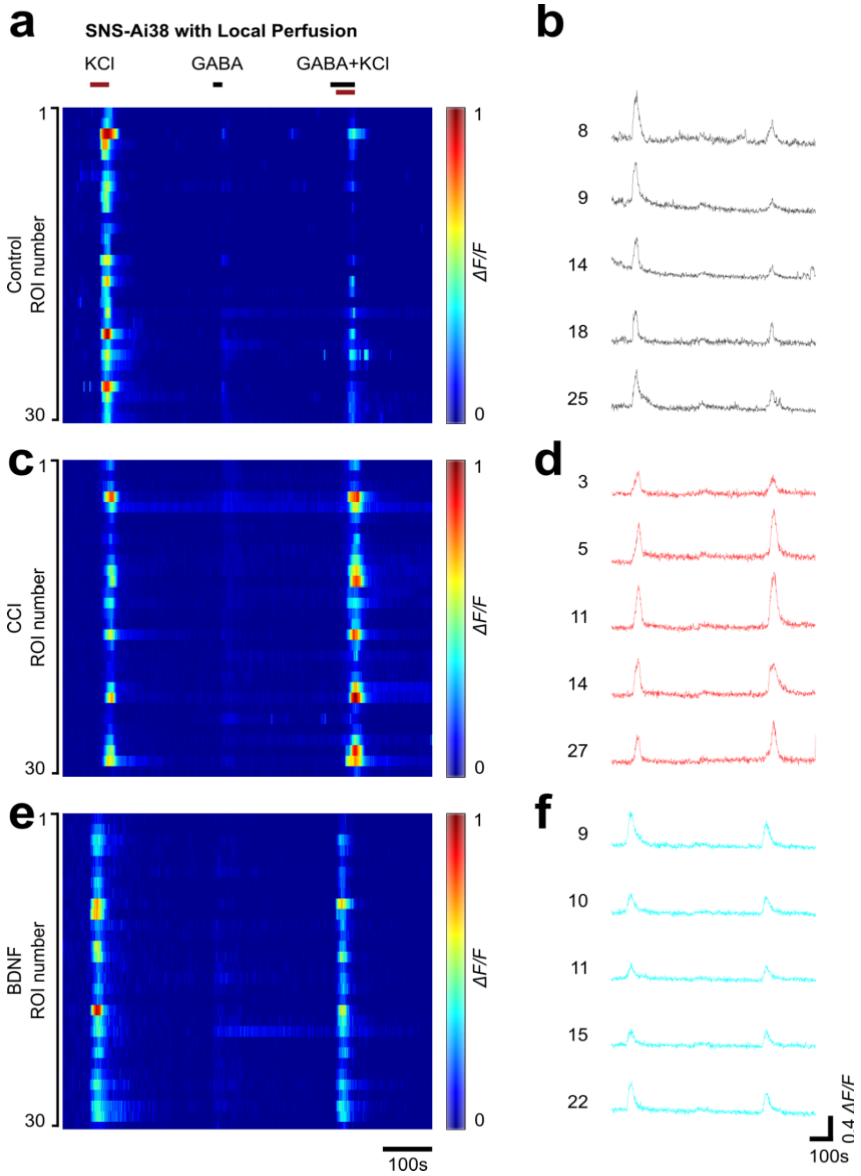


Figure 10: The color maps and representative traces of 2-photon calcium imaging of acutely dissected spinal cord slices from SNS-Ai38 mice (control, CCI and BDNF). (**a, c, e**) Each color map represents presynaptic calcium intensity in 30 ROIs. (**b, d, f**) Selected representative traces showing calcium intensity. The figures for control (**a, b**), CCI (**c, d**) and BDNF (**e, f**) groups are correlated with the example 2-photon images show in **Figure 9**.

recording area) in addition to whole chamber perfusion were applied to ensure the activation of $GABA_A$ receptors. Clear calcium transient ($\Delta F/F_0$) was observed when high KCl Ringer's solution, with or without GABA, was applied (**Figure 9d, f, h, j; 10a - d**). Noticeably, when GABA was co-applied with high KCl Ringer's solution, majority of high KCl responding regions of interest (ROIs) either showed similar amplitude of calcium transient or attenuated calcium influx or even no influx (Whole chamber perfusion: No-change: 58 %; More $Ca^{2+}$ transient: 7 %; Less $Ca^{2+}$ transient: 36 %. Local perfusion: No-change: 49 %; More $Ca^{2+}$ transient: 9 %; Less $Ca^{2+}$ transient: 41 %. **Figure 11a**). And nerve injury dramatically decreased the proportion of ROIs where GABA exhibited such inhibitory effect on KCl evoked calcium transient, and boosted the proportion showing elevated calcium transient when GABA was co-applied with high KCl (Whole chamber perfusion: CCI: No-change: 46 %; More $Ca^{2+}$ transient: 45 %; Less $Ca^{2+}$ transient: 9 %. Local perfusion: CCI: No-change: 67 %; More $Ca^{2+}$ transient: 30 %; Less $Ca^{2+}$ transient: 3 %. **Figure 11a**). 1 mM GABA perfused to the recording chamber could trigger calcium transient in a small percentage of ROIs in spinal cord from intact SNS-Ai38 mice (Whole chamber perfusion: 2.7 ± 1.3 %. Local perfusion: 12.5 ± 2.3 %. **Figure 11b**), and nerve injury did not show significant influence on this percentage (Whole chamber perfusion: 1.3 ± 0.7 %. Local perfusion: 19.8 ± 4.7 %. **Figure 11b**). In conclusion, these results showed the considerable inhibitory effect of GABA on nociceptor central terminals, and nerve injury significantly disturbed this negative control. However, presynaptic GABAergic control, unlike postsynaptic inhibition, was not reversed to be excitatory, but was only disinhibited, since GABA did not generate more calcium influx after nerve injury.

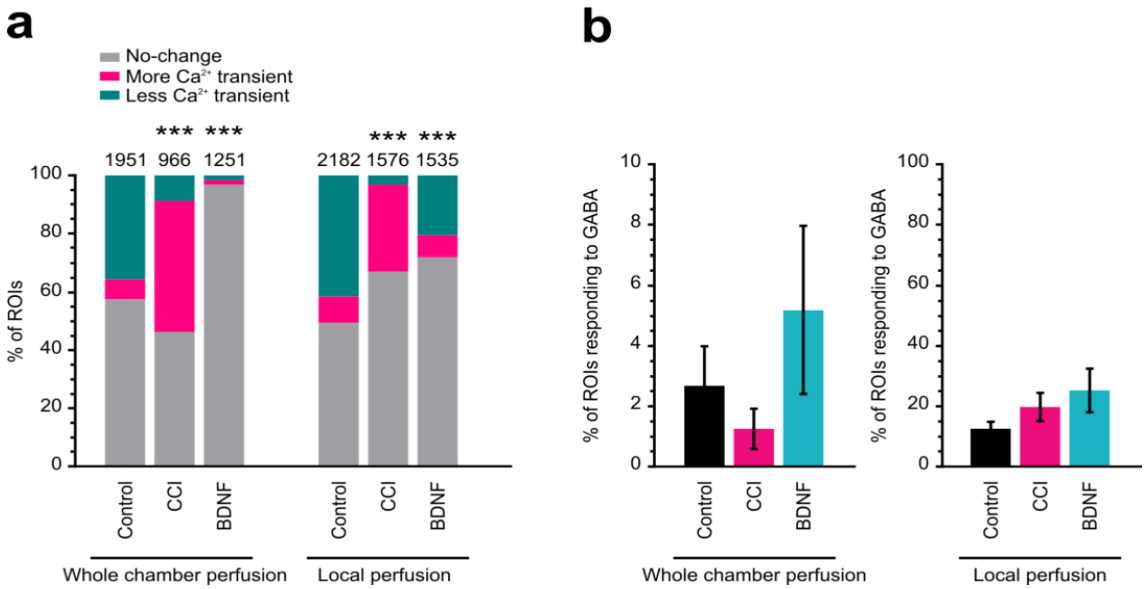


Figure 11: statistics results of 2-photon calcium imaging on spinal cord from SNS-Ai38 mice (control, CCI and BDNF). (**a**) The proportions of ROIs where no-change, more $Ca^{2+}$ transient, and less $Ca^{2+}$ transient were observed when 1 mM GABA was applied with high KCl compare to sole high KCl perfusion. The number of ROIs recorded is indicated on top of each bar. (whole chamber perfusion: Control mice n = 5; CCI mice n = 4; BDNF mice n=3. chi-squared test, Control vs CCI, $P < 0.001$; Control vs BDNF, $P < 0.001$. local perfusion: Control mice n = 4; CCI mice n = 3; BDNF mice n=3. chi-squared test, Control vs CCI, $P < 0.001$; Control vs BDNF, $P < 0.001$). (**b**) The proportion of ROIs displaying GABA evoked calcium transient was not changed by CCI or BDNF incubation (whole chamber perfusion: Control slice, n = 6; CCI slice, n = 5; BDNF slice, n = 5. student t-test, Control vs CCI, $P > 0.05$; Control vs BDNF, $P > 0.05$. Local perfusion: Control slice, n = 8; CCI slice, n = 7; BDNF slice, n = 4. student t-test, Control vs CCI, student t-test, $P > 0.05$; Control vs BDNF, student t-test, $P > 0.05$.). Error bars indicate SEM. ***$P < 0.001$.

### 4.1.4 Lost of presynaptic inhibition after nerve injury contributes to mechanical hypersensitivity and fully responsible for thermal hyperalgesia (experiments carried by Jeremy Tsung-chieh Chen)

The group of De Koninck[50,51] provided evidence that mechanical allodynia and thermal hyperalgesia in peripheral nerve injured mice were at least partially caused by the increased postsynaptic chloride gradient which alters inhibitory GABAergic input from interneurons. Witschi et al.[69] recently selectively knockout $GABA_A$ receptor α2 subunit on DRG nociceptors (SNS-$\alpha2^{-/-}$) by utilizing Cre-loxP method. Although, the antinociceptive effect of Diazepam (DZP) was found to be reduced in these SNS-$\alpha2^{-/-}$ mice, the thresholds to thermal and mechanical stimulation were normal, which might because of the upregulation of bensodiazepine insensitive $GABA_A$ receptors. My colleague, by using SNS-cre and Gabrb3-loxP mice, generated conditional knockout mouse line (SNS-$\beta3^{-/-}$) in which another $GABA_A$ receptor subunit, β3, was specifically knockout in nociceptors. Compare to control litter mates, $\beta3^{fl/fl}$ mice, SNS-$\beta3^{-/-}$ mice were significantly more sensitive to both thermal and mechanical stimulation, yet nerve injury was still capable of further sensitizing mechanical sensitivity (**Figure 12a**). However, heat hypersensitivity could not be further developed (**Figure 12b**). My calcium imaging data and these behavior results together suggest that nerve injury disrupts presynaptic inhibition, and this lost of inhibition contributes to mechanical hypersensitivity and is fully responsible for thermal hyperalgesia.

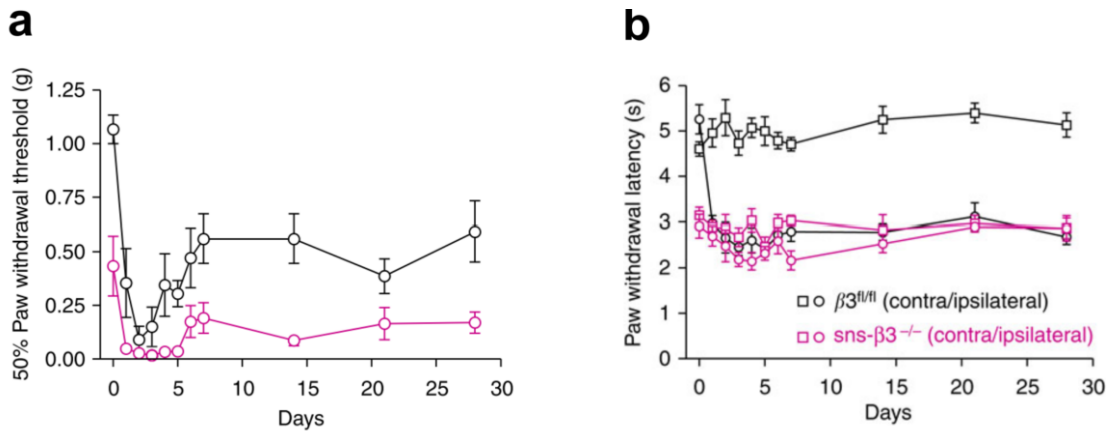


Figure 12: SNS-$\beta3^{-/-}$ mice were more sensitive to both mechanical and thermal stimuli. (**a**) Von Frey test showed mechanical hypersensitivity was significantly reduced in SNS-$\beta3^{-/-}$ mice, and mechanical allodynia was further developed after CCI. n = 6 mice per group. (repeated two-way ANOVA, $\beta3^{fl/fl}$ ipsilateral versus SNS-$\beta3^{-/-}$ ipsilateral, factor time, $P < 0.001$; factor genotype, $P < 0.001$. Bonferroni post hoc test, $\beta3^{fl/fl}$ ipsilateral versus SNS-$\beta3^{-/-}$ ipsilateral 0d, $P < 0.05$). (**b**) SNS-$\beta3^{-/-}$ mice failed to develop thermal hypersensitivity after CCI. n = 6 mice per group. (Two-way analysis of variance (ANOVA): $\beta3^{fl/fl}$ contralateral versus ipsilateral, $P < 0.001$; SNS-$\beta3^{-/-}$ contralateral versus ipsilateral, $P < 0.05$; $\beta3^{fl/fl}$ ipsilateral versus SNS-$\beta3^{-/-}$ ipsilateral after injury, $P > 0.05$). Error bars indicate SEM.

### 4.1.5 BDNF causes the lost of presynaptic inhibition after nerve injury

Coull et al. revealed that the elevated [$Cl^-$] in lamina I neurons after nerve injury were caused by microglia released BDNF which down-regulates KCC2 by binding to TrkB receptors[51]. BDNF-TrkB signaling had been suggested to modulating intracellular [$Cl^-$] by regulating NKCC1, which is mainly expressed by DRG neurons, as well as KCC2[70,71]. In addition, TrkB receptors had been reported to also expressed at axonal terminals of primary afferent fibers in nociceptors, and depolarizing shift of chloride reversal potential was observed in BDNF treated DRG neurons as well[61,72]. Therefore, it is likely that the microglia-derived BDNF after nerve injury also has an impact on presynaptic [$Cl^-$]. To examine this assumption, calcium imaging on overnight BDNF (50 ng $ml^{-1}$) treated DRG cell culture was applied. GABA induced calcium transient didn't appear in bigger proportion of neurons compare to control, which is similar to result acquired from injured mice (BDNF: small, 43 %; large, 43 %. **Figure 8c**).

2-Photon calcium imaging was also applied to examine the effect of BDNF on presynapses (**Figure 9k – n; 10e – f; 11**). 2h BDNF incubated spinal cord slice from SNS-Ai38 mice exhibited a prominent loss of GABAergic inhibition on high KCl induced calcium influx in presynapses located in superficial layer (Whole chamber perfusion: No-change: 97 %; More $Ca^{2+}$ transient: 2 %; Less $Ca^{2+}$ transient: 2 %. Local perfusion: No-change: 72 %; More $Ca^{2+}$ transient: 7 %; Less $Ca^{2+}$ transient: 21 %.), which is identical to the change in CCI spinal cord (**Figure 11a**). Similarly, the proportion of ROIs displaying GABA-evoked calcium transient (Whole chamber perfusion: 5.2 ± 2.8 %. Local perfusion: 25.3 ± 7.2 %) was also unaffected (**Figure 11b**).

In addition, our group previously provided behavior evidence showing BDNF and CCI had similar effect on presynaptic terminals[61]. Taken together, these similarities between CCI and BDNF groups implied the nerve injury induced lost of presynaptic inhibition is regulated by BDNF.

## 4.2 GABAergic presynaptic modulation after peripheral inflammation

### 4.2.1 Increased [$Cl^-$] associated with unchanged $G_{GABA}$ in nociceptors after inflammation (experiments carried by Jeremy Tsung-chieh Chen)

Willis had reviewed dorsal root reflex (DRR), which is only observed after peripheral inflammation but not nerve injury, and discussed the possible mechanism causing it[52]. Pharmacological studies strongly suggested that the enhanced PAD mediated by presynaptic $GABA_A$ receptors after inflammation was essential for DRR. Therefore, we reasoned that peripheral inflammation, similar to nerve injury, also likely to elevate the intracellular [$Cl^-$], which may cause a depolarization strong enough to trigger an action potential. Indeed, Patch clamp study from our lab revealed that CFA injection did induce a depolarizing shift of $E_{Cl}$ in small sized DRG neurons (**Figure 13**). Moreover, the whole cell $G_{GABA}$ did not decrease like neurons from nerve injured animal and rather show a trend towards increasing (**Figure 13**). Together, these electrophysiology results implied that the activation of $GABA_A$ receptors probably generated a stronger depolarization after peripheral inflammation than after nerve injury, which possibly underlied why DRR was not observed after nerve injury.

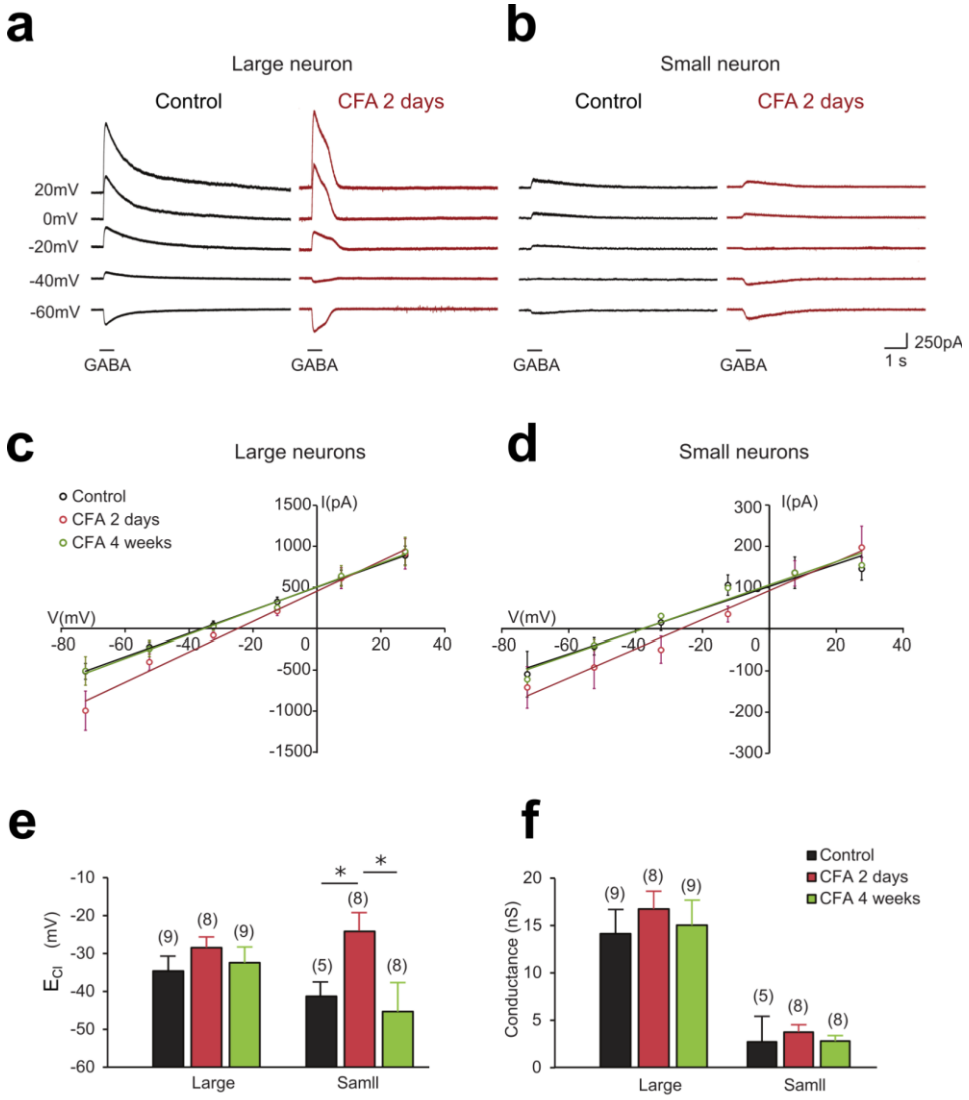


Figure 13: The influence of CFA induced inflammation on $E_{Cl}$ and $G_{GABA}$ of cultured DRG neurons. (**a - b**) Representative traces displaying GABA generated currents in large (**a**) and small (**b**) neurons at various holding potential. (**c - d**) The current – voltage curve of GABA induced cell responses in large (**c**) and small (**d**) neurons. (**e**) $E_{Cl}$ was depolarizingly shifted in small neurons 2 days after CFA injection. This shift was recovered after 4 weeks. (student t-test, Large: Control vs CFA 2 days, $P > 0.05$; Control vs CFA 4 weeks, $P > 0.05$; CFA 2 days vs CFA 4 days, $P > 0.05$. Small: Control vs CFA 2 days, $P < 0.05$; Control vs CFA 4 weeks, $P > 0.05$; CFA 2 days vs CFA 4 days, $P < 0.05$). (**f**) The conductance of $GABA_A$ receptors was not affected by CFA injection in neither larger nor small DRG neurons. (student t-test, Large: Control vs CFA 2 days, $P > 0.05$; Control vs CFA 4 weeks, $P > 0.05$; CFA 2 days vs CFA 4 days, $P > 0.05$. Small: Control vs CFA 2 days, $P > 0.05$; Control vs CFA 4 weeks, $P > 0.05$; CFA 2 days vs CFA 4 days, $P > 0.05$). The number of recorded neurons in indicated on top of each bar in (**e**) and (**f**). Error bars indicate SEM. *$P < 0.05$.

My colleague found both similarities and distinctions between nerve injured and CFA injected SNS-$\beta3^{-/-}$ mice with behavior test. CFA injection induced peripheral inflamma-

tion further developed the mechanical and thermal hyperalgesia in SNS-$\beta3^{-/-}$ mice as CCI (**Figure 14a, b**), yet mechanical allodynia was not fully developed after inflammation (**Figure 14c**). This indicates that presynaptic $GABA_A$ receptors are crucial for mechanical allodynia development after inflammation which was not observed in nerve injured animal.

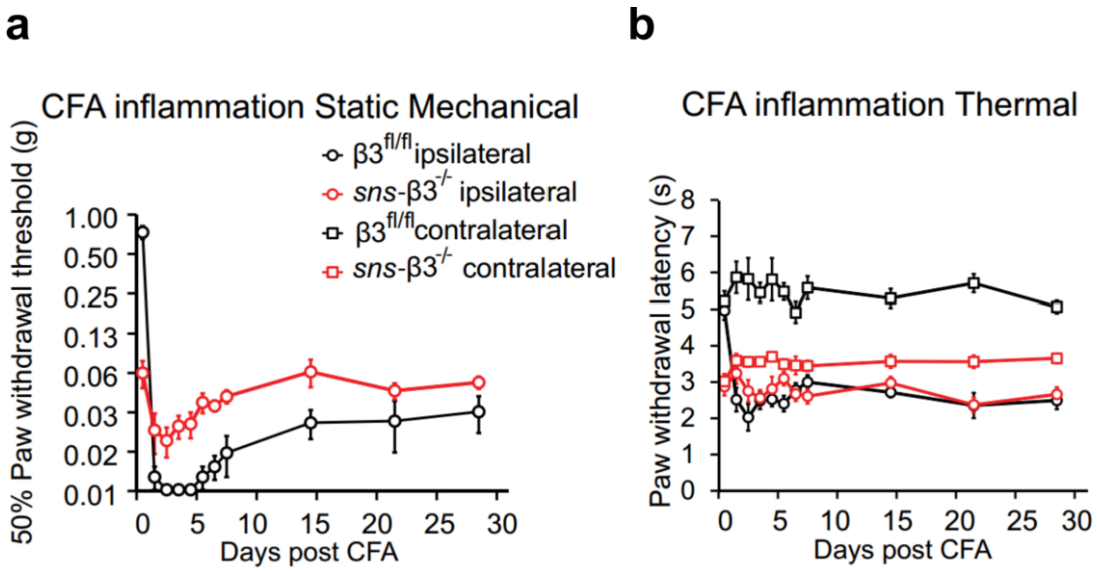


Figure 14: CFA induced peripheral inflammation further sensitized SNS-$\beta3^{-/-}$ mice. (**a**) The mechanical allodynia was developed in SNS-$\beta3^{-/-}$ mice after CFA injection, but it was less sensitive than that in $\beta3^{fl/fl}$ mice. ($\beta3^{fl/fl}$, n = 6; SNS-$\beta3^{-/-}$, n = 8. Repeated two-way ANOVA (0 - 28d): factor time $P < 0.0001$, factor genotype $P < 0.0001$, Bonferroni post hoc, $\beta3^{fl/fl}$ vs SNS-$\beta3^{-/-}$ on 0d, $P < 0.0001$. Repeated two-way ANOVA (1 – 28d): factor time $P < 0.0001$, factor genotype $P < 0.01$). (**b**) The development of thermal hyperalgesia was similar in SNS-$\beta3^{-/-}$ and its control litter mates ($\beta3^{fl/fl}$, n = 6; SNS-$\beta3^{-/-}$, n = 8. Repeated two-way ANOVA (0 - 28d): factor CFA injection, $\beta3^{fl/fl}$ contralateral vs ipsilateral, $P < 0.0001$; SNS-$\beta3^{-/-}$ contralateral vs ipsilateral, $P < 0.0001$. Repeated two-way ANOVA (1 – 28d) $\beta3^{fl/fl}$ vs SNS-$\beta3^{-/-}$ ipsilateral, $P > 0.05$). (**c**) Error bars indicate SEM.

### 4.2.2 Excitatory effect of GABA on presynapses in inflamed mice

Therefore, I studied the function of presynaptic $GABA_A$ receptors with spinal cord (SC) slices from CFA injected animal to investigated whether the increased [$Cl^-$] abolishes the inhibitory effect of GABA as it does in nerve injured animal, and whether the difference in $G_{GABA}$ between CCI and CFA groups leads to functional difference.

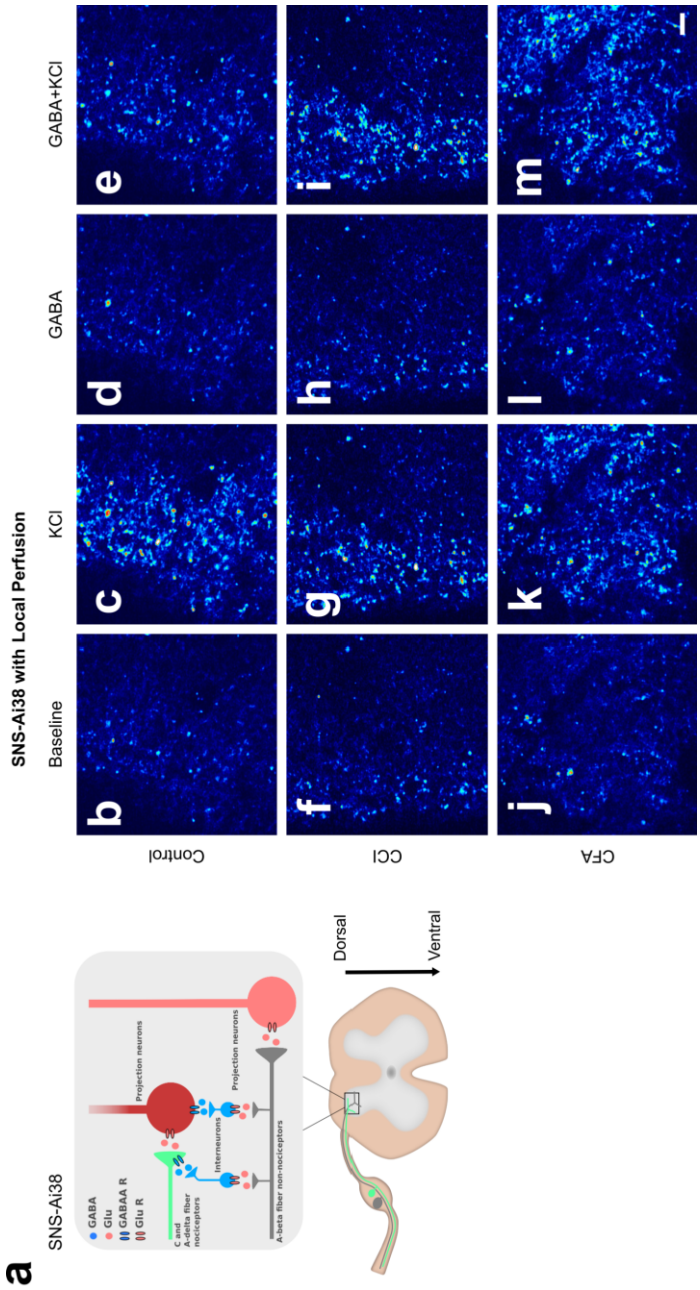


Figure 15: 2-photon images of acutely dissected spinal cord slices from SNS-Ai38 mice.(**a**) A diagram showing expression patter of GCaMP3 signal in SNS-Ai38 mice. (**b**) 2-photon microscope imaged GCaMP3 signal indicating [Ca2+] in Control (**b - e**), CCI (**f - i**) and CFA (**j - m**) spinal cord superficial layer in response to various stimuli. Scale bars, (**b – m**) 10 µm (only shown in m).

2-day after CFA injection, GABA was found, like in nerve injured mice, failing to suppress high KCl Ringer's solution generated calcium transient in spinal cord from SNS-Ai38 mice (Whole chamber perfusion: No-change: 66 %; More $Ca^{2+}$ transient: 21 %; Less $Ca^{2+}$ transient: 13%. Local perfusion: No-change: 68 %; More $Ca^{2+}$ transient: 31 %; Less $Ca^{2+}$ transient: 1 %. **Figure 15; 16; 17a**). In addition, GABA itself alone could generate calcium influx in more presynapses in spinal cord from CFA injected SNS-Ai38

mice (Whole chamber perfusion: Control: 2.7 ± 1.3 %; CFA: 6.6 ± 0.9 %. Local perfusion: Control: 13 ± 2.3 %; CFA: 57 ± 12 %. **Figure 15i; 16e,f; 17b**).

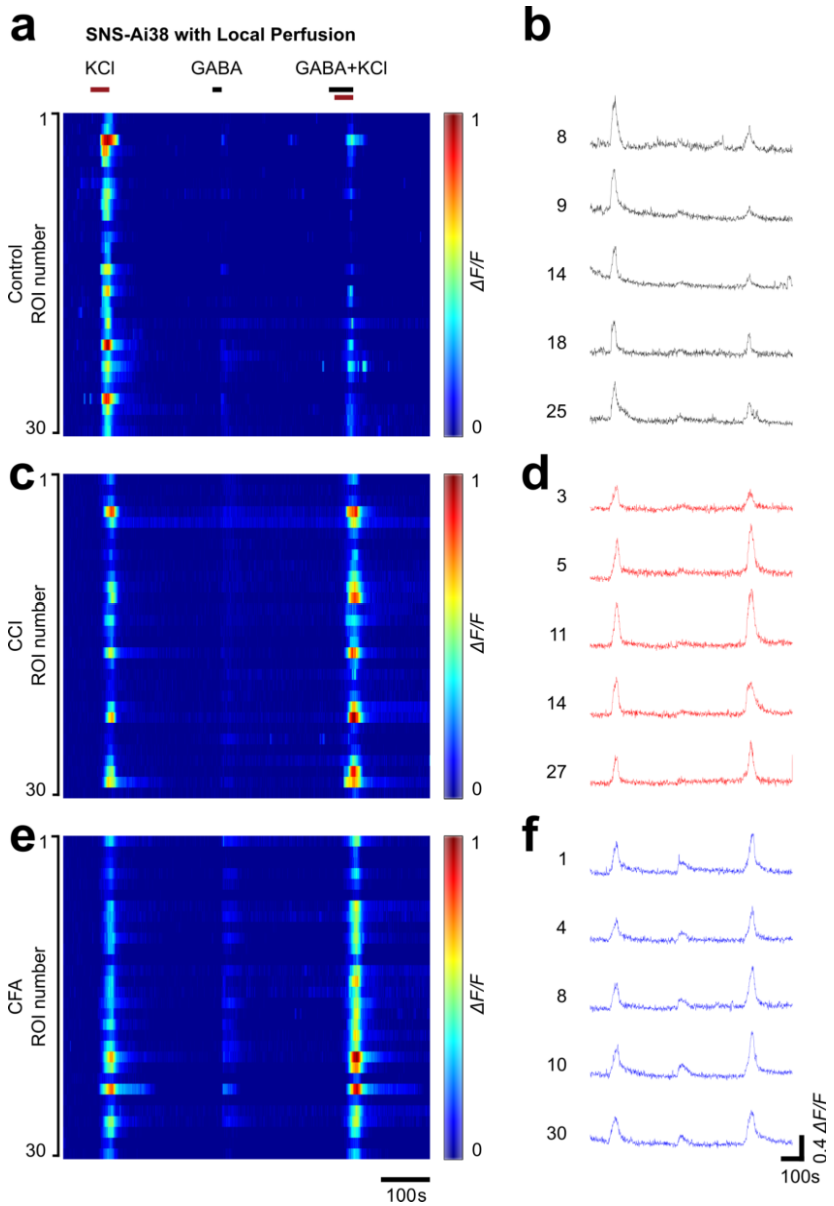


Figure 16: The color maps and representative traces of 2-photon calcium imaging of acutely dissected spinal cord slices from SNS-Ai38 mice (control, CCI, CFA). (**a, c, e**) Each color map represents presynaptic calcium intensity in 30 ROIs. (**b, d, f**) Selected representative traces showing calcium intensity. The figures for control (**a, b**), CCI (**c, d**) and CFA (**e, f**) groups are correlated with the example 2-photon images show in **Figure 15**.

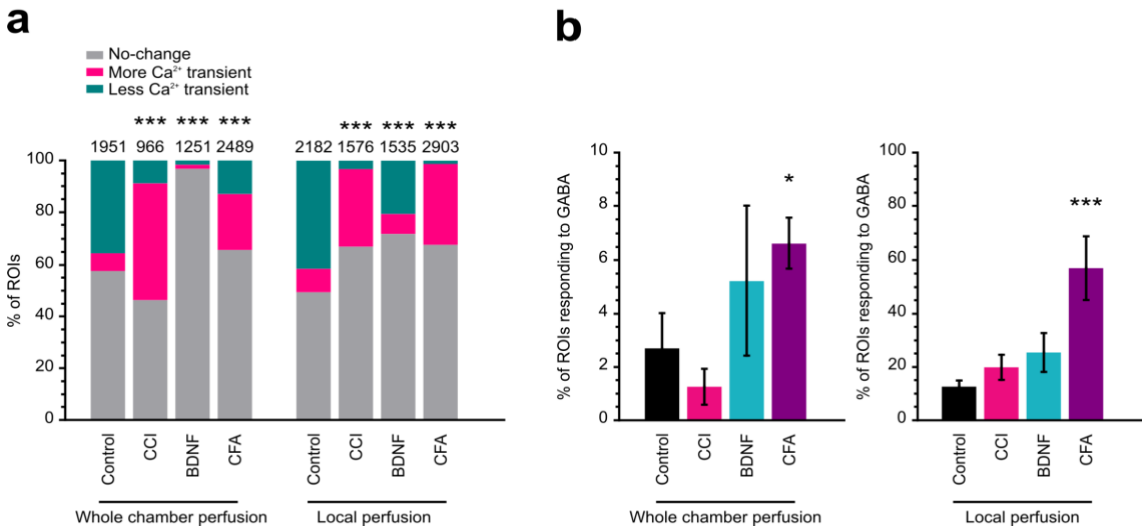


Figure 17: Statistics data of 2-photon calcium imaging on spinal cord from nerve injured SNS-Ai38 mice. (**a**) The proportions of ROIs where no-change, more $Ca^{2+}$ transient, and less $Ca^{2+}$ transient were observed when 1 mM GABA was applied with high KCl compare to sole high KCl perfusion. The number of ROIs recorded is indicated on top of each bar. (whole chamber perfusion: Control mice n = 5; CCI mice n = 4; BDNF mice n = 3; CFA mice n = 6. chi-squared test, Control vs CCI,P < 0.001; Control vs BDNF, P < 0.001; Control vs CFA, P < 0.001. Local perfusion: Control mice n = 4; CCI mice n = 3; BDNF mice n=3; CFA mice n = 3. chi-squared test, Control vs CCI, P < 0.001; Control vs BDNF, P < 0.001; Control vs CFA, P < 0.001). (**b**) The proportion of ROIs displaying GABA evoked calcium transient. (whole chamber perfusion: Control, n = 6; CCI, n = 5; BDNF, n = 5; CFA, n = 12. student t-test, Control vs CCI, P > 0.05; Control vs BDNF, P > 0.05; Control vs CFA, P < 0.05. Local perfusion: Control, n = 8; CCI, n = 7; BDNF, n = 4; CFA, n = 8. student t-test, Control vs CCI, P > 0.05; Control vs BDNF, P > 0.05; Control vs CFA, P < 0.01.). Error bars indicate SEM. *P < 0.05, ***P < 0.001.

2-photon calcium imaging with GABA receptor antagonists was performed to investigated the contribution of $GABA_A$ and $GABA_B$ receptors to this increased calcium influx after inflammation. As expected, GABA only induced calcium transient in few ROIs in spinal cord from intact SNS-Ai38 mice, and neither $GABA_B$ receptor antagonist, CGP55845, nor $GABA_A$ receptor antagonists, bicuculline and picrotoxin, changed this (GABA: 4.6 ± 0.8 %; GABA+CGP55845: 4.7 ± 2.4 %; GABA+CGP55845+Bicuculline+Picrotoxin: 5.9 ± 2.9 %. **Figure 18c – e; 19a, c**). In spinal slices from CFA injected SNS-Ai38 mice, CGP55845 did not show any influence on GABA-evoked calcium transient (GABA: 31 ± 5.8 %; GABA+CGP55845: 31 ± 5.0 %. **Figure 18h – i; 19b, c**). However, bicuculline and picrotoxin successfully suppressed the calcium transient in majority of ROIs, indicating the essential role of $GABA_A$ receptors in the inflammation induced increase of GABA activity (GABA+CGP55845+Bicu-

culline+Picrotoxin: 6.8 ± 3.0 %. **Figure 18j; 19b, c**).In conclusion, these results implies GABA does not only lose inhibitory effect, but also acquires excitatory effect in inflammatory pain model, which supports the previous report that the increased DRRs were mediated by the activation of $GABA_A$ receptors after peripheral inflammation[73]. And the incomplete developed allodynia of CFA injected SNS-$\beta3^{-/-}$ mice observed by my colleague may be due to the lack of GABA excitatory effect on presynapses after inflammation.

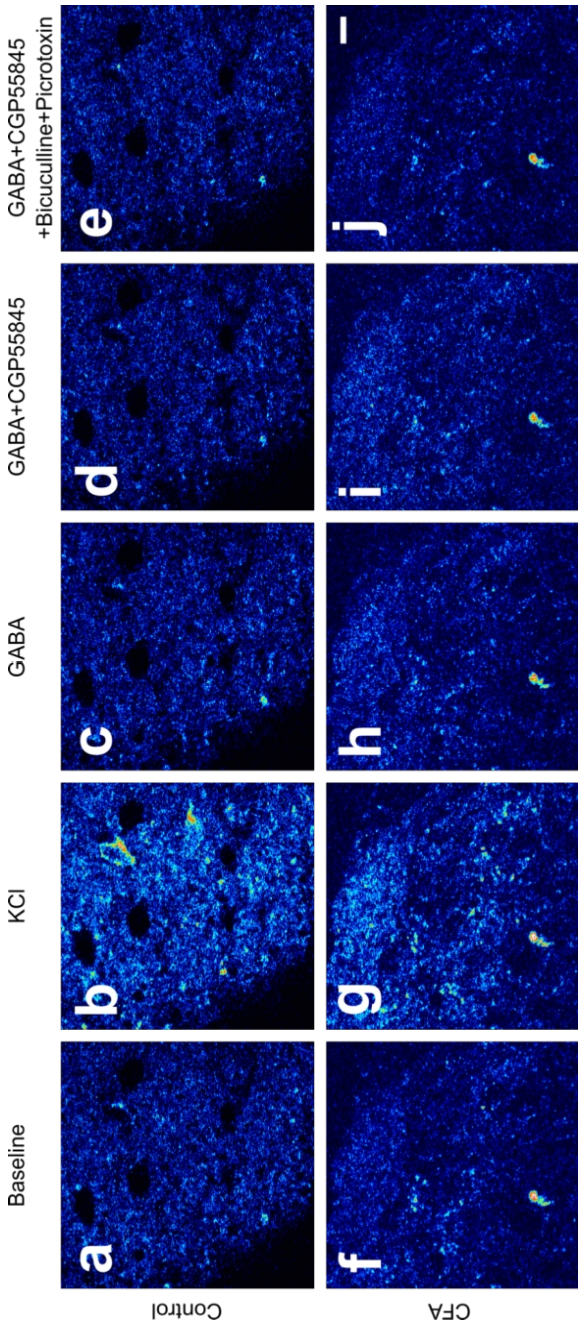


Figure 18: 2-photon images of acutely dissected spinal cord slices from SNS-Ai38 mice showing the effect of antagonists of $GABA_A$ and $GABA_B$ receptors. (**a – e**) The 2-photon images taken from Control group. (**f – j**) The 2-photon images taken from CFA group. Scale bars, (**a – j**) 10 µm (only shown in **j**)

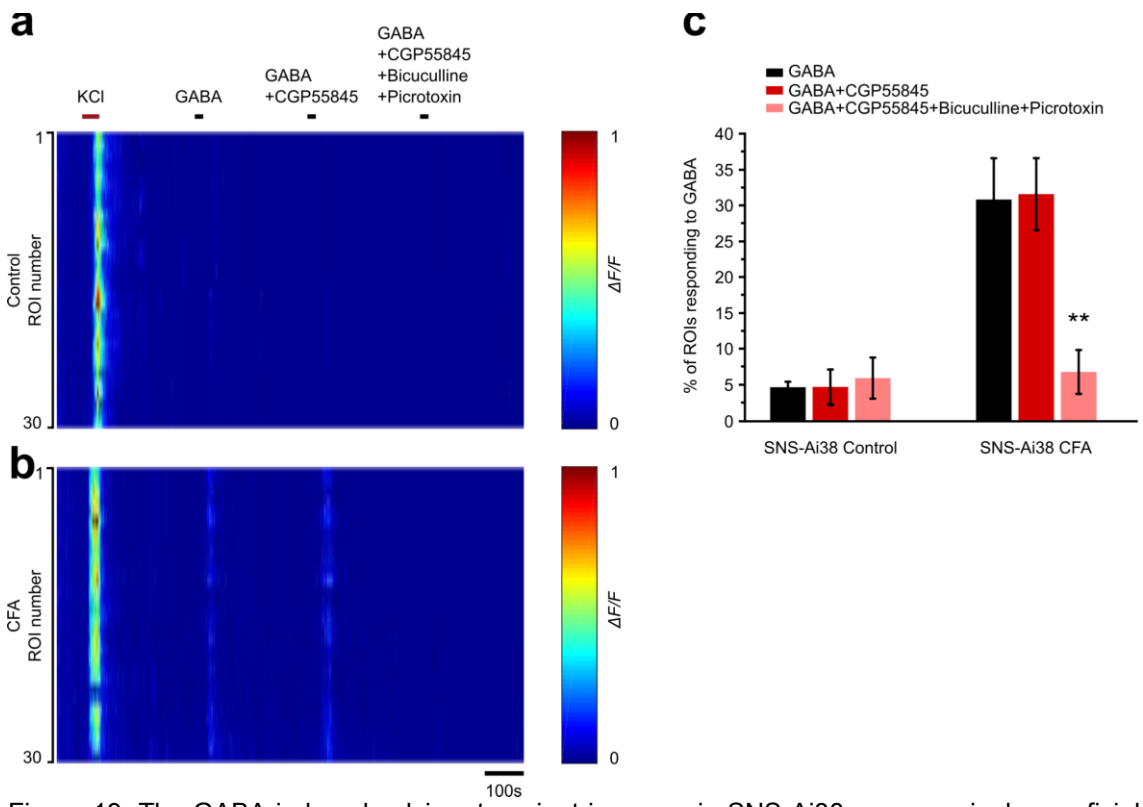


Figure 19: The GABA induced calcium transient increase in SNS-Ai38 mouse spinal superficial layer after peripheral inflammation is mediated by $GABA_A$ receptors. (**a**) Color map displaying intact SNS-Ai38 mouse spinal superficial layer presynaptic [$Ca^{2+}$] change in 30 ROIs chosen from the area shown in Figure 18a – e. (**b**) Color map displaying CFA injected SNS-Ai38 mouse spinal superficial layer presynaptic [$Ca^{2+}$] change in 30 ROIs chosen from the area shown in Figure 18f – j. (**c**) The proportion of ROIs displaying GABA evoked calcium transient grew after CFA injection. This increase was prohibited by co-application of $GABA_A$ receptor antagonists, bicuculline and picrotoxin, with 1 mM GABA (SNS-Ai38 Control, n = 5; SNS-Ai38 CFA, n = 8. SNS-Ai38 Control: GABA vs GABA+CGP55845, student t-test, P > 0.05; GABA vs GABA+CGP55845+Bicuculline+Picrotoxin, student t-test, P > 0.05; SNS-Ai38 CFA: GABA vs GABA+CGP55845, student t-test, P > 0.05; GABA vs GABA+CGP55845+Bicuculline+Picrotoxin, student t-test, P < 0.01). Error bars indicate SEM. **P < 0.01.

### 4.2.3 mRNA level of proteins related to the function of presynaptic $GABA_A$ receptors

The effect of $GABA_A$ receptors mainly depends on 3 factors, the $Cl^-$ gradient, GABA concentration and the density of $GABA_A$ receptors. If the $Cl^-$ gradient is larger, the electrochemical driven force would be bigger at the same resting potential. Previous studies reported that the sodium potassium chloride co-transporter (NKCC1) is crucial for the

$Cl^-$ homeostasis in DRG neurons[38,74,75]. And our group had provided evidence that the activity of NKCC1 is important for transient hypersensitivity of mice after nerve injury[61]. Our previous study also showed BDNF-TrkB signaling on DRG neurons generate a raise in intracellular [$Cl^-$] in nerve injured animal[61]. I therefore examined mRNA levels of all these proteins (NKCC1, BDNF, full length and truncated TrkB), which might be in the signaling pathway upregulating intracellular [$Cl^-$], in DRGs (**Figure 20**) and spinal cord dorsal horn (**Figure 21**) from intact and CFA injected mice with qRT-PCR. BDNF was found increased in ipsilateral side of both DRGs (Control: 1.00 ± 0.01; CFA: 11.68 ± 2.59) and spinal dorsal horn (Control: 1.00 ± 0.04; CFA: 1.69 ± 0.13) after CFA injection, which is consistent with previous studies, while mRNA of full-length (DRG: Control: 1.00 ± 0.01; CFA: 1.00 ± 0.12. SC: Control: 1.01 ± 0.02; CFA: 0.97 ± 0.03), truncated TrkB receptors (DRG: Control: 1.00 ± 0.01; CFA: 1.23 ± 0.19. SC: Control: 1.03 ± 0.02; CFA: 1.08 ± 0.05) and NKCC1 did not show significant change (DRG: Control: 1.00 ± 0.01; CFA: 1.04 ± 0.13. SC: Control: 1.05 ± 0.03; CFA: 1.11 ± 0.06).

The concentration of GABA can be regulated by 2 glutamic acid decarboxylase (GAD), GAD65 and GAD67, which are enzymes catalyzing the decarboxylation of glutamate to

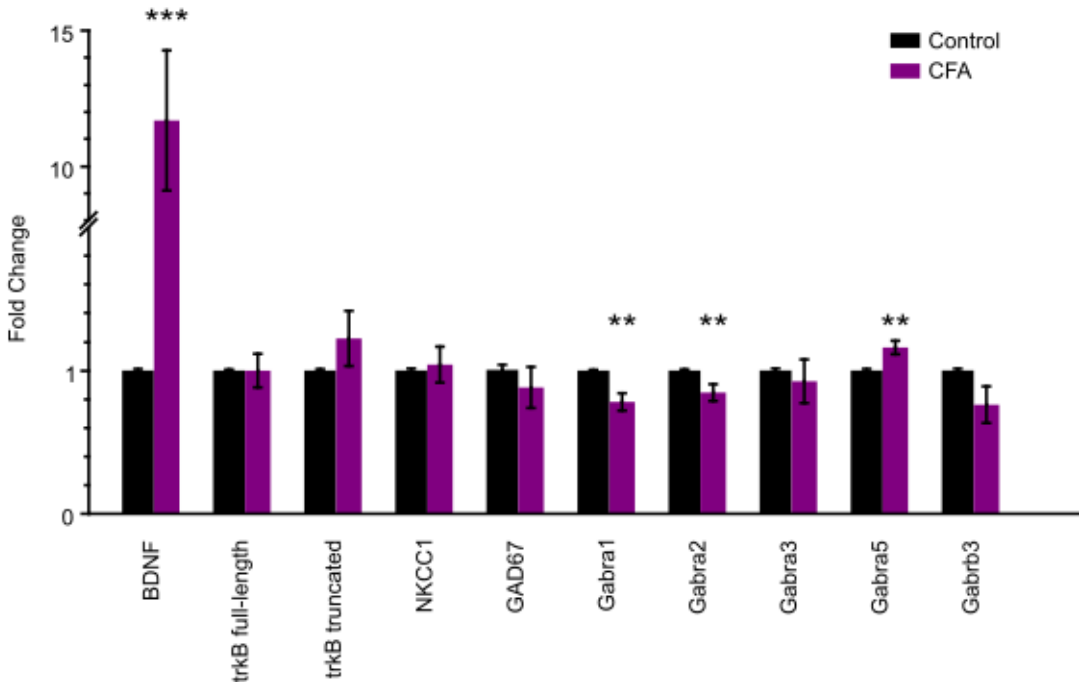


Figure 20: mRNA levels of proteins potentially influencing presynaptic GABAergic control in DRG (Control, n = 9; CFA, n = 9. Student t-test, Control vs CFA: BDNF, $P < 0.001$; trkB full-length, $P > 0.05$; trkB truncated, $P > 0.05$; NKCC1, $P > 0.05$; GAD67, $P > 0.05$; Gabra1, $P < 0.01$; Gabra2, $P < 0.01$; Gabra3, $P > 0.05$; Gabra5, $P < 0.01$; Gabrb3, $P > 0.05$). Error bars indicates SEM. **P < 0.01, ***P < 0.001

GABA, and GABA transporter 1 (GAT1) functioning as a GABA remover. None of them had a change on mRNA level in spinal cord after CFA injection (GAD65: Control: 1.03 ± 0.04; CFA: 1.01 ± 0.06. GAD67: Control: 1.00 ± 0.02; CFA: 0.96 ± 0.04. GAT1: Control: 1.01 ± 0.03; CFA: 0.97 ± 0.05), likewise GAD67 mRNA remained at the same level in DRGs (Control: 1.01 ± 0.04; CFA: 0.88 ± 0.14). $C_T$ value of GAD65 was found very high (> 30) in DRGs, which represented the mRNA level was too low for reliable test, and thus not used for analysis. mRNA level of GABA remover, GAT1, in DRGs was not examined, since all primary afferents are excitatory[13].

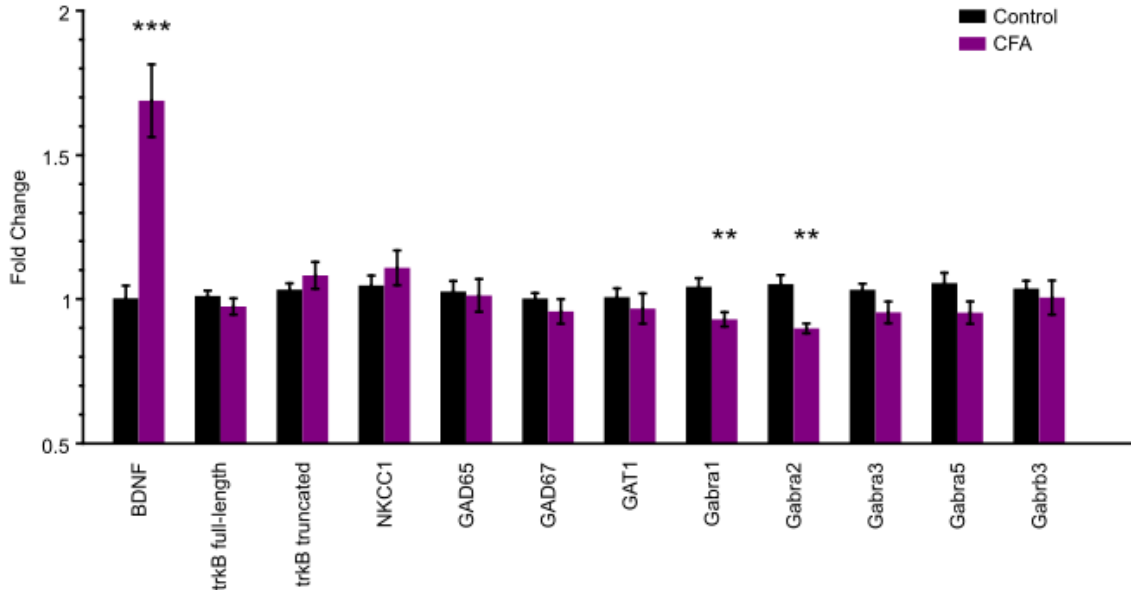


Figure 21: mRNA levels of proteins potentially influencing presynaptic GABAergic control in spinal dorsal horn ipsilateral side (Control, n = 18; CFA, n = 15. Student t-test, Control vs CFA: BDNF, P < 0.001; trkB full-length, P > 0.05; trkB truncated, P > 0.05; NKCC1, P > 0.05; GAD65, P > 0.05; GAD67, P > 0.05; GAT1, P > 0.05; Gabra1, P < 0.01; Gabra2, P < 0.01; Gabra3, P > 0.05; Gabra5, P > 0.05; Gabrb3, P > 0.05). Error bars indicates SEM. **P < 0.01, ***P < 0.001

Each $GABA_A$ receptors is composed of 5 subunits, and interface(s) between α and β subunit is/are binding site(s) for GABA[76]. α1-3, α5, and β3 subunits were reportedly expressed in DRG neurons[77]. Any change of these subunits may lead to the unexpected efficacy of GABA, therefore mRNA levels of these subunits were examined (**Figure 20; 21**). α1 and α2 subunits were found decreased in both DRG (gabra1: Control: 1.00 ± 0.004; CFA: 0.78 ± 0.06. gabra2: Control: 1.00 ± 0.01; CFA: 0.85 ± 0.06) and spinal cord (gabra1: Control: 1.04 ± 0.03; CFA: 0.93 ± 0.02. gabra2: Control: 1.05 ± 0.01; CFA: 0.90 ± 0.02) after inflammation, while α5 subunit was elevated only in DRG

(DRG: Control: 1.00 ± 0.01; CFA: 1.16 ± 0.05. SC: Control: 1.06 ± 0.04; CFA: 0.95 ± 0.04). No change was observed for mRNA levels of α3 (DRG: Control: 1.00 ± 0.01; CFA: 0.93 ± 0.15. SC: Control: 1.03 ± 0.02; CFA: 0.95 ± 0.04) and β3 subunits (DRG: Control: 1.00 ± 0.01; CFA: 0.76 ± 0.13. SC: Control: 1.04 ± 0.03; CFA: 1.01 ± 0.06).

In summary, a raise of BDNF may influence the BDNF-TrkB signaling pathway, but no significant change of NKCC1 mRNA was observed. The proteins responsible for GABA production and removal were not affected by CFA injection on mRNA level in both DRGs and spinal dorsal horn. Variations in mRNA levels of $GABA_A$ receptor subunits were observed after inflammation. However, the conduction of $GABA_A$ receptors in DRG neurons was not significantly shifted by CFA injection, which might due to the increase of α1 and α2 subunits and decrease of α5 subunits compensate each other.

### 4.2.4 Upregulated NKCC1 contributed to mechanical hypersensitivity development after peripheral inflammation (experiments carried by Flavia Frattini)

Although mRNA level of NKCC1 in DRGs was not altered after peripheral inflmmation, this does not rule out that intracellular [$Cl^-$] increase depends on the enhanced activity of NKCC1, which is determined by the protein level of plasma membrane NKCC1. My colleague did NKCC1 staining on DRG cryosections from intact and CFA injected mice and quantified the fluorescence intensity on cell membrane. The result revealed that the CFA induced peripheral inflammation significantly upregulated NKCC1 level in plasma membrane of both small and large neurons (**Figure 22**).

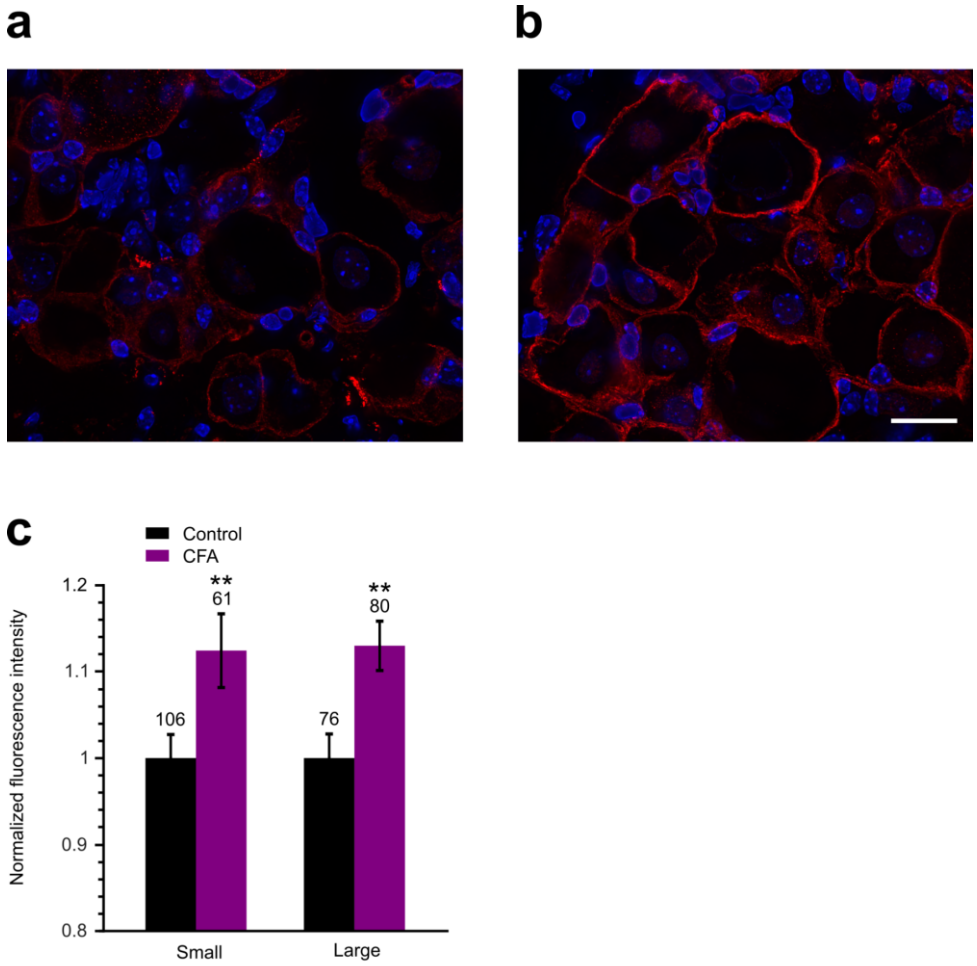


Figure 22: Peripheral inflammation upregulated cell surface NKCC1 level in DRG neurons. NKCC1 (red) and DAPI (blue) were labeled on DRG slices from control (**a**) and CFA injected mice (**b**). (**c**) the normalized fluorescence intensity of NKCC1 increased in both small and large DRG neurons 2-day after CFA injection from 3 control and 3 CFA injected mice (small control: n = 106; small CFA: n = 61; large control: n = 76; large CFA n= 80; small control vs small CCI, unpaired student t-test, $P < 0.01$; large control vs large CCI, unpaired student t-test, $P < 0.01$). Error bars indicates SEM. **$P < 0.01$. Scale bars, (**a, b**) 20 μm (only shown in **b**).

Our previous study had shown that bumetanide, a NKCC1 inhibitor, is able to alleviate the thermal hyperalgesia caused by nerve injury[61], likely via lightening the upregulated NKCC1 induced intracellular [$Cl^-$] uprise. Due to the fact that the CFA injection also leads to the increase of [$Cl^-$] and NKCC1 in DRG neurons, we reasoned that bumetanide probably had an analgesic effect in inflammatory pain. Mice were treated with bumetanide 2, 7, 14, and 28 days after CFA injection (**Figure 23**). The paw withdraw latency upon mechanical stimulation was significantly increased on the 2$^{nd}$ day and

even furthered on the 7th day, and the increased baseline level of withdraw latency from the 7th day suggested a long term effect of bumetanide (**Figure 23a**). Interestingly, bumetanide treatment did not show any influence on inflammation induced thermal hyperalgesia (**Figure 23b**).

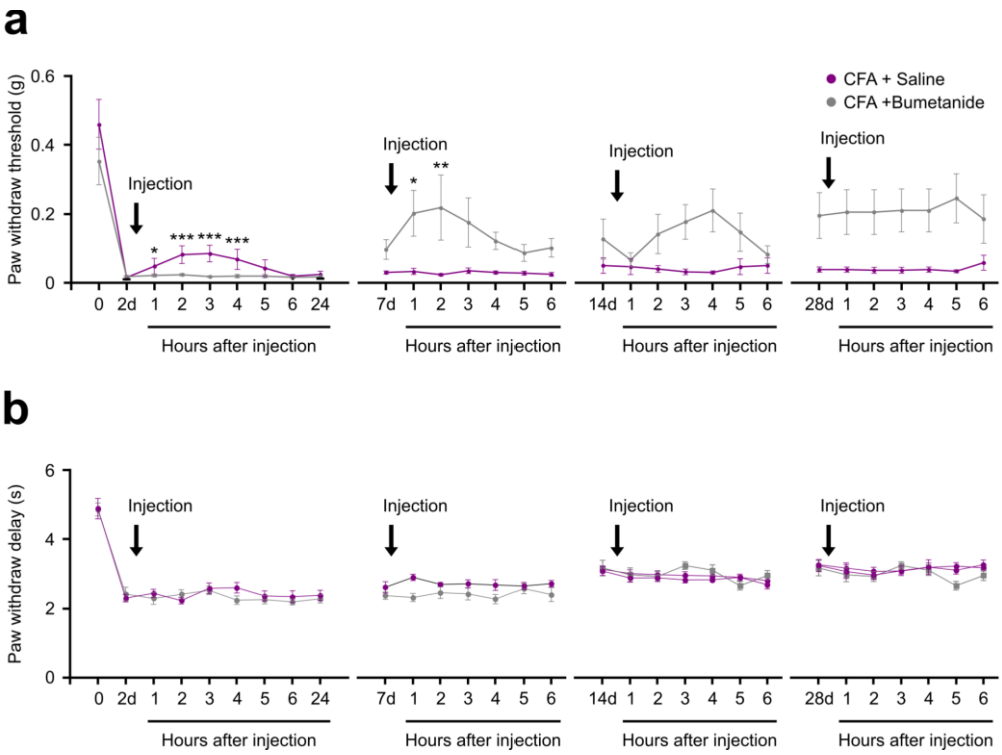


Figure 23: Intraperitoneal administration of NKCC1 inhibitor bumetanide alleviated mechanical but not thermal hypersensitivity caused by peripheral inflammation. Saline or bumetanide were intraperitonealy injected in mice (CFA + Saline: n = 6; CFA + Bumetanide: n = 6) on the 2nd, 7th, 14th and 28th day after CFA injection. Both mechanical and thermal sensitivity were evaluated in these mice. (**a**) Bumetanide injection alleviated mechanical allodynia on the 2nd and 7th day ( Bumetanide effect was analyzed with repeated two-way analysis of variance (ANOVA) (factor 1: time; factor 2: injection): variance of sensitivity according to time (factor 1), 2nd day, $p < 0.01$; 7th day, $p > 0.05$; 14th day, $p > 0.05$; 28th day, $p > 0.05$. post-hoc Bonferroni: 2d vs 2d-1h, $p < 0.05$; 2d vs 2d-2h, $p < 0.001$; 2d vs 2d-3h, $p < 0.001$; 2d vs 2d-4h, $p < 0.001$; 7d vs 7d-1h, $p < 0.05$; 7d vs 7d-2h, $p < 0.01$). Although no further anti-nociceptive effect was observed on the 14th and 28th day, the baseline mechanical sensitivity was upregulated for the 7th day after CFA injection (repeated two-way ANOVA: variance of sensitivity according to injection (factor 2), 2nd day, $p > 0.05$; 7th day, $p < 0.05$; 14th day, $p < 0.05$; 28th day, $p < 0.05$). (**b**) CFA induced thermal hypersensitivity could not be alleviated by bumetanide injection (repeated two-way ANOVA: factor 1, $p > 0.05$ for 2nd, 7th, 14th and 28th day; factor 2, $p > 0.05$ for 2nd, 7th, 14th, and 28th day). Error bars indicate SEM. *P < 0.05; **P < 0.01; ***P < 0.001.

Taken together, these results indicated that the putative nociceptor NKCC1 upregulation, which is likely responsible for the depolarizing shift of $E_{Cl}$ in small diameter neurons, caused by CFA injection induced inflammation specifically contributes to the development of mechanical hypersensitivity. This is consistent with the idea that the

$GABA_A$ receptors mediated presynaptic control contributes to the inflammation induced mechanical hypersensitivity suggested by the behavior result of SNS-Ai38 mice (**Figure 14c**).

## 4.3 A subpopulation of nociceptors crucial for presynaptic mediated mechanical allodynia in inflammatory pain

### 4.3.1 Difference between SNS-Cre and advillin-Cre

In addition to SNS-Ai38 mice, advillin-Ai38 mice were also used for 2-photon calcium imaging to study presynaptic GABAergic control. Advillin-Ai38 mice were generated by crossing advillin-cre mice, which express Cre recombinase in majority of sensory neurons including both nociceptors and non nociceptors. Due to the fact that superficial layer of spinal dorsal horn is only innervated by nociceptors, 2-photon calcium imaging using spinal cords from SNS-Ai38 and advillin-Ai38 mice in this area was expected to show accordant results. Indeed, the inhibitor effect of GABA on KCl induced calcium transient was also observed in advillin-Ai38 mice spinal cord (Whole chamber perfusion: No-change: 43 %; More $Ca^{2+}$ transient: 8 %; Less $Ca^{2+}$ transient: 49 %. Local perfusion: No-change: 41 %; More $Ca^{2+}$ transient: 14 %; Less $Ca^{2+}$ transient: 45 %. **Figure 24c, e; 25a**), and this inhibition could be abolished after nerve injury (Whole chamber perfusion: No-change: 52 %; More $Ca^{2+}$ transient: 35 %; Less $Ca^{2+}$ transient: 13 %. Local perfusion: No-change: 67 %; More $Ca^{2+}$ transient: 27 %; Less $Ca^{2+}$ transient: 7 %), BDNF treatment (Whole chamber perfusion: No-change: 57 %; More $Ca^{2+}$ transient: 28 %; Less $Ca^{2+}$ transient: 14 %. Local perfusion: No-change: 70 %; More $Ca^{2+}$ transient: 26 %; Less $Ca^{2+}$ transient: 4 %) and CFA injection induced inflammation (Whole chamber perfusion: No-change: 65 %; More $Ca^{2+}$ transient: 9 %; Less $Ca^{2+}$ transient: 25 %. Local perfusion: No-change: 55 %; More $Ca^{2+}$ transient: 43 %; Less $Ca^{2+}$ transient: 2 %) (**Figure 24; 25; 26a**). And the calcium influx caused by GABA (Whole chamber perfusion: 1.7 ± 0.9 %. Local perfusion: 10.7 ± 2.3 %) was also not significantly altered by nerve injury (Whole chamber perfusion: 2.1 ± 1.4 %. Local perfusion: 10.3 ± 8.3 %) and BDNF

treatment in advillin-Ai38 spinal cord (Whole chamber perfusion: 1.6 ± 0.7 %. Local perfusion: 18.8 ± 2.3 %) (**Figure 24; 25; 26b**). However, the CFA injection induced increase of GABA generated calcium influx observed in SNS-Ai38 mice spinal cord (**Figure 17b**), suggesting an enhanced excitatory effect of GABA, was absent in advillin-Ai38 mice spinal cord (Whole chamber perfusion: CFA: 1.1 ± 0.4 %. Local perfusion: CFA: 18.7 ± 4 %. **Figure 24p; 25d; 26b**). Meanwhile, my colleague found that the mechanical allodynia was only partially developed in SNS-$\beta3^{-/-}$ mice after CFA injection (**Figure 14c**), while advillin-$\beta3^{-/-}$ mice, generated by crossing advillin-Cre and $\beta3^{fl/fl}$ mice developed mechanical allodynia to the same level as their control litter mates ($\beta3^{fl/fl}$) (**Figure 27**). These difference between advillin-Cre and SNS-Cre generated transgenic mice strongly suggested the different expression patterns between 2 Cre mouse lines, and this difference may be used to study the subpopulation of nociceptors important for peripheral inflammation induced mechanical allodynia.

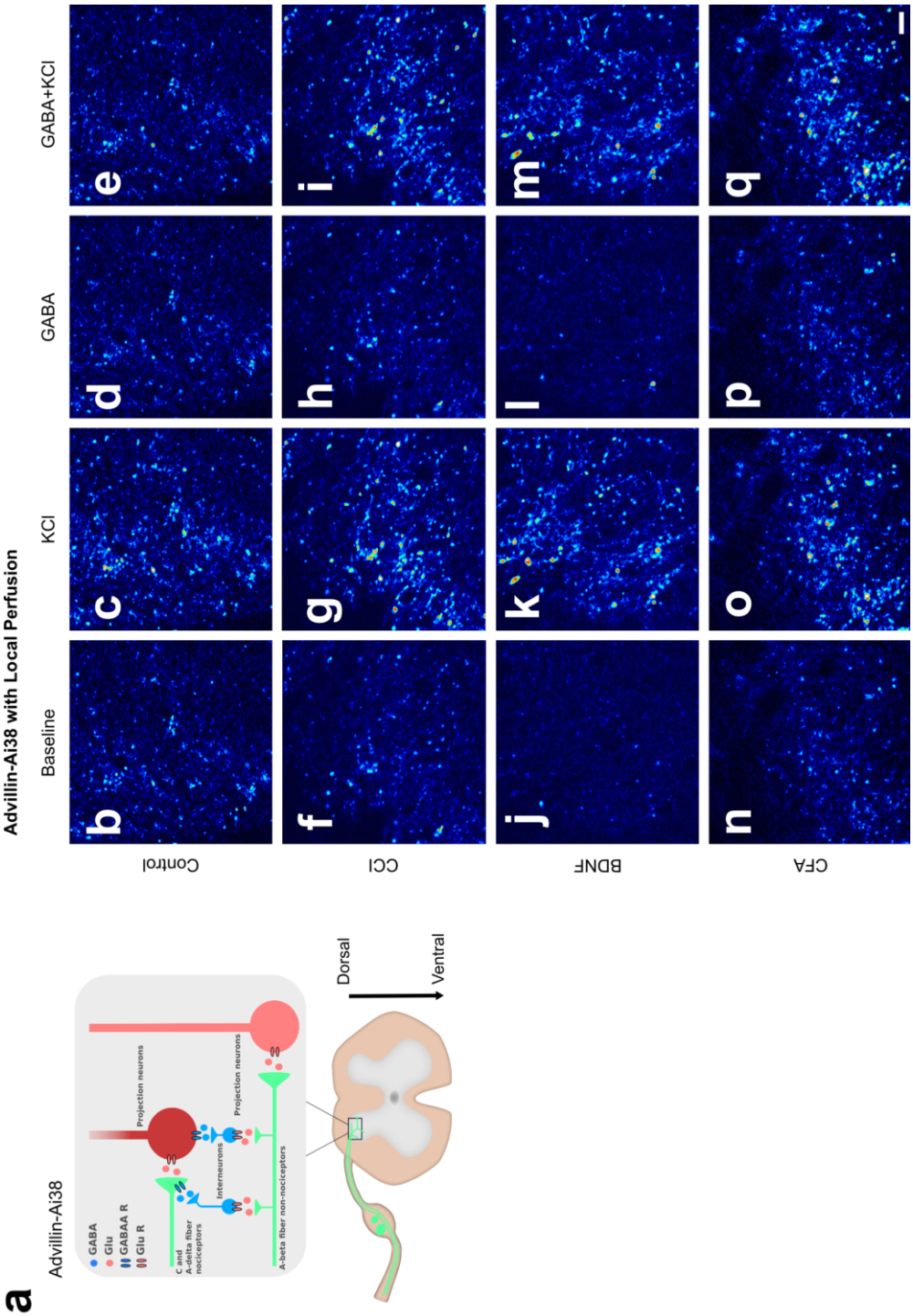


Figure 24: 2-photon images of acutely dissected spinal cord slices from advillin-Ai38 mice (control, CCI, BDNF, CFA).(**a**) A diagram showing expression patter of GCaMP signal in advillin-Ai38 mice. 2-photon microscope imaged GCaMP3 signal indicating [Ca2+] in Control (**b - e**), CCI (**f – l**), BDNF (**j – m**) CFA (**n - q**) spinal cord superficial layer in response to various stimuli. Scale bars, (**b – q**) 10 µm (only shown in **q**)

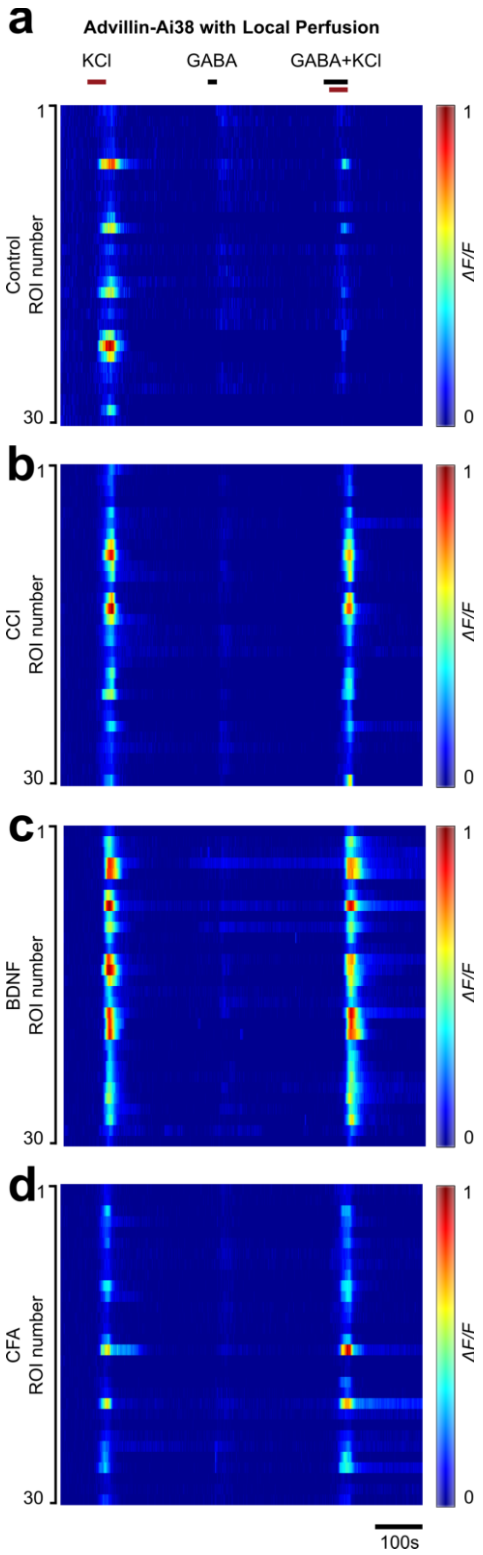


Figure 25: The color maps of 2-photon calcium imaging of acutely dissected spinal cord slices from advillin-Ai38 mice. Each color map represents presynaptic calcium intensity in 30 ROIs. The figures for control (**a**), CCI (**b**), BDNF (**c**) and CFA (**d**) groups are correlated with the example 2-photon images show in Figure 24.

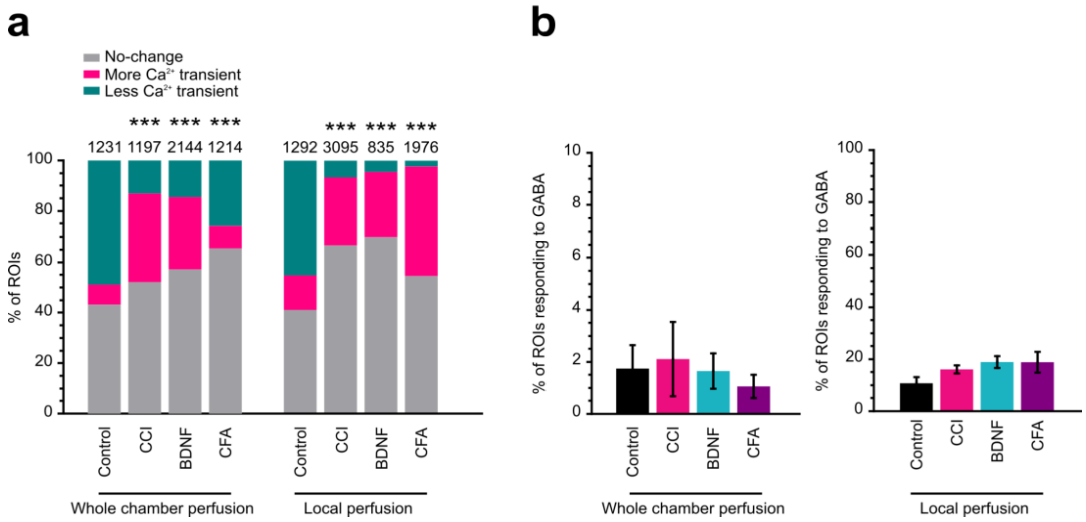


Figure 26: The influence of GABA on presynaptic activity in acutely dissected spinal cord slices from advillin-Ai38. The effect of GABA was examined by using 2 different application methods, whole chamber perfusion and local perfusion, which can influence the concentration of applied chemicals. (**a**) The inhibitory effect of 1 mM GABA on high KCl induced $Ca^{2+}$ influx was attenuated by CCI, BDNF treatment and CFA injection (Whole chamber perfusion: Control mice n = 5; CCI mice n = 6; BDNF mice n = 3; CFA mice n = 3. chi-squared test, Control vs CCI, $P < 0.001$; Control vs BDNF, $P < 0.001$; Control vs CFA, $P < 0.001$. Local perfusion: Control mice n = 3; CCI mice n = 3; BDNF mice n = 3; CFA mice n = 3. chi-squared test, Control vs CCI, $P < 0.001$; Control vs BDNF, $P < 0.001$; Control vs CFA, $P < 0.001$.). (**b**) GABA induced $Ca^{2+}$ transient was not influenced by CCI, BDNF treatment or CFA injection (Whole chamber perfusion: Control slice, n = 4; CCI slice, n = 5; BDNF slice, n = 6; CFA slice, n = 6. Student t-test, Control vs CCI, $P > 0.05$; Control vs BDNF, $P > 0.05$; Control vs CFA, $P > 0.05$. Local perfusion: Control slice, n = 6; CCI slice, n = 11; BDNF slice, n = 3; CFA slice, n = 6. Student t-test, Control vs CCI, $P > 0.05$; Control vs BDNF, $P > 0.05$; Control vs CFA, $P > 0.05$.). Error bars indicate SEM. ***$P < 0.001$.

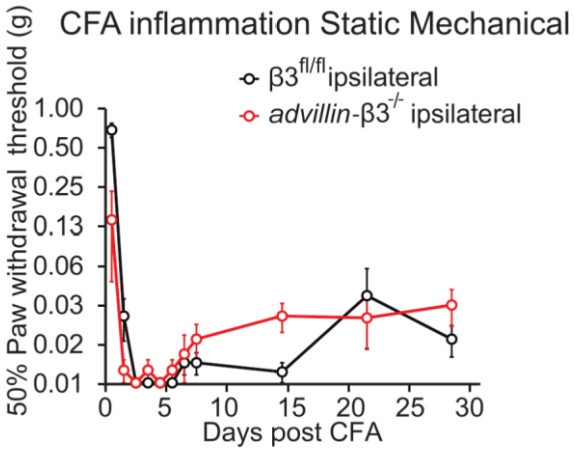


Figure 27: Mechanical allodynia induced by peripheral inflammation developed to similar level in advillin-$\beta3^{-/-}$ and $\beta3^{fl/fl}$ ($\beta3^{fl/fl}$: n = 7; advillin-$\beta3^{-/-}$: n = 6. Repeated two-way ANOVA (0 - 28d): factor time P < 0.0001, factor genotype P < 0.01, Bonferroni post hoc $\beta3^{fl/fl}$ vs advillin-$\beta3^{-/-}$ on 0d, P < 0.0001. Repeated two-way ANOVA (1 – 28 day): factor time P < 0.01, factor genotype P > 0.05).

### 4.3.2 Advillin-Cre is not expressed in all peptidergic nociceptors as SNS-Cre

SNS-Cre and advillin-Cre lines are widely used to study nociceptors and all sensory neurons respectively. However, N Agawal et al., who originally produced SNS-Cre mice used in my study, showed that about 93% of small neurons in DRG are Cre positive[55]. And S Zurborg et al. Suggested Cre recombinase could be found in more than 80% of DRG neurons in advillin-Cre mouse[56]. Considering about 70% of DRG neurons are nociceptors[78], it is very possible that a subpopulation of SNS-Cre expressing nociceptors would not express advillin, i.e. this subpopulation falls into the 20% of DRG neurons which are advillin negative. And they might be responsible for the difference in 2-photon calcium imaging between SNS-Ai38 and advilllin-Ai38 mice, and difference in mechanical allodynia development between SNS-$\beta3^{-/-}$ and advillin-$\beta3^{-/-}$ mice as well.

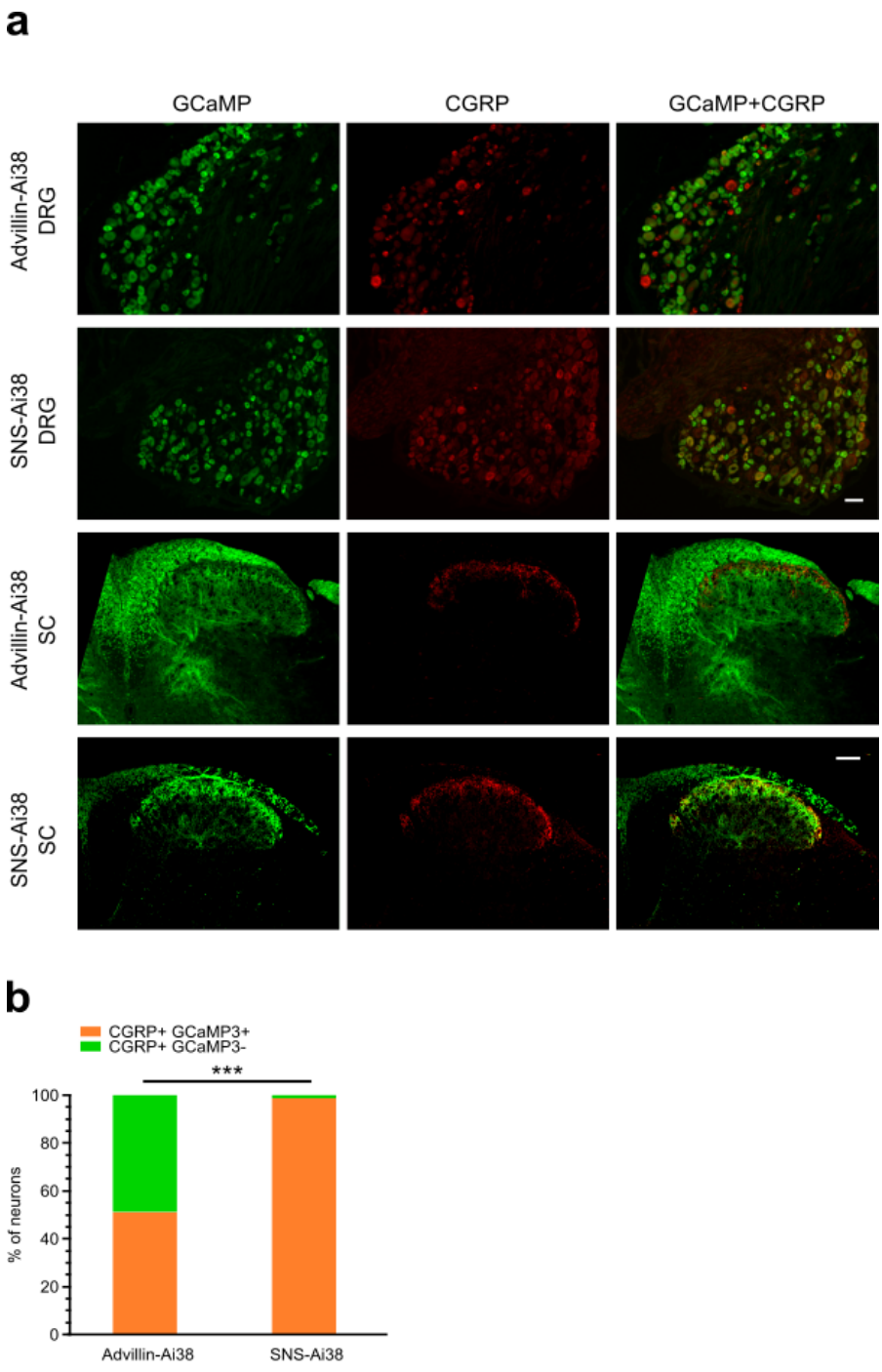


Figure 28: A big proportion of CGRP positive neurons are GCaMP3 negative in advillin-Ai38 mice. (**a**) upper 2 panels showed GCaMP3 and CGRP signals in DRGs from advillin-Ai38 and SNS-Ai38 mice. Lower 2 panels showed GCaMP3 and CGRP signals in spinal cords from advillin-Ai38 and SNS-Ai38 mice. (**b**) 51% and 99% of CGRP positive DRG neurons expressed GCaMP3 in advillin-Ai38 and SNS-Ai38 mice respectively (advillin-Ai38, 3 mice, n = 197; SNS-Ai38, 3 mice, n = 156. Fisher's exact test, $p < 0.001$). Scale bars (**a**) DRG: 50 μm; SC: 100 μm.*** $p < 0.0001$

Nociceptors can be divided into 2 classes, peptidergic and non-peptidergic nociceptors. Calcitonin gene-related peptide (CGRP) and isolectin B4 (IB4) are commonly used to

mark these 2 classes respectively. DRGs and spinal cords with fluorescent calcium indicator, GCaMP, from SNS-Ai38 and advillin-Ai38 animal were cryosectioned and stained with CGRP (**Figure 28**) and IB4 (**Figure 29**) to investigate the expression patterns of corresponding Cre recombinases. Interestingly, Almost all (99 %) CGRP positive neurons carried GCaMP signal in SNS-Ai38 DRGs compare to 51 % in advillin-Ai38 DRGs (**Figure 28b**), while GCaMP signal were found in virtually all IB4 positive neurons from both SNS-Ai38 (97 %) and advillin-Ai38 DRGs (100 %) (**Figure 29)**. The staining on spinal cords exhibited consistent results. As expected, CGRP positive area, lamina I and lamina II out layer, perfectly overlaps the very dorsal region of GCaMP signal in spinal cord from SNS-Ai38 mice (**Figure 28a**). However, the CGRP staining on spinal cord from *advillin-Ai38* mice reveals that the CGRP positive area has weaker GCaMP signal compare to other GCaMP positive area (**Figure 28a**). IB4 staining, on the other hand, co-localized with GCaMP signal in spinal cord from both SNS-Ai38 and advillin-Ai38 mice (**Figure 29**).

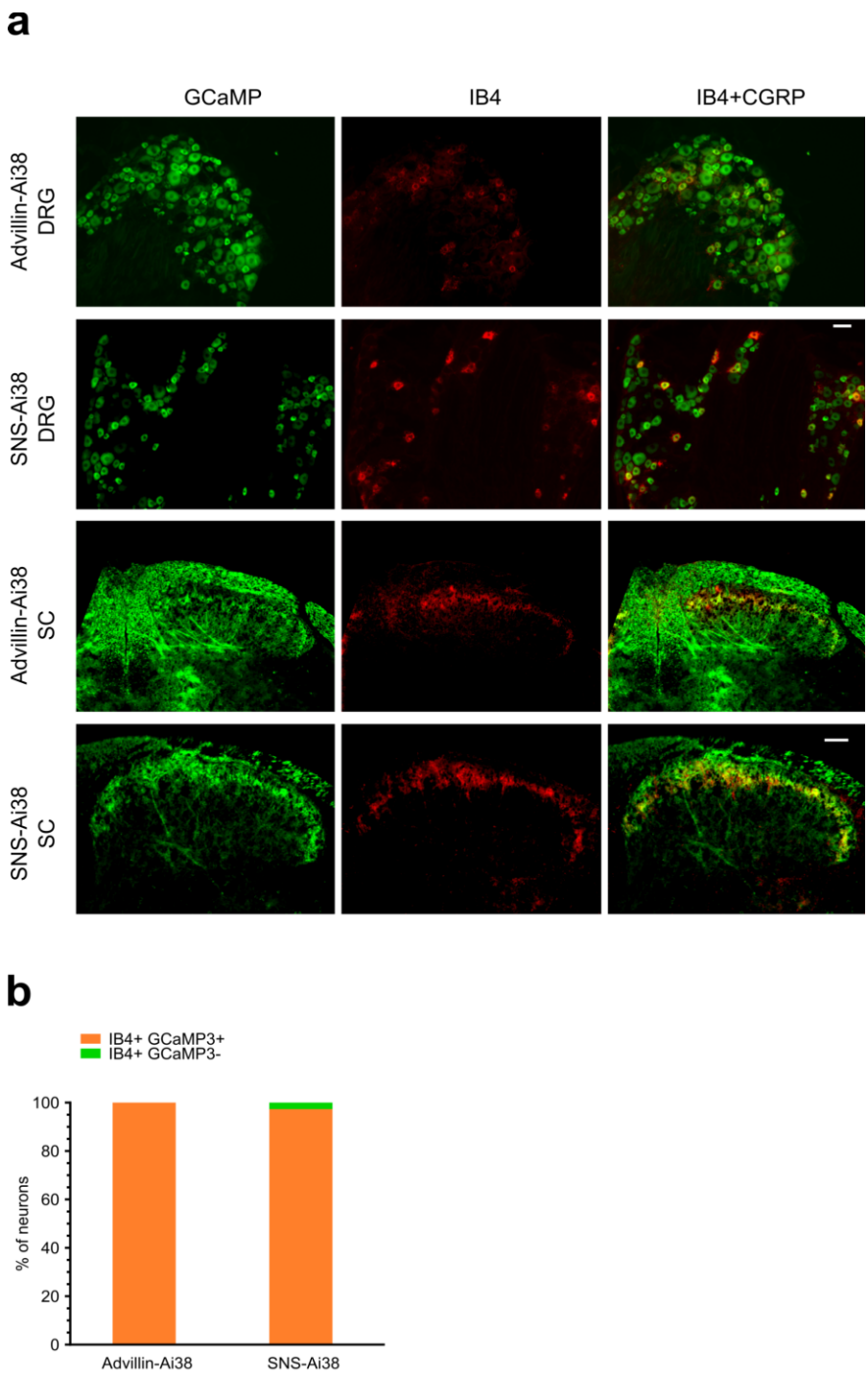


Figure 29: All IB4 positive DRG neurons expressed GCaMP3 signal in both advillin-Ai38 and SNS-Ai38 mice. (**a**) upper 2 panels showed GCaMP3 and IB4 signals in DRGs from advillin-Ai38 and SNS-Ai38 mice. Lower 2 panels showed GCaMP3 and CGRP signals in spinal cords from advillin-Ai38 and SNS-Ai38 mice.(**b**) 100% and 97% of IB4 positive DRG neurons expressed GCaMP3 in advillin-Ai38 and SNS-Ai38 mice respectively (advillin-Ai38, 3 mice, n = 108; SNS-Ai38, 3 mice, n = 111. Fisher's exact test, $p > 0.05$). Scale bars (**a**) DRG: 50 μm; SC: 100 μm.

In conclusion, these immunohistochemistry results revealed that there is a expression difference of Cre recombinase in peptidergic nociceptors between SNS-Cre and advillin-Cre lines. This difference suggests that the excitatory effect of GABA observed in SNS-Ai38 after inflammation was contributed by central terminals of a subpopulation of peptidergic nociceptors, which does not express Cre in advillin-Cre animal. And the fully developed mechanical allodynia of advillin-$\beta3^{-/-}$ mice might be due to the incomplete knockout of $GABA_A$ receptor $\beta3$ subunits in peptidergic nociceptors.

### 4.3.3 IB4 negative and positive putative nociceptor were similar changed by peripheral inflammation

To further investigate the difference between peptidergic and non-peptidergic nociceptors after inflammation, I labeled non-peptidergic DRG neurons with IB4 and thus separated them from peptidergic nociceptors in primary cell culture. Calcium imaging was applied to examine their physiological properties. CFA injection, different from CCI and BDNF incubation, successfully altered the response of small-sized DRG neurons to GABA. The percentages of neurons displaying calcium transient were significantly increased by CFA injection in small-sized neurons (IB4- Control: 17 %; IB4- CFA: 38 %; IB4+ Control: 32 %; IB4+ CFA: 63 %. **Figures 30**). This result is consistent with my observation of presynapses after inflammation and offers more evidence of excitatory effect switch of GABA on DRG nociceptors caused by CFA injection. However, a bigger proportion of IB4+ neurons exhibited GABA-evoked calcium transient compare to IB4- neurons in both control and CFA groups (**Figures 30**).

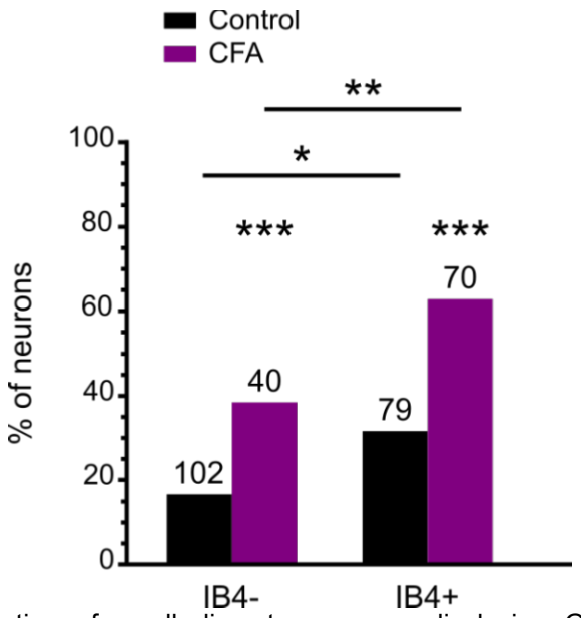


Figure 30: The proportion of small diameter neurons displaying GABA evoked calcium transient significantly increased in IB4- and IB4+ subpopulations after peripheral inflammation (IB4- Control vs IB4- CFA, chi-squared test, $P < 0.001$; IB4+ Control vs IB4+ CFA, chi-squared test, $P < 0.001$). The proportion of GABA activated neurons is higher in IB4+ subpopulation despite of CFA injection (IB4- Control vs IB4+ Control, chi-squared test, $P < 0.05$; IB4- CFA vs IB4+ CFA, chi-squared test, $P < 0.01$). Control mice, n = 4; CFA mice, n = 3. The number of recorded neurons is on top of each bar. *P < 0.05, **P < 0.01, ***P < 0.001.

The amplitude of calcium transient ($R_{340/380} - R_0$) induced by high KCl in IB4- and IB4+ neurons was raised by inflammation (IB4- Control: 1.06 ± 0.07; IB4- CFA: 1.49 ± 0.07; IB4+ Control: 1.04 ± 0.08; IB4+ CFA: 1.54 ± 0.09. **Figure 31a**), and co-application of GABA could not significantly change this increase (IB4- Control: 0.85 ± 0.06; IB4- CFA: 1.09 ± 0.07; IB4+ Control: 0.82 ± 0.07; IB4+ CFA: 1.18 ± 0.08. **Figure 31a**). However, GABA effectively decreased KCl generated calcium transient in all small diameter neurons in spite of CFA injection (**Figure 31b**), which is different from the result of 2-photon calcium imaging on presynapses (**Figure 17a, c**). This may be due to the prominent shunting effect caused by $GABA_A$ receptors activation in cell soma in both control and CFA groups. This effect could weaken KCl induced depolarization and in turn decrease the calcium transient. The amplitude of GABA-evoked calcium transient was only seen increased in IB4- neurons but not in IB4+ neurons after inflammation (IB4- Control: 0.06 ± 0.02; IB4- CFA: 0.13 ± 0.03; IB4+ Control: 0.07 ± 0.02; IB4+ CFA: 0.10 ± 0.02. **Figure 30b**) suggesting a stronger GABA induced depolarization in IB4- putative nociceptors.

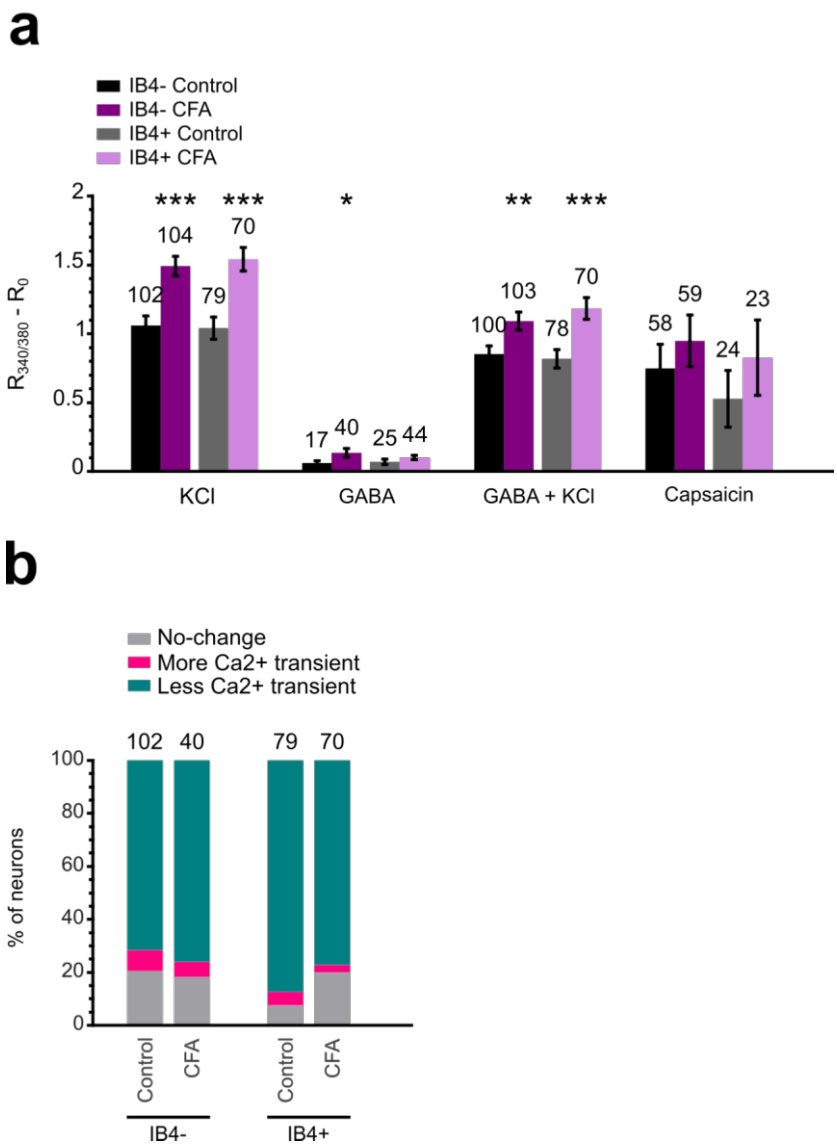


Figure 31: GABA inhibited the high KCl triggered calcium transient in IB4- and IB4+ small diameter neurons. (**a**) CFA injection caused the increase of peak value of calcium transient ($R_{340/380}$ - $R_0$) triggered by high KCl (IB4- Control vs IB4- CFA, $P < 0.001$; IB4+ Control vs IB4+ CFA, $P < 0.001$. Student t-test) and GABA (1mM) +KCl (IB4- Control vs IB4- CFA, $P < 0.01$; IB4+ Control vs IB4+ CFA, $P < 0.001$. Student t-test) in IB4- and IB4+ neurons. The rise of 1 mM GABA evoked calcium peak only appeared in IB4- group after inflammation (IB4- Control vs IB4- CFA, $P < 0.05$; IB4+ Control vs IB4+ CFA, $P > 0.05$. Student t-test), and 1 μM capsaicin evoked calcium peak was not altered by inflammation (IB4- Control vs IB4- CFA, $P > 0.05$; IB4+ Control vs IB4+ CFA, $P > 0.05$. Student t-test). (**b**) GABAergic inhibition on high KCl induced calcium transient was not influenced by CFA induced inflammation in IB4- and IB4+ small diameter neurons (IB4-: Control vs CFA, $P > 0.05$. IB4+: Control vs CFA, $P > 0.05$). Control mice, n = 4; CFA mice, n = 3. The number of recorded neurons is on top of each bar. Error bars indicate SEM. *P < 0.05, **P < 0.01, ***P < 0.001.

It is well-known that the intracellular calcium concentration ($[Ca^{2+}]$) is crucial for various neuronal processes including neuronal excitability, transmitter release, gene tran-

scription etc[79]. Therefore, the homeostasis of [$Ca^{2+}$] is profoundly important for proper function of neurons. Calcium dysregulation in brain neurons had been reported in numerous pathological conditions[80]. Although an upregulation of resting [$Ca^{2+}$] was mostly observed in brain neurons in pathological conditions[80], previous studies suggested that resting [$Ca^{2+}$] decreased in DRG neurons after nerve injury[81]. Consistently, my results showed the resting [$Ca^{2+}$] ($R_{340/380}$) in CCI small diameter neurons (CCI: 0.59 ± 0.03) was significantly lower than that in Control neurons (Control: 0.77 ± 0.02) (**Figure 32a**). In addition, CFA induced peripheral inflammation also significantly downregulated the resting [$Ca^{2+}$] in both IB4- and IB4+ small diameter neurons (IB4- Control: 0.83 ± 0.04; IB4- CFA: 0.72 ± 0.03; IB4+ Control: 0.24 ± 0.06; IB4+ CFA: 0.96 ± 0.04. **Figure 32b**). Interestingly, the resting [$Ca^{2+}$] of IB4- neurons was lower than that of IB4+ neurons in both control and CFA injected groups (**Figure 32b**). Noticeably, BDNF treatment increased the resting [$Ca^{2+}$] rather than decreasing it (BDNF: 0.89 ± 0.03. **Figure 32a**) despite it could mimic the effect of CCI on both cellular and behavior levels[61].

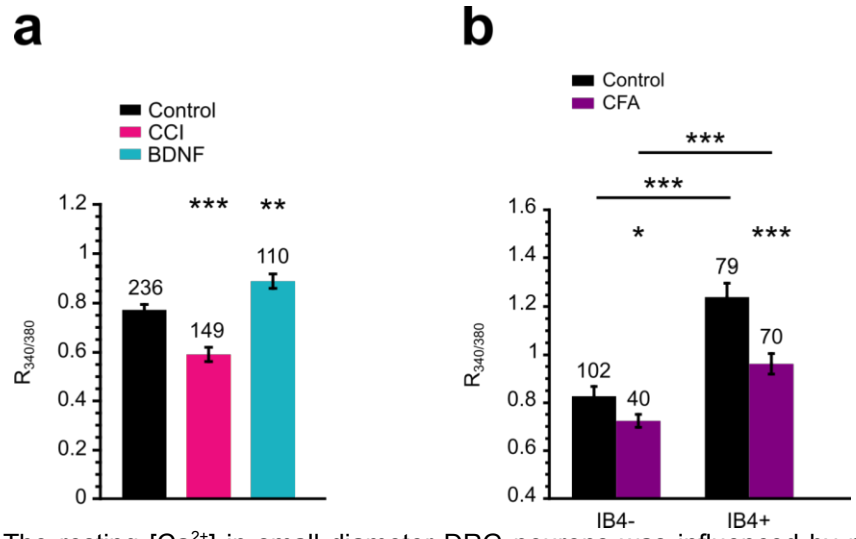


Figure 32: The resting [$Ca^{2+}$] in small diameter DRG neurons was influenced by nerve injury, BDNF and peripheral inflammation. (**a**) The resting [$Ca^{2+}$] was downregulated in small diameter neurons from CCI mice (Control vs CCI, student t-test, $P < 0.001$). BDNF treatment elevated the resting [$Ca^{2+}$] in small diameter neurons (Control vs BDNF, student t-test, $P < 0.001$). (**b**) The resting [$Ca^{2+}$] was downregulated in IB4- and IB4+ small diameter neurons from CFA injected mice (IB4-: Control vs CFA, $P < 0.05$. IB4+: Control vs CFA, $P < 0.001$. Student t-test). The resting [$Ca^{2+}$] in IB4+ neurons is higher than IB4- neurons despite of CFA injection (Control: IB4- vs IB4+, $P < 0.001$. CFA: IB4- vs IB4+, $P < 0.001$. Student t-test). Control mice, n = 4; CFA mice, n = 3. The number of recorded cells is on top of each bar. Error bars indicate SEM. *$P < 0.05$, **$P < 0.01$, ***$P < 0.001$.

In general, these calcium imaging data showed dramatic changes of small sized DRG neurons after inflammation, and it suggested there is a considerable variation between IB4- and IB4+ neurons. GABA exhibited a more excitatory effect after inflammation, which is consistent with 2-photon imaging data from spinal cords of SNS-Ai38 mice. However, whether the differences between SNS-cre and advillin-cre generated transgenic mice in 2-photon calcium imaging (SNS-Ai38 and advillin-Ai38) and behavior tests (SNS-$\beta3^{-/-}$ and advillin-$\beta3^{-/-}$) are due to the different Cre expression in peptidergic neurons cannot be concluded yet. First, IB4- and IB4+ neurons were generally changed towards the same direction by inflammation; Second, cultured DRG neurons may offer valuable information, but the recordings on somas may also provide different results compare to recordings on central terminals. Therefore, further approach with clear labeling of peptidergic and/or non-peptidergic central terminals is required to answer this question.

# 5 Discussion

## 5.1 GABAergic presynaptic control in neuropathic pain

### 5.1.1 Intracellular [$Cl^-$] and presynaptic GABAergic inhibition

The principle inhibitory effect of GABA is mediated by the activation of ionotropic $GABA_A$ receptors which increase membrane permeability to chloride. Thus the intracellular [$Cl^-$] is critical for a proper functioning GABAergic inhibition. The cation chloride cotransporters, such as inwardly directed NKCCs and outwardly directed KCCs, play a major role in maintaining intracellular [$Cl^-$]. In CNS, highly expressed KCC2 keeps low intracellular [$Cl^-$] in mature neurons[34], so the activation of $GABA_A$ receptors generates an inward flow of $Cl^-$ and hyperpolarizes the neurons. Mature DRG neurons, unlike CNS neurons, do not extrude chloride ions to the level lower than extracellular space due maintain a relatively high intracellular [$Cl^-$][34] compare to CNS neurons due to the predominantly expressed NKCC1 and low or absent expression of KCC2, and the reversal potential of Chloride is more positive than membrane potential. Therefore, the mechanism of GABAergic inhibition on DRG neurons is different from that on CNS neurons. The opening of ionotropic $GABA_A$ receptors permits an outflow of $Cl^-$ and depolarized the DRG neurons, which is named as PAD (primary afferent depolarization) when this happens on central terminals. PAD rather inhibits transmitter release than facilitates it. Two explanations had been proposed for its inhibitory effect: suppressing the transmitter release by inactivating the voltage gated calcium channels; hampering the action potential by either inactivating the voltage gated sodium channels or shunting effect, or both of them. It is reasonable to speculate that the stronger PAD may fail the inhibition based on these proposed mechanisms, and it may even be converted to excitation and activate the transmitter release when itself could directly evoke action potentials.

Previous studies have suggested an increase of intracellular [$Cl^-$] in DRG neurons after nerve injury by showing the increased activity of NKCC1 and a depolarizing shift of

$E_{Cl}$[61,74,82–84]. My chloride imaging on Clomeleon mice DRGs and my colleague's perforated patch clamp results confirmed the rise of intracellular [$Cl^-$] in both small and large DRG neurons on ex vivo level 2 days after nerve injury. And it seems like this increase is not strong enough for GABA to switch its role from inhibitory to excitatory, since the proportion of neurons displaying GABA-evoked calcium transient was not changed by nerve injury. Takkala et al., by using computer simulations and dynamic clamp experiments, provided evidence that the depolarizing shift of $E_{Cl}$ and increased intrinsic excitability were both necessary for PAD-induced spiking[85]. Therefore, the reason that no change of GABA-evoked calcium transient was observed after nerve injury may because that the intrinsic excitability of DRG neurons probably was not affected. Besides, the reduced $G_{GABA}$ may also limit the depolarization caused by GABA. Nevertheless, all these evidences about elevated [$Cl^-$] in pathological conditions were acquired from neuron soma studies; whether the [$Cl^-$] increases in central terminals after nerve injury and therefore enhances PAD was still unclear.

### 5.1.2 Nerve injury elevates presynaptic [$Cl^-$] and abolishes GABAergic presynaptic inhibition

The 2-photon calcium imaging on central terminals of nociceptors was employed to investigate the effect of GABA on presynapses. Acute spinal cord slices were prepared from advillin-Ai38 and SNS-Ai38 mice, where calcium indicator GCaMP3 was expressed in advillin-Cre positive (sensory neurons) and SNS-Cre positive (nociceptors) cells respectively. The recordings on superficial layers demonstrated that GABA-evoked calcium transient in nociceptor central terminals was not affected by nerve injury, which is consistent with result acquired from cultured neurons. However, GABA showed presynaptic inhibitory effect by suppressing the high KCl induced calcium transient in these presynaptic terminals, and nerve injury could disrupt such presynaptic inhibition. These evidence suggest that nerve injury abolishes the GABA mediated presynaptic inhibition rather than converts it to excitation. This disinhibition effect may be due to the combine effect of upregulated intracellular [$Cl^-$] and reduced $G_{GABA}$ [61]. The latter one probably restrains the increased strength of PAD. Since the intrinsic excitability of DRG neurons is essential for PAD-induced spikes, it probably not affected in central terminals after nerve injury. Yet, further study is required to address this. My colleagues also discovered that the NKCC1 inhibitor bumetanide effectively alleviated nerve injury induced thermal hypergesia while did not show any influence on mechani-

cal allodynia suggesting presynaptic chloride concentration is crucial for thermal hyperagesia in neuropathic[61]. Interestingly, the efficacy of bumetanide decreased along time: strong on 2nd day after injury, weak on 14th day after injury, and no analgesic effect on 21st day after injury. This time dependent effect is consistent with the depolarizingly shifted $E_{Cl}$ 2-day post nerve injury, which further indicates that the lost of presynaptic inhibition caused by intracellular chloride elevation contributes to thermal hyperagesia in the early stage of neuropathic pain.

To clarify the function of presynaptic inhibition in vivo, our group tried to generate nociceptor specific $GABA_A$ receptor deficient mice. Every $GABA_A$ receptor is assembled from 5 subunits. α and γ subunits form the BZD binding site at their interface, and α and β subunits form the binding site for GABA[20]. Mutation of α and γ subunits was reported that only affect bensodiazepine sensitivity without changing the response to GABA[69,86]. On the other hand, β subunits are only responsible for GABA but not BZD binding effect, and β3 subunit-containing $GABA_A$ receptors selectively mediate the action of intravenous general anesthetics[87]. Moreover, β3 subunits, the most dominant β subunits expressed by DRG neurons[88,89], are widely expressed in spinal cord and DRG suggesting a possible role in presynaptic inhibition[90,91]. Therefore, β3 subunits were chosen to knock out in nociceptors by crossing SNS-Cre to floxed β3 mice to create SNS-$\beta3^{-/-}$ mice[61]. The SNS-$\beta3^{-/-}$ mice showed hypersensitivity to both mechanical and thermal stimulations compare to their control litter mates. Moreover, nerve injury could further develop their mechanical sensitivity but not the thermal sensitivity. These observations indicated presynaptic inhibition contributes to modulation of both mechanical and thermal nociceptive signal, especially the latter one, which is almost solely controlled by presynaptic inhibition.

### 5.1.3 BDNF-TrkB signaling regulates nerve injury induced lost of GABAergic presynaptic inhibition

BDNF-TrkB signaling is crucially involved in regulating the survival and differentiation of neuronal populations during development stage, and plays an important role in modulating synaptic transmission and plasticity in CNS in adult stage[92,93]. Previous studies had indicated BDNF-TrkB signaling could decrease GABAergic inhibition by rising intracellular [$Cl^-$] through down-regulation of KCC2[94,95]. When intracellular [$Cl^-$] is elevated, the activation of $GABA_A$ receptors will generated less or no hyperpolariza-

tion, i.e. less or no inhibition. The group of De Koninck reported that the inverted postsynaptic inhibition on nociceptive signal transmission after nerve injury was due to the same mechanism, and the source of BDNF is ATP activated microglias[51]. Although DRG neurons barely express KCC2, previous studies suggested BDNF-TrkB signaling might also modulate intracellular [$Cl^-$] via regulating NKCC1, which is heavily expressed by sensory neurons[35–38,70,71]. Indeed, my colleague observed a depolarizing shift of $E_{cl}$ in BDNF treated DRG neurons, which is similar to the $E_{cl}$ of neurons from nerve injury animal[61]. In addition, the depolarizing shift of $E_{cl}$ was successfully reversed by BDNF scavenger TrkB-Fc[61]. Consistently, disinhibition effect of GABA observed in nerve injury group also appeared in BDNF treatment group in 2-photon calcium imaging. Together, these results suggested the presynaptic inhibition caused by nerve injury is regulated by BDNF-TrkB signaling.

# 5.2 GABAergic presynaptic control in inflammatory pain

## 5.2.1 The GABAergic presynaptic control in inflammatory pain is different from the one in neuropathic pain

A declined inhibitory control in spinal cord dorsal horn after peripheral inflammation had been addressed by several reviews[13,28]. It is widely agreed that the hypersensitivity caused by inflammation is due to the diminished glycinergic inhibition proposed by Zeilhofer's group: the peripheral inflammation increases the expression of cyclooxygenase-2 (COX-2), in turn, leads to the release of pronociceptive and proinflammatory prostaglandin E2 (PGE2) in spinal cord; The PGE2 binds to neuronal EP2 receptors expressed by interneurons, and decreases the glycinergic inhibitory control on these neurons via a protein kinase A (PKA) dependent phosphorylation of the glycine receptor 3 (GlyR3) subtype of strychnine-sensitive glycine receptors[96]. Nevertheless, this well-established mechanism only covers postsynaptic control, because there is no evidence indicating glycine plays any role in PAD or presynaptic inhibition[97–100], and glycine receptors are not expressed by nociceptors[101].

Besides the different postsynaptic disinhibition mechanisms, the behavior results of GABAergic studies also set the inflammatory pain apart from neuropathic pain. We had previously reviewed that most studies showed $GABA_A$ receptor agonists still exhibited analgesic effect in neuropathic pain condition, while their effect is controversial in inflammatory pain: both agonists and antagonists of $GABA_A$ receptor had been suggested to regulate analgesia[77]. This ambiguous effect of GABAergic pathway may be attributed to a special event - DRR, which is only observed after inflammation but not after nerve injury[52]. DRR had been well reviewed by Willis[52]. Briefly, DRR is generated by an intense form of PAD capable of triggering action potential. At this moment, PAD rather performs an excitatory effect instead of inhibition. Therefore, the balance of postsynaptic GABAergic inhibition and presynaptic GABAergic excitation caused by intensified PAD might decide whether GABA holds an analgesic effect after peripheral inflammation. It had been proposed that action potentials of nociceptive fibers could be presynapticlly evoked by non-nociceptive activated Aβ fibers through GABAergic interneurons, and this action potential would travel both retrogradely and anterogradely to induce neurogenic inflammation by DRR and contribute to hypersensitivity respectively[43,77,102,103].

### 5.2.2 Peripheral inflammation induces the GABAergic presynaptic disinhibition and excitation

A possible cause of the vigorous PAD after inflammation, similar to presynaptic disinhibition in neuropathic pain, is the increase of intracellular $[Cl^-]$ regulated by NKCC1[77]. In fact, CFA injection could induce a depolarizing shift of $E_{Cl}$ without changing the $G_{GABA}$ in nociceptors. The presynaptic disinhibition effect of GABA was also observed in spinal dorsal horn superficial layers by using 2-photon calcium imaging. In addition, the activation of $GABA_A$ receptors even generated presynaptic calcium transient in a bigger proportion of ROIs, which suggests a switch to excitatory effect of GABA. Considering that the activity of NKCC1 can be upregulated by inflammation[53,82], and NKCC1 inhibitor, bumetanide, is able to abolish DRR, the increase of intracellular $[Cl^-]$ possibly depends on NKCC1[104]. Although the mRNA level of NKCC1 was not changed by peripheral inflammation, an upregulation of NKCC1 expression on membrane was observed in both small and large DRG neurons. Interestingly, the depolarizing shift of $E_{Cl}$ was only observed in small neurons. The mechanism underlying this is still unknown. An intracellular $[Cl^-]$ related negative feedback system to regulate the activity of NKCC1 had

been suggested by previous study[39]. It is possible that this feedback system was still intact in large neurons after CFA injection. Further study on this feedback system and its possible change in various pathological conditions would be helpful to understand the role of NKCC1 in pathological pain. On behavior level, the NKCC1 inhibitor bumetanide was found to reduce mechanical sensitivity developed by CFA injection without affecting the thermal hypersensitivity, and this treatment exhibited a long term effect. Noticeably, bumetanide only alleviated thermal hyperalgesia in our neuropathic pain model[61]. Both mechanical and thermal sensitivity of SNS-$\beta3^{-/-}$ mice could be furthered by CFA injection suggesting that presynaptic element only partially contributes to mechanical and thermal hypersensitivity induced by CFA injection.

In addition to intracellular [$Cl^-$], the effect of GABA also depends on the release of GABA and the density of $GABA_A$ receptors. The first one can be regulated by GABA catalyzing enzymes, GAD65 and GAD67, and the GABA remover GAT1. The mRNA level of three were unchanged neither in DRG nor in spinal cord after inflammation. α and β $GABA_A$ receptor subunits form binding sites for GABA. Five of them were found expressed in DRG neurons[77]. α1 subunits were reported to have low expression level in superficial layer and rather concentrate in lamina III[19,21]. The upregulation of α1 mRNA implies an increase of this subunit in non-nociceptor terminals. $GABA_A$ receptors containing α2 subunits are predominantly expressed by C fibers[21], and had been reported to be crucial for spinal anti-hyperalgesic effects of BZD[105] in inflammatory and neuropathic pain. Here I showed significant decrease of α2 subunits mRNA in both DRG and spinal cord dorsal horn samples. It's likely that there was a downregulation of α2 subunits on both presynaptic and postsynaptic sides, though further study, such as in situ hybridization and immunohistochemistry, should be employed to confirm this. A reduction of KCC2 had been observed in spinal cord after peripheral inflammation as well as after nerve injury. This implies a similar postsynaptic disinhibition happens in neuropathic pain. And the downregulation of α2 subunits in postsynaptic neurons may weaken the BZD induced analgesic effect. If the α2 subunits are decreased in primary afferent central terminals, the effect of BZD is also lessened, which may decrease the strength of PAD. Interestingly, an increase of α5 subunits mRNA was also observed but only in DRG. α5 subunits are mainly expressed by extrasynaptic $GABA_A$ receptors, which generate a tonic conductance and produce a shunt affecting excitability and gain control[106–110]. CNS studies, especially on hippocampus, strongly indicated $GABA_A$ receptors containing α5 subunits play a critical role in the regulation of plasticity which is important for learning and memory[109,111]. Recently, Perez-Sanchez et al. showed that

these receptors in spinal cord also contributed to a tonic current. In spite of no hypersensitivity was observed in mice lacking α5 subunits, these mice had a prolonged recovery from inflammatory and neuropathic pain, and increased response in the late phase of the formalin test[112]. These results imply that α5 subunits are important for central sensitization and synapse plasticity. However, the contributions from presynaptic and postsynaptic sides remain to be determined. The mRNA level of β3 subunits was not influenced by CFA injection induced inflammation. But the inflammation may change β3 subunits in another way. There is evidence that PGE2, which is released in spinal cord after inflammation, is able to increase cAMP level in DRG neurons as well as in spinal neurons[96,113], which is able to subsequently upregulate PKA mediated protein phosphorylation. And McDonald et al. showed that the phosphorylation of β3 subunits could enhance the activity of $GABA_A$ receptors[114]. Together, these results imply that the release of PGE2 boosts $GABA_A$ receptors containing β3 subunits via PKA mediated phosphorylation in presynaptic and postsynaptic neurons. Factors described above imply that the slightly increased $G_{GABA}$ after inflammation may be due to the balance of downregulation of α2 subunits and enhanced activity of β3 subunits containing receptors.

In conclusion, the NKCC1-dependent increase of intracellular [$Cl^-$] causes the malfunction of presynaptic inhibition in inflammatory pain as well as in neuropathic pain. Although this presynaptic malfunction contributes to both mechanical and thermal hypersensitivity in neuropathic and inflammatory pain, its role is more prominent in thermal hyperalgesia induced by nerve injury and in mechanical allodynia generated by inflammation. The later one is likely due to the excitatory switch of GABA effect, which is caused by enhanced PAD strong enough to trigger action potentials.

## 5.3 A subpopulation of peptidergic nociceptors is essential for inflammation induced mechanical allodynia

### 5.3.1 Difference between SNS-Cre and advillin-Cre generated transgenic mice

Nociceptors can be classified based on conduction velocities (caused by different level of myelination), innervation patterns, specificity to various sensory modalities, and molecular markers. And these various classifications also correlated, for example, TRPV1 positive and Mrgprd positive nociceptors mediate noxious thermal and mechanical stimuli respectively[115,116]. Nerve injury and peripheral inflammation not only disturb spinal circuit controlling nociceptive signal transmission, but can also cause sensitization of DRG neurons which is attributable to hypersensitivity[117–119]. Study on TRPV1$^{-/-}$ mice revealed that these transgenic mice did not develop heat hyperalgesia after CFA injection, but nerve injury successfully generated heat hyperalgesia in them[117]. This finding suggests that the population of neurons sensitized by different pathological conditions are different. Here, my 2-photon calcium imaging results provide evidence supporting this idea by showing that primary afferent central terminals in advillin-Ai38 and SNS-Ai38 mice had similar change after nerve injury, disinhibition effect of GABA was observed in both of them, yet the excitatory effect of GABA generated by peripheral inflammation was only seen in SNS-Ai38 spinal cord slices. Consistent with this, the difference between advillin-β3$^{-/-}$ and SNS-β3$^{-/-}$ in behavior test was also observed: mechanical and thermal sensitivities were both further developed by CFA injection in these two transgenic mouse lines, but SNS-β3$^{-/-}$ did not fully develop the mechanical allodynia.

### 5.3.2 Different expression patterns of SNS-Cre and advillin-Cre in nociceptors

Zurborg et al., who generated advillin-Cre mice, reported that the Cre recombinase was expressed in 82.28% or 87.74% of all-sized sensory neurons depends on different investigation methods[56]. On the other hand, Cre recombinase was reported to be expressed in 93% of small sensory neurons in SNS-Cre transgenic mice[55]. Therefore, the possible

explanation of the different results between advillin-Cre and SNS-Cre generated transgenic mice is the different Cre expression patterns in nociceptors from there two mouse lines. Indeed, I found almost all (99%) CGRP positive DRG neurons from SNS-Ai38 mice expressed GCaMP3, and half (49%) of CGRP positive neurons from advillin-Ai38 mice did not express GCaMP3. Yet, virtually all IB4 positive DRG neurons from adillin-Ai38 (100%) and SNS-Ai38 (97%) mice are GCaMP3 positive. These immunohistochemistry results indicates that the Cre expression driven by the regulatory elements of advillin gene is absent in a big proportion of peptidergic nociceptors.

Together with presynaptic calcium imaging and behavior study from advillin-Cre and SNS-Cre generated mice, these immunochemistry results imply that the peptidergic nociceptors, at least part of them, are responsible for the presynaptic excitatory effect of GABA and mechanical allodynia in inflammatory pain. This is strongly supported by the observation of Brenneis et al.[119]. They found that the silencing of TRPV1 receptors, which are mainly expressed in peptidergic neurons[12], only abolished mechanical hypersensitivity developed by peripheral inflammation but not by nerve injury.

### 5.3.3 Comparison between peptidergic and non-peptidergic nociceptors

Further investigation of peptidergic and non-peptidergic nociceptors was carried on cultured DRG neurons thanks to IB4 labeling of alive neurons. The calcium imaging results revealed that the peptidergic and non-peptidergic small diameter neurons had similar changes after peripheral inflammation. The proportion responding to GABA application was increased in both peptidergic and non-peptidergic neurons. This is only partially consistent with the result of the 2-photon calcium imaging on spinal cords, since the difference between advillin-Ai38 and SNS-Ai38 mice implied that the increased of GABA triggered calcium transient in nociceptor central terminals was mainly contributed by peptidergic nociceptors. One possible explanation for this controversy between calcium imaging on cultured neurons and central terminals is that the expression pattern of $GABA_A$ receptors in the somas of cultured neurons is different from central terminals. The GABA induced depolarization may be enhanced in both peptidergic and non-peptidergic nociceptor central terminals after inflammation, likely due to intracellular $[Cl^-]$ increase and the change of $GABA_A$ receptor expression, but it is only strong enough to trigger calcium transient in former ones, which is supported by the re-

sult showing the amplitude of GABA-evoked calcium transient was only upregulated in IB4- neurons after inflammation. In primary neuron culture, the GABA generated depolarization could be more intensive in neuron somas due to the higher density of $GABA_A$ receptors, and triggered calcium transient in non-peptidergic neurons as well.

The increased amplitude of calcium transient caused by high KCl, with and without GABA, suggested an upregulated sensitivity of all putative nociceptors after inflammation. This probably is contributed by the upregulated activity of voltage gated sodium channels[120] and the lowered resting [$Ca^{2+}$], which built up a larger driven force for $Ca^{2+}$ influx. Noticeably, GABA suppressed high KCl triggered calcium influx in majority of putative nociceptors from both intact and CFA injected mice. This may be due to the more intense shunting effect of GABA in somas than central terminals.

Although peptidergic and non-peptidergic neurons were similarly modulated after inflammation, the discrepancy between these 2 subpopulations should not be neglected. In cell culture, GABA triggered calcium transient in more IB4+ neurons than in IB4- neurons regardless of CFA injection. The resting [$Ca^{2+}$] of IB4- neurons is lower than that of IB4+ neurons. However, whether these differences are consistent in central terminals, and the functional difference underlain by them remains to be investigated.

### 5.3.4 Calcium homeostasis in pathological condition

Homeostasis of [$Ca^{2+}$] is crucial for neurons to function properly, because [$Ca^{2+}$] influences action potential transportation and transmitter release, and $Ca^{2+}$ is also an 2$^{nd}$ messenger in various signaling pathways[79]. The rise of neuronal [$Ca^{2+}$] is usually initiated by action potential, which opens voltage gated calcium channels, and generates a $Ca^{2+}$ influx which can then trigger the release of endoplasmic reticulum (ER) and mitochondrion stored $Ca^{2+}$ via signaling pathway. The excessive $Ca^{2+}$ can be purged away to extracellular space or organelles by various $Ca^{2+}$ pumps and exchangers, such as $Na^+/Ca^{2+}$ exchanger (NCX) and plasma membrane $Ca^{2+}$-ATPase (PMCA) in cell membrane, sarcoendoplasmic reticulum $Ca^{2+}$-ATPase (SERCA) in ER membrane and $Ca^{2+}$ uni-porter (CUP) in mitochondrion membrane (reviewed by Gleichmann and Mattson[121] and Zündorf and Reiser[80]).

It had been reported that nerve injury rather decreased the resting intracellular [$Ca^{2+}$] of DRG neurons than increases it[122], which is often observed in brain neurons in patho-

logical conditions[80]. My calcium imaging result indicats that not only nerve injury but peripheral inflammation also reduces the intracellular [$Ca^{2+}$] of DRG nociceptors. Gemes et at. indicated that the upregulated activity of PMCA leads to the reduction of resting $Ca^{2+}$ level in axotomized sensory neurons. Compare to the elevated PMCA, the activity of SERCA responsible for returning $Ca^{2+}$ to ER decreased after injury[123], which can disturb the role of ER as a calcium sink. CUP and other calcium transporters on mitochondrion have not been investigated in DRG neurons. The important role of mitochondrion in calcium homeostasis is to sequester excess $Ca^{2+}$ during the development of calcium transient[124]. Interruption of presynaptic mitochondrial $Ca^{2+}$ uptake may significantly influence the recovery from high [$Ca^{2+}$] and the transmitter release. The altered dynamic control of [$Ca^{2+}$] due to the changed resting [$Ca^{2+}$] and modulated $Ca^{2+}$ transporters can also influence the calcium-sensitive signaling pathways regulating gene expression and enzyme activity. Nevertheless, the activities of all these $Ca^{2+}$ pumps and exchangers in DRG neurons and their contributions to the homeostasis of $Ca^{2+}$ remain to be examined in pathological conditions.

Noticeably, there was a rise of resting [$Ca^{2+}$] level in BDNF treated DRG neurons which is consistent with previous study indicating BDNF elevates intracellular [$Ca^{2+}$][125]. Although BDNF is released in spinal dorsal horn after nerve injury and inflammation[51,126,127], the resting [$Ca^{2+}$] was rather lowered in DRG neurons. These phenomena suggest a spatial specific effect of BDNF, which is limited in central terminals of DRG neurons, and the [$Ca^{2+}$] change in neural soma is possibly regulated by other factors.

## 5.4 Brief summary

### 5.4.1 Summary of results

In present study I explored the character of GABAergic presynaptic control for nociceptive signal transmission in spinal dorsal horn in physiological and pathological conditions. I found GABAergic presynaptic disinhibition in neuropathic and inflammatory pain animal models. The disinhibition after nerve injury, which most likely mediated by spinal BDNF, is essential for thermal hyperagesia. In inflammatory pain model, in addition to disinhibition, GABA also acquired more excitatory effect on central terminals

of CGRP positive neurons (peptidergic nociceptors), which leaded to mechanical allodynia.

Half a century ago, Melzack and Wall proposed the classic GCT which describes a spinal circuit where the dorsal horn inhibitory interneurons occupy the key position and regulate the nociceptive signal transmission from PNS to CNS. Nowadays, the improved GCT suggests this regulation is employed by both presynaptic and postsynaptic inhibition. GABA is the major inhibitory neurotransmitter in the nervous system, and $GABA_A$ receptors had been found to express on both central terminals of primary afferents and spinal neurons[21]. Pharmacological studies with GABA and its antagonists provided huge body of evidence indicating GABAergic inhibition has an analgesic effect. However, the contribution of pre- inhibition to this analgesic effect had never been clearly addressed separately.

Previously, most direct recording for presynaptic inhibition study on cellular level were carried on cultured DRG neurons. Recently, Zeilhofer's group tried to study the genuine presynaptic control by generating a conditional nociceptor-specific $GABA_A$ receptor α2 subunit deficient mouse line (SNS-$\alpha2^{-/-}$)[69]. It was reported that DZP lost its potentiating effect on PAD and a major part of its spinal anti-hyperalgesic action against inflammatory hyperalgesia in these mice. However, This SNS-$\alpha2^{-/-}$ mouse line exhibited normal $GABA_A$ receptor currents, and behavior to mechanical and thermal stimulation, and developed neuropathic and inflammatory pain sensitization as wild type animal. These characters of SNS-$\alpha2^{-/-}$ mice make it an excellent tool to study the effect of positive allosteric modulator on presynaptic $GABA_A$ receptors, but the contribution of $GABA_A$ receptors mediated PAD in physiological and various pathological conditions kept unsolved.

Here in addition to investigation on neuron somas in cell culture and acutely dissected whole mount DRG, I managed to selectively record presynaptic activity by specifically express GCaMP3 in sensory neurons. All-sensory neuron- and nociceptor-specific GECI mice (advillin-Ai38 and SNS-Ai38) were generated by crossing two different Cre mouse lines, advillin-Cre[56] and SNS-Cre[55], to Ai38 mice carrying a floxed STOP cassette preventing GCaMP3 expression. Recording on these slices, for the first time, provided ex vivo evidence for GABAergic inhibition on presynapses, and its change after nerve injury and inflammation. These results together with the work of my colleagues, for the first time, confirmed the contribution of presynaptic inhibition on nociceptive signal regulation. We discovered that nerve injury and peripheral inflmmation could disturb

GABAergic presynaptic inhibition, mainly due to the upregulation of intracellular [$Cl^-$] and change of $G_{GABA}$, and leaded to the lost of GABAergic presynaptic inhibition and the GABAergic presynaptic excitation respectively (**Figure 33**). These malfunctioning presynaptic inputs contributed to neuropathic and inflammatory pain differently. Further more, The difference between advillin-Cre and SNS-Cre generated transgenic mice and study with non-peptidergic marker, IB4, further indicated that the malfunction of GABAergic presynaptic inhibition on peptidergic and non-peptidergic nociceptors contributed to the hypersensitivity responding to different modality inputs. These new understandings suggest, from a presynaptic point of view, neuropathic and inflammatory pain should be treated accordingly. Furthermore, modality specific pain treatment in various condition can focus on specific subpopulation.

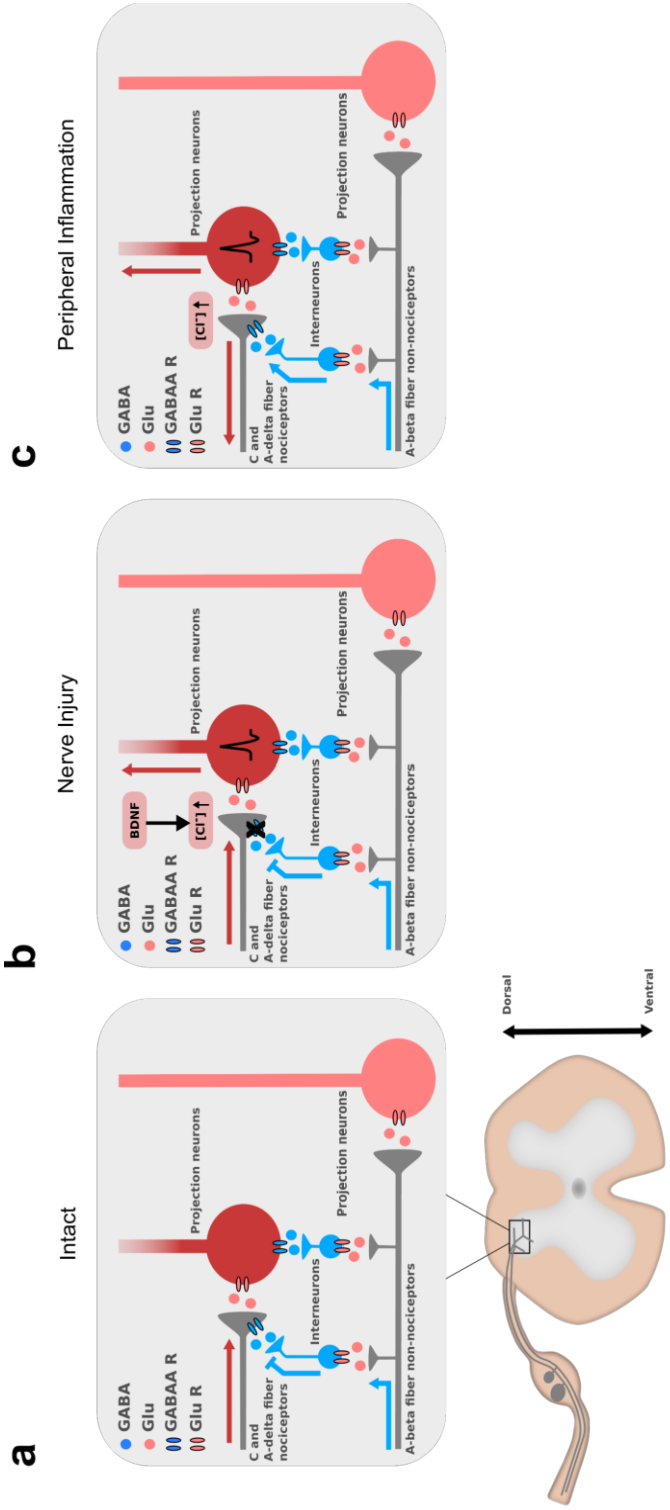


Figure 33: Hypothetical scheme showing the presynaptic control on nociceptors in different conditions. High threshold nociceptors are activated by nociceptive stimuli and transmit action potentials to their central terminals innervating postsynaptic projection neurons which can transport the nociceptive signals to brain. Both the presynaptic central terminals of nociceptors and postsynaptic projection neurons are regulated by GABAergic inhibitory interneurons receiving input from non-peptidergic sensory neurons. (**a**) In pathological condition, the

activation of non-nociceptive sensory neurons can suppress the nociceptive signal, i.e., close the gate of pain, by inhibiting the presynaptic central terminals. This presynaptic inhibition is disturbed in pathological conditions. (**b**) After nerve injury, the presynaptic [$Cl^-$] is upregulated by a BDNF-TrkB signaling activated pathway. This [$Cl^-$] alteration ceases the presynaptic inhibition mediated by $GABA_A$ receptors. In other words, presynaptic GABA losses its ability to close the gate of pain, and nociceptive stimuli generates stronger pain. (**c**) The peripheral inflammation also elevates [$Cl^-$] in presynaptic nociceptors. However, $G_{GABA}$ is not diminished as in neuropathic pain condition. This probably further enhances the $GABA_A$ receptors mediated depolarization, which is strong enough to trigger action potentials in nociceptor central terminals. This action potential anterogradely activates postsynaptic projection neurons and retrogradely facilitates peripheral inflammation. In this case, the gate of pain is opened, and low threshold stimuli could generate pain which is termed as allodynia.

# 6 References


1. Merskey, H. & Bogduk, N. *Classification of Chronic Pain*. *IASP Pain Terminology* (1994). doi:10.1002/ana.20394

2. Campbell, J. N. & Meyer, R. a. Mechanisms of neuropathic pain. *Neuron* **52,** 77–92 (2006).

3. Van Hecke, O., Torrance, N. & Smith, B. H. Chronic pain epidemiology and its clinical relevance. *British Journal of Anaesthesia* **111,** 13–18 (2013).

4. Tsang, A. *et al.* Common Chronic Pain Conditions in Developed and Developing Countries: Gender and Age Differences and Comorbidity With Depression-Anxiety Disorders. *J. Pain* **9,** 883–891 (2008).

5. Elliott, A. M., Smith, B. H., Hannaford, P. C., Smith, W. C. & Chambers, W. A. The course of chronic pain in the community: Results of a 4-year follow-up study. *Pain* **99,** 299–307 (2002).

6. Snider, W. D. & McMahon, S. B. Tackling pain at the source: New ideas about nociceptors. *Neuron* **20,** 629–632 (1998).

7. Zwick, M. *et al.* Glial cell line-derived neurotrophic factor is a survival factor for isolectin B4-positive, but not vanilloid receptor 1-positive, neurons in the mouse. *J. Neurosci.* **22,** 4057–4065 (2002).

8. Cavanaugh, D. J. *et al.* Restriction of Transient Receptor Potential Vanilloid-1 to the Peptidergic Subset of Primary Afferent Neurons Follows Its Developmental Downregulation in Nonpeptidergic Neurons. *J Neurosci* **31,** 10119–10127 (2011).

9. Price, T. J. *et al.* Treatment of trigeminal ganglion neurons in vitro with NGF, GDNF or BDNF: effects on neuronal survival, neurochemical properties and TRPV1-mediated neuropeptide secretion. *BMC Neurosci* **6,** 4 (2005).

10. Petruska, J. C., Napaporn, J., Johnson, R. D., Gu, J. G. G. & Cooper, B. Y. Subclassified acutely dissociated cells of rat DRG: Histochemistry and patterns of capsaicin-, proton-, and ATP-activated currents. *J. Neurophysiol.* **84,** 2365–2379 (2000).

11. Petruska, J. C., Napaporn, J., Johnson, R. D. & Cooper, B. Y. Chemical responsiveness and histochemical phenotype of electrophysiologically classified cells of the adult rat dorsal root ganglion. *Neuroscience* **115,** 15–30 (2002).

12. Price, T. J. & Flores, C. M. Critical evaluation of the colocalization between calcitonin gene-related peptide, substance P, transient receptor potential vanilloid

subfamily type 1 immunoreactivities, and isolectin B4 binding in primary afferent neurons of the rat and mouse. *J. Pain* **8,** 263–72 (2007).

13. Braz, J., Solorzano, C., Wang, X. & Basbaum, A. I. Transmitting pain and itch messages: a contemporary view of the spinal cord circuits that generate gate control. *Neuron* **82,** 522–36 (2014).

14. Todd, A. J. Neuronal circuitry for pain processing in the dorsal horn. *Nat. Rev. Neurosci.* **11,** 823–36 (2010).

15. Melzack, R. & Wall, P. D. Pain mechanisms: a new theory. *Science* **150,** 971–9 (1965).

16. Grudt, T. J. & Perl, E. R. Correlations between neuronal morphology and electrophysiological features in the rodent superficial dorsal horn. *J. Physiol.* **540,** 189–207 (2002).

17. Proudlock, F., Spike, R. C. & Todd, A. J. Immunocytochemical study of somatostatin, neurotensin, GABA, and glycine in rat spinal dorsal horn. *J. Comp. Neurol.* **327,** 289–297 (1993).

18. Todd, A. J. & McKenzie, J. GABA-immunoreactive neurons in the dorsal horn of the rat spinal cord. *Neuroscience* **31,** 799–806 (1989).

19. Bohlhalter, S., Weinmann, O., Mohler, H. & Fritschy, J. M. Laminar compartmentalization of GABAA-receptor subtypes in the spinal cord: an immunohistochemical study. *J. Neurosci.* **16,** 283–297 (1996).

20. Sigel, E. & Steinmann, M. E. Structure, function, and modulation of GABAA receptors. *J. Biol. Chem.* **287,** 40224–40231 (2012).

21. Paul, J., Zeilhofer, H. U. & Fritschy, J.-M. Selective distribution of GABA(A) receptor subtypes in mouse spinal dorsal horn neurons and primary afferents. *J. Comp. Neurol.* **520,** 3895–911 (2012).

22. Polgár, E. *et al.* Selective loss of spinal GABAergic or glycinergic neurons is not necessary for development of thermal hyperalgesia in the chronic constriction injury model of neuropathic pain. *Pain* **104,** 229–239 (2003).

23. Lu, Y. & Perl, E. R. A specific inhibitory pathway between substantia gelatinosa neurons receiving direct C-fiber input. *J. Neurosci.* **23,** 8752–8758 (2003).

24. Roberts, L. A., Beyer, C. & Komisaruk, B. R. Nociceptive responses to altered GABAergic activity at the spinal cord. *Life Sci.* **39,** 1667–74 (1986).

25. Sawynok, J. GABAergic mechanisms of analgesia: An update. *Pharmacol. Biochem. Behav.* **26,** 463–474 (1987).

26. Melcangic, M. & Bowery, N. G. GABA and its receptors in the spinal cord. *Trends Pharmacol. Sci.* **17,** 457–462 (1996).

27. Dickenson, a. H., Chapman, V. & Green, G. M. The pharmacology of excitatory and inhibitory amino acid-mediated events in the transmission and modulation of pain in the spinal cord. *Gen. Pharmacol.* **28,** 633–638 (1997).

28. Zeilhofer, H. U., Wildner, H., Yevenes, G. E. & Yévenes, G. E. Fast synaptic inhibition in spinal sensory processing and pain control. *Physiol. Rev.* **92,** 193–235 (2012).

29. Sivilotti, L. & Woolf, C. J. The contribution of GABAA and glycine receptors to central sensitization: disinhibition and touch-evoked allodynia in the spinal cord. *J Neurophysiol* **72,** 169–179 (1994).

30. Sorkin, L. S., Puig, S. & Jones, D. L. Spinal bicuculline produces hypersensitivity of dorsal horn neurons: effects of excitatory amino acid antagonists. *Pain* **77,** 181–190 (1998).

31. Loomis, C. W., Khandwala, H., Osmond, G. & Hefferan, M. P. Coadministration of Intrathecal Strychnine and Bicuculline Effects Synergistic Allodynia in the Rat: An Isobolographic Analysis. *J. Pharmacol. Exp. Ther.* **296,** 756–761 (2001).

32. Zhang, Z., Hefferan, M. P. & Loomis, C. W. Topical bicuculline to the rat spinal cord induces highly localized allodynia that is mediated by spinal prostaglandins. *Pain* **92,** 351–361 (2001).

33. Malan, T. P., Mata, H. P. & Porreca, F. Spinal GABA(A) and GABA(B) receptor pharmacology in a rat model of neuropathic pain. *Anesthesiology* **96,** 1161–7 (2002).

34. Kahle, K. T. *et al.* Roles of the cation-chloride cotransporters in neurological disease. *Nat. Clin. Pract. Neurol.* **4,** 490–503 (2008).

35. Alvarez, F. J., Anto, B., Leo, M. & Gardun, R. Immunolocalization of the Na(+)-K(+)-2Cl(-) cotransporter in peripheral nervous tissue of vertebrates. **104,** 569–582 (2001).

36. Kanaka, C. *et al.* The differential expression patterns of messenger RNAs encoding K-Cl cotransporters (KCC1,2) and Na-K-2Cl cotransporter (NKCC1) in the rat nervous system. *Neuroscience* **104,** 933–46 (2001).

37. Price, T. J., Hargreaves, K. M. & Cervero, F. Protein expression and mRNA cellular distribution of the NKCC1 cotransporter in the dorsal root and trigeminal ganglia of the rat. *Brain Res.* **1112,** 146–58 (2006).

38. Mao, S. *et al.* Molecular and functional expression of cation-chloride cotransporters in dorsal root ganglion neurons during postnatal maturation. *J. Neurophysiol.* **108,** 834–52 (2012).

39. Rocha-González, H. I., Mao, S. & Alvarez-Leefmans, F. J. Na+,K+,2Cl− Cotransport and Intracellular Chloride Regulation in Rat Primary Sensory Neurons: Thermodynamic and Kinetic Aspects. *J. Neurophysiol.* **100,** (2008).

40. Levy, R. A. The role of gaba in primary afferent depolarization. *Progress in Neurobiology* **9,** 211–267 (1977).

41. Kullmann, D. M. *et al.* Presynaptic, extrasynaptic and axonal GABA A receptors in the CNS: Where and why? *Progress in Biophysics and Molecular Biology* **87,** 33–46 (2005).

42. Prescott, S. a, Ma, Q. & De Koninck, Y. Normal and abnormal coding of somatosensory stimuli causing pain. *Nat. Neurosci.* **17,** 183–91 (2014).

43. Price, T. J., Cervero, F., Gold, M. S., Hammond, D. L. & Prescott, S. A. Chloride regulation in the pain pathway. *Brain Res. Rev.* **60,** 149–70 (2009).

44. Sandkühler, J. Models and mechanisms of hyperalgesia and allodynia. *Physiol. Rev.* 707–758 (2009). doi:10.1152/physrev.00025.2008.

45. Yaksh, T. L. Behavioral and autonomic correlates of the tactile evoked allodynia produced by spinal glycine inhibition: effects of modulatory receptor systems and excitatory amino acid antagonists. *Pain* **37,** 111–123 (1989).

46. Minami, T. *et al.* Allodynia evoked by intrathecal administration of prostaglandin E2 to conscious mice. *Pain* **57,** 217–223 (1994).

47. Baba, H. *et al.* Removal of GABAergic inhibition facilitates polysynaptic A fiber-mediated excitatory transmission to the superficial spinal dorsal horn. *Mol. Cell. Neurosci.* **24,** 818–830 (2003).

48. Baba, H., Doubell, T. P. & Woolf, C. J. Peripheral Inflammation Facilitates A $^{N}_{L}$ Fiber-Mediated Synaptic Input to the Substantia Gelatinosa of the Adult Rat Spinal Cord. *J. Neurosci.* **19,** 859–867 (1999).

49. Moore, K. A. *et al.* Partial peripheral nerve injury promotes a selective loss of GABAergic inhibition in the superficial dorsal horn of the spinal cord. *J Neurosci* **22,** 6724–6731 (2002).

50. Coull, J. A. M. *et al.* Trans-synaptic shift in anion gradient in spinal lamina I neurons as a mechanism of neuropathic pain. *Nature* **424,** 938–942 (2003).

51. Coull, J. A. M. *et al.* BDNF from microglia causes the shift in neuronal anion gradient underlying neuropathic pain. *Nature* **438,** 1017–1021 (2005).

52. Willis, W. D. Dorsal root potentials and dorsal root reflexes: a double-edged sword. *Exp. brain Res.* **124,** 395–421 (1999).

53. Funk, K. *et al.* Modulation of chloride homeostasis by inflammatory mediators in dorsal root ganglion neurons. *Mol. Pain* **4,** 32 (2008).

54. Duebel, J. *et al.* Two-photon imaging reveals somatodendritic chloride gradient in retinal ON-type bipolar cells expressing the biosensor Clomeleon. *Neuron* **49,** 81–94 (2006).

55. Agarwal, N., Offermanns, S. & Kuner, R. Conditional gene deletion in primary nociceptive neurons of trigeminal ganglia and dorsal root ganglia. *Genesis* **38,** 122–9 (2004).

56. Zurborg, S. *et al.* Generation and characterization of an Advillin-Cre driver mouse line. *Mol. Pain* **7,** 66 (2011).

57. Shields, S. D. *et al.* Nav1.8 expression is not restricted to nociceptors in mouse peripheral nervous system. *Pain* **153,** 2017–2030 (2012).

58. Ravenall, S. J., Gavazzi, I., Wood, J. N. & Akopian, A. N. A peripheral nervous system actin-binding protein regulates neurite outgrowth. *Eur. J. Neurosci.* **15,** 281–90 (2002).

59. Akopian, A. N. & Wood, J. N. Peripheral nervous system-specific genes identified by subtractive cDNA cloning. *J. Biol. Chem.* **270,** 21264–70 (1995).

60. Shibata, M. *et al.* Type F scavenger receptor SREC-I interacts with advillin, a member of the gelsolin/villin family, and induces neurite-like outgrowth. *J. Biol. Chem.* **279,** 40084–90 (2004).

61. Chen, J. T. *et al.* Presynaptic GABAergic inhibition regulated by BDNF contributes to neuropathic pain induction. *Nat. Commun.* **5,** 5331 (2014).

62. Wetzel, C. *et al.* A stomatin-domain protein essential for touch sensation in the mouse. *Nature* **445,** 206–9 (2007).

63. Fehrenbacher, J. C., Vasko, M. R. & Duarte, D. B. Models of inflammation: Carrageenan- or unit 5.4 complete freund's adjuvant (CFA)-induced edema and hypersensitivity in the rat. *Curr. Protoc. Pharmacol.* 5.4.1-5.4.4 (2012). doi:10.1002/0471141755.ph0504s56

64. Chaplan, S. R., Bach, F. W., Pogrel, J. W., Chung, J. M. & Yaksh, T. L. Quantitative assessment of tactile allodynia in the rat paw. *J. Neurosci. Methods* **53,** 55–63 (1994).

65. Kuner, T., Augustine, G. J. & Carolina, N. A Genetically Encoded Ratiometric Indicator for ChlorideCapturing Chloride Transients in Cultured Hippocampal Neurons. *Neuron* **27,** 447–459 (2000).

66. Jayaraman, S., Haggie, P., Wachter, R. M., Remington, S. J. & Verkman, A. S. Mechanism and cellular applications of a green fluorescent protein-based halide sensor. *J. Biol. Chem.* **275,** 6047–50 (2000).

67. Schmittgen, T. D. & Livak, K. J. Analyzing real-time PCR data by the comparative CT method. *Nat. Protoc.* **3,** 1101–1108 (2008).

68. Farrant, M. & Nusser, Z. Variations on an inhibitory theme: phasic and tonic activation of GABA(A) receptors. *Nat. Rev. Neurosci.* **6,** 215–229 (2005).

69. Witschi, R. *et al.* Presynaptic alpha2-GABAA receptors in primary afferent depolarization and spinal pain control. *J. Neurosci.* **31,** 8134–42 (2011).

70. Lee, S. W. *et al.* GABAergic inhibition is weakened or converted into excitation in the oxytocin and vasopressin neurons of the lactating rat. *Mol. Brain* **8,** 34 (2015).

71. Eftekhari, S. *et al.* BDNF modifies hippocampal KCC2 and NKCC1 expression in a temporal lobe epilepsy model. *Acta Neurobiol. Exp. (Wars).* **74,** 276–287 (2014).

72. Salio, C., Lossi, L., Ferrini, F. & Merighi, A. Ultrastructural evidence for a pre- and postsynaptic localization of full-length trkB receptors in substantia gelatinosa (lamina II) of rat and mouse spinal cord. *Eur. J. Neurosci.* **22,** 1951–66 (2005).

73. Rees, H., Sluka, K. a, Westlund, K. N. & Willis, W. D. The role of glutamate and GABA receptors in the generation of dorsal root reflexes by acute arthritis in the anaesthetized rat. *J. Physiol.* **484 ( Pt 2,** 437–45 (1995).

74. Pieraut, S. *et al.* NKCC1 phosphorylation stimulates neurite growth of injured adult sensory neurons. *J. Neurosci.* **27,** 6751–9 (2007).

75. Sung, K.-W., Kirby, M., McDonald, M. P., Lovinger, D. M. & Delpire, E. Abnormal GABAA Receptor-Mediated Currents in Dorsal Root Ganglion Neurons Isolated from Na-K-2Cl Cotransporter Null Mice. *J. Neurosci.* **20,** 7531–7538 (2000).

76. Macdonald, R. L. & Olsen, R. W. GABAA receptor channels. *Annu. Rev. Neurosci.* **17,** 569–602 (1994).

77. Guo, D. & Hu, J. Spinal presynaptic inhibition in pain control. *Neuroscience* **283,** 95–106 (2014).

78. McMahon, S. B. (Stephen B. . *Wall and Melzack's textbook of pain*. (Elsevier/Saunders, 2013).

79. Berridge, M. J. Neuronal calcium signaling. *Neuron* **21,** 13–26 (1998).

80. Zündorf, G. & Reiser, G. Calcium dysregulation and homeostasis of neural calcium in the molecular mechanisms of neurodegenerative diseases provide multiple targets for neuroprotection. *Antioxid. Redox Signal.* **14,** 1275–1288 (2011).

81. Fuchs, A., Lirk, P., Stucky, C., Abram, S. E. & Hogan, Q. H. Painful nerve injury decreases resting cytosolic calcium concentrations in sensory neurons of rats. *Anesthesiology* **102,** 1217–1225 (2005).

82. Pieraut, S. *et al.* An autocrine neuronal interleukin-6 loop mediates chloride accumulation and NKCC1 phosphorylation in axotomized sensory neurons. *J. Neurosci.* **31,** 13516–26 (2011).

83. Wei, B. *et al.* Pre- and post-synaptic switches of GABA actions associated with Cl- homeostatic changes are induced in the spinal nucleus of the trigeminal nerve in a rat model of trigeminal neuropathic pain. *Neuroscience* **228,** 334–48 (2013).

84. Mòdol, L., Cobianchi, S. & Navarro, X. Prevention of NKCC1 phosphorylation avoids downregulation of KCC2 in central sensory pathways and reduces neuropathic pain after peripheral nerve injury. *Pain* **155,** 1577–1590 (2014).

85. Takkala, P., Zhu, Y. & Prescott, S. A. Combined Changes in Chloride Regulation and Neuronal Excitability Enable Primary Afferent Depolarization to Elicit Spiking without Compromising its Inhibitory Effects. *PLoS Comput. Biol.* **12,** e1005215 (2016).

86. Möhler, H., Fritschy, J. M. & Rudolph, U. A new benzodiazepine pharmacology. *J. Pharmacol. Exp. Ther.* **300,** 2–8 (2002).

87. Jurd, R. *et al.* General anesthetic actions in vivo strongly attenuated by a point mutation in the GABA(A) receptor beta3 subunit. *FASEB J.* **17,** 250–252 (2002).

88. Ma, W., Saunders, P. A., Somogyi, R., Poulter, M. O. & Barker, J. L. Ontogeny of GABAA receptor subunit mRNAs in rat spinal cord and dorsal root ganglia. *J. Comp. Neurol.* **338,** 337–359 (1993).

89. Coggeshall, R. E. & Carlton, S. M. Receptor localization in the mammalian dorsal horn and primary afferent neurons. *Brain Res. Rev.* **24,** 28–66 (1997).

90. Ma, W., Saunders, P. A., Somogyi, R., Poulter, M. O. & Barker, J. L. Ontogeny of GABAA receptor subunit mRNAs in rat spinal cord and dorsal root ganglia. *J. Comp. Neurol.* **338,** 337–59 (1993).

91. T, A. J. *et al.* Colocalization of GABA , Glycine , and their Receptors Synapses in the Rat Spinal Cord. *J. Neurosci.* **16,** 974–982 (1996).

92. Lewin, G. R. & Barde, Y.-A. PHYSIOLOGY OF THE NEUROTROPHINS. *ANIU Rev. Neumsciem* **19,** 289–317 (1996).

93. Gottmann, K., Mittmann, T. & Lessmann, V. BDNF signaling in the formation, maturation and plasticity of glutamatergic and GABAergic synapses. *Experimental Brain Research* **199,** 203–234 (2009).

94. Rivera, C. *et al.* Mechanism of Activity-Dependent Downregulation of the Neuron-Specific K-Cl Cotransporter KCC2. *J. Neurosci.* **24,** (2004).

95. Rivera, C. *et al.* BDNF-induced TrkB activation down-regulates the K+–Cl− cotransporter KCC2 and impairs neuronal Cl− extrusion. *J. Cell Biol.* **159,** (2002).

96. Ahmadi, S., Lippross, S., Neuhuber, W. L. & Zeilhofer, H. U. PGE(2) selectively blocks inhibitory glycinergic neurotransmission onto rat superficial dorsal horn neurons. *Nat. Neurosci.* **5,** 34–40 (2002).

97. Willis, W. D. John Eccles' studies of spinal cord presynaptic inhibition. *Prog. Neurobiol.* **78,** 189–214 (2006).

98. Maxwell, D. J. & Riddell, J. S. Axoaxonic synapses on terminals of group II muscle spindle afferent axons in the spinal cord of the cat. *Eur. J. Neurosci.* **11,** 2151–2159 (1999).

99. Eccles, J. C., Schmidt, R. & Willis, W. D. Pharmacological Studies on Presynaptic Inhibition. *J. Physiol.* **168,** 500–530 (1963).

100. Jiménez, I., Rudomin, P. & Solodkin, M. Mechanisms involved in the depolarization of cutaneous afferents produced by segmental and descending inputs in the cat spinal cord. *Exp. Brain Res.* **69,** 195–207 (1987).

101. Lorenzo, L.-E. *et al.* Gephyrin clusters are absent from small diameter primary afferent terminals despite the presence of GABA(A) receptors. *J. Neurosci.* **34,** 8300–17 (2014).

102. Garcia-Nicas, E., Laird, J. M. A. & Cervero, F. Vasodilatation in hyperalgesic rat skin evoked by stimulation of afferent Aβ-fibers: Further evidence for a role of dorsal root reflexes in allodynia. *Pain* **94,** 283–291 (2001).

103. Cervero, F., Laird, J. M. A. & García-Nicas, E. Secondary hyperalgesia and presynaptic inhibition: an update. *Eur. J. Pain* **7,** 345–51 (2003).

104. Valencia-de Ita, S., Lawand, N. B., Lin, Q., Castañeda-Hernandez, G. & Willis, W. D. Role of the Na+-K+-2Cl- cotransporter in the development of capsaicin-induced neurogenic inflammation. *J. Neurophysiol.* **95,** 3553–61 (2006).

105. Knabl, J. *et al.* Reversal of pathological pain through specific spinal GABAA receptor subtypes. *Nature* **451,** 330–4 (2008).

106. Semyanov, A., Walker, M. C., Kullmann, D. M. & Silver, R. A. Tonically active GABAA receptors: Modulating gain and maintaining the tone. *Trends in Neurosciences* **27,** 262–269 (2004).

107. Glykys, J. & Mody, I. Activation of GABAA Receptors: Views from Outside the Synaptic Cleft. *Neuron* **56,** 763–770 (2007).

108. Semyanov, A., Walker, M. C., Kullmann, D. M. & Silver, R. A. Tonically active GABAA receptors: Modulating gain and maintaining the tone. *Trends in Neurosciences* **27,** 262–269 (2004).

109. Caraiscos, V. B. *et al.* Tonic inhibition in mouse hippocampal CA1 pyramidal neurons is mediated by alpha5 subunit-containing gamma-aminobutyric acid type A receptors. *Proc. Natl. Acad. Sci. U. S. A.* **101,** 3662–3667 (2004).

110. Bai, D. *et al.* Distinct functional and pharmacological properties of tonic and quantal inhibitory postsynaptic currents mediated by g -aminobutyric acid(A) receptors in hippocampal neurons. *Mol. Pharmacol.* **59,** 814–824 (2001).

111. Dawson, G. R. *et al.* An inverse agonist selective for alpha5 subunit-containing GABAA receptors enhances cognition. *J. Pharmacol. Exp. Ther.* **316,** 1335–1345 (2006).

112. Perez-Sanchez, J. *et al.* α5GABA A Receptors Mediate Tonic Inhibition in the Spinal Cord Dorsal Horn and Contribute to the Resolution Of Hyperalgesia. *J. Neurosci. Res.* **0,** 1–12 (2016).

113. Smith, J. A. M., Davis, C. L. & Burgess, G. M. Prostaglandin E 2 -induced sensitization of bradykinin-evoked responses in rat dorsal root ganglion neurons is mediated by cAMP-dependent protein kinase A. *Eur. J. Neurosci.* **12,** 3250–3258 (2000).

114. McDonald, B. J. *et al.* Adjacent phosphorylation sites on GABAA receptor beta subunits determine regulation by cAMP-dependent protein kinase. *Nat. Neurosci.* **1,** 23–8 (1998).

115. Zhang, J., Cavanaugh, D. J., Nemenov, M. I. & Basbaum, A. I. The modality-specific contribution of peptidergic and non-peptidergic nociceptors is manifest at the level of dorsal horn nociresponsive neurons. *J. Physiol.* **591,** 1097–110 (2013).

116. Cavanaugh, D. J. *et al.* Distinct subsets of unmyelinated primary sensory fibers mediate behavioral responses to noxious thermal and mechanical stimuli. *Proc Natl Acad Sci U S A* **106,** 9075–9080 (2009).

117. Caterina, M. J. *et al.* Impaired nociception and pain sensation in mice lacking the capsaicin receptor. *Science* **288,** 306–13 (2000).

118. Obata, K. *et al.* TRPA1 induced in sensory neurons contributes to cold hyperalgesia after inflammation and nerve injury. *J. Clin. Invest.* **115,** 2393–2401 (2005).

119. Brenneis, C. *et al.* Phenotyping the Function of TRPV1-Expressing Sensory Neurons by Targeted Axonal Silencing. *J Neurosci* **33,** 315–326 (2013).

120. Wood, J. N., Boorman, J. P., Okuse, K. & Baker, M. D. Voltage-gated sodium channels and pain pathways. *Journal of Neurobiology* **61,** 55–71 (2004).

121. Gleichmann, M. & Mattson, M. P. Neuronal calcium homeostasis and dysregulation. *Antioxid. Redox Signal.* **14,** 1261–73 (2011).

122. Fuchs, A., Lirk, P., Stucky, C., Abram, S. E. & Hogan, Q. H. Painful Nerve Injury Decreases Resting Cytosolic Calcium Concentrations in Sensory Neurons of Rats. *J. Am. Soc. Anesthesiol.* **102,** 1217–1225 (2005).

123. Duncan, C. *et al.* Painful nerve injury decreases sarco-endoplasmic reticulum Ca2+-ATPase activity in axotomized sensory neurons. *Neuroscience* **231,** 247–257 (2013).

124. Berridge, M. J., Lipp, P. & Bootman, M. D. The versatility and universality of calcium signalling. *Nat. Rev. Mol. Cell Biol.* **1,** 11–21 (2000).

125. Berninger, B., García, D. E., Inagaki, N., Hahnel, C. & Lindholm, D. BDNF and NT-3 induce intracellular Ca2+ elevation in hippocampal neurones. *Neuroreport* **4,** 1303–1306 (1993).

126. Mannion, R. J. *et al.* Neurotrophins: peripherally and centrally acting modulators of tactile stimulus-induced inflammatory pain hypersensitivity. *Proc. Natl. Acad. Sci. U. S. A.* **96,** 9385–90 (1999).

127. Jovanovic, J. N., Thomas, P., Kittler, J. T., Smart, T. G. & Moss, S. J. Brain-derived neurotrophic factor modulates fast synaptic inhibition by regulating GABA(A) receptor phosphorylation, activity, and cell-surface stability. *J. Neurosci.* **24,** 522–30 (2004).

# 7 Acknowledgements

I would like to thank Dr. Jing Hu for her excellent mentoring. Her patience and effort in discussion trained my scientific thinking, and her passion for science is always rousing. I also would like to thank my advisory board members, Dr. Maria Kukley and Dr. Eva Küppers, for their support and helpful suggestions for my project.

It is a great experience to work with my supportive colleagues, Flavia Frattini, Dr. Yanmei Qi, Dr. Florian Mayer and Dr. Jeremy Tsung-Chieh Chen. Your friendliness makes our lab such a pleasant place to work. I also would like to express my appreciation to my other CIN friends, Bálint Nagy, Ting-jun Chen, Bartosz, Saad Idrees, Dr. Ivana Nikić-Spiegel, Aleksandra Arsic, and Nevena Stajkovic, for their help when I was looking for advices, chemicals, tools, devices, coffee, sweets, etc. I wish all my friends a bright future.

In the end, I would like to thank my parents for their long term support and understanding, without which it would not be possible for me to achieve this.